

DISCLAIMER

This report was prepared as an account of work sponsored by an agency of the United States Government. Neither the United States Government nor any agency thereof, nor any of their employees, makes any warranty, expressed or implied, or assumes any legal liability or responsibility for the accuracy, completeness, or usefulness of any information, apparatus, product, or process disclosed, or represents that its use would not infringe privately owned rights. Reference herein to any specific commercial product, process, or service by trade name, trademark, manufacturer, or otherwise does not necessarily constitute or imply its endorsement, recommendation, or favoring by the United States Government or any agency thereof. The views and opinions of authors expressed herein do not necessarily state or reflect those of the United States Government.

This report has been reproduced directly from the best available copy.

Available to DOE and DOE contractors from the Office of Scientific and Technical Information, P.O. Box 62, Oak Ridge, TN 37831; prices available from (615) 576-8401.

Available to the public from the National Technical Information Service, U.S. Department of Commerce, 5285 Port Royal Rd., Springfield VA 22161

DOE/BC/14884-15
Distribution Category UC-122

Surfactant Loss Control in Chemical Flooding
Spectroscopic and Calorimetric Study of Adsorption and
Precipitation on Reservoir Minerals

Annual Report for the Period
September 30, 1992 to September 30, 1995

By
Columbia University in the city of New York

July 1996

Work Performed Under Contract No. DE-AC22-92BC14884

Prepared for
U.S. Department of Energy
Assistant Secretary for Fossil Energy

Jerry Casteel, Project Manager
Bartlesville Project Office
P.O. Box 1398
Bartlesville, OK 74005

Prepared by
Columbia University in the city of New York
Box 20, Low Memorial Library
New York, NY 10027

TABLE OF CONTENTS

LIST OF FIGURES	v
LIST OF TABLES	x
LIST OF SYMBOLS	xi
ABSTRACT	xii
EXECUTIVE SUMMARY	1
MATERIALS & METHODS	6
Materials	6
Surfactants	6
Minerals	6
Other Chemicals	7
Methods	7
Analytical Techniques	7
Adsorption	7
Surface tension	8
Flotation test	8
Zeta potential	8
Fluorescence spectroscopy	8
Ultrafiltration	8
RESULTS & DISCUSSION	9
Effect of surfactant structure on adsorption of xylene sulfonates	9
Interfacial behavior of nonionic surfactants	11
Adsorption	11
Electrokinetics	15
Wettability	17
Microstructure studies	19
Interfacial and solution behavior of anionic - nonionic surfactant mixtures	20

Adsorption of surfactant mixtures at solid-liquid interfaces	24
Effect of hydrocarbon chain length of nonionic surfactant on its adsorption	28
Sodium dodecyl sulfate (SDS)/octaethyleneglycol mono-n-alkyl ether (C ₁₂ EO ₈) mixture adsorption	29
Fluorescence probing of mixed-surfactant adsorbed layers	32
Adsorption/desorption of cationic surfactant at the alumina-water interface	40
Desorption of cationic surfactant from alumina-water interface	45
Adsorption of cationic-nonionic surfactant mixtures	48
Changes in surfactant ratios of tetradecyl trimethyl ammonium chloride (TTAC) to pentadecyl ethoxylated nonyl phenol (NP-15) after adsorption	55
Theoretical and Thermodynamic Modelling of Cationic - Nonionic Surfactant Interactions	62
Desorption of surfactant mixtures from alumina-water interface	68
Measurement of monomer concentration by ultrafiltration	74
Monomer concentrations of tetradecyl trimethyl ammonium chloride (TTAC) and pentadecyl ethoxylated nonyl phenol (NP-15) in their mixed solutions	76
Relationship between adsorption at the alumina-water interface and monomer concentration in a 4:1 tetradecyl trimethyl ammonium chloride (TTAC) to pentadecyl ethoxylated nonyl phenol (NP-15) mixture system	83
SUMMARY	90
REFERENCES	93
PUBLICATIONS AND PRESENTATION	94

LIST OF FIGURES

Figure 1	4C11 2,4 Meta xylene sulfonate (Meta)	9
Figure 2	4C11 3,5 Paraxylene sulfonate (Para1)	9
Figure 3	4C11 2,5 Paraxylene sulfonate (Para2)	9
Figure 4	4C11 4,5 Orthoxylene sulfonate (OXS)	9
Figure 5	Adsorption of xylene sulfonates on alumina	10
Figure 6	Polyethoxylated nonyl phenol (NP) surfactant (n: 10, 15, 20, 40).	11
Figure 7	Surface tension of polyethoxylated nonyl phenols with 10, 15, 20 & 40 ethylene oxide groups	12
Figure 8	Effect of change in number of ethylene oxide groups on the adsorption of polyethoxylated nonyl phenols on silica	13
Figure 9	Effect of pH on the adsorption of polyethoxylated nonyl phenol (NP-10) on silica	14
Figure 10	Zeta potential of silica	15
Figure 11	Effect of NP-10 adsorption on the zeta potential of silica (pH \approx 6)	16
Figure 12	Effect of NP-15 adsorption on the zeta potential of silica (pH \approx 6)	16
Figure 13	Wettability of silica after NP-10 adsorption	17
Figure 14	Wettability of silica after NP-40 adsorption	18
Figure 15	Adsorption of NP-40 on silica and characterization of the adsorbed layer using pyrene	20
Figure 16	Surface tension of mixtures of sodium dodecyl sulfate (SDS) and polyethoxylated dodecyl phenol (TRITON)	21
Figure 17	Correlation of CMC of a mixture of SDS and TRITON with mole fraction of TRITON	23
Figure 18	Effect of pH on the adsorption on kaolinite of (a) SDS and (b) C ₁₂ EO ₈ from SDS/C ₁₂ EO ₈ mixtures.	26
Figure 19	Schematic representation of pH effect on the adsorption of SDS/C ₁₂ EO ₈ mixtures on kaolinite	27

Figure 20	Effect of hydrocarbon chain length of nonionic surfactant on its adsorption on kaolinite	28
Figure 21	Effect of nonionic surfactant hydrocarbon chain length on the adsorption of sodium dodecyl sulfate (SDS) on kaolinite from 1:1 SDS/C _n EO ₈ mixtures. 0.03 M NaCl, pH 5.	29
Figure 22	Effect of hydrocarbon chain length (C _n EO ₈) on the adsorption of nonionic surfactant on kaolinite. 0.03 M NaCl, pH 5.	30
Figure 23	Effect of nonionic surfactant hydrocarbon chain length on the adsorption of C _n EO ₈ (n=10,12,14,16) on kaolinite from its 1:1 mixtures with SDS. 0.03 M NaCl, pH 5	31
Figure 24	Schematic representation of the effect of nonionic surfactant hydrocarbon chain length on the adsorption of the anionic surfactant SDS when the nonionic surfactant hydrocarbon chain is (a) longer than SDS, (b) equal to SDS and (c) shorter than SDS.	32
Figure 25	Polarity parameter of pyrene in the adsorbed layer of 1:1 SDS/C ₁₂ EO ₈ mixtures on alumina	33
Figure 26	Total adsorption of sodium dodecyl sulfate (SDS) and 1:1 SDS/C ₁₂ EO ₈ mixtures on alumina and aggregation numbers of surfactant.	36
Figure 27	Isotherms for individual surfactant adsorption on alumina from 1:1 SDS/C ₁₂ EO ₈ mixtures.	38
Figure 28	Adsorption isotherm of tetradecyl trimethyl ammonium chloride (TTAC) on alumina at pH 10.	40
Figure 29	Zeta potential of alumina after adsorption of tetradecyl trimethyl ammonium chloride (TTAC) at pH 10.	41
Figure 30	Settling rate of alumina suspensions after tetradecyl trimethyl ammonium chloride (TTAC) adsorption at pH 10.	42
Figure 31	Adsorption isotherm of tetradecyl trimethyl ammonium chloride (TTAC) on alumina and corresponding changes in pyrene monomer fluorescence from the alumina water interface and the supernatant.	44

Figure 32	Desorption of TTAC from alumina upon dilution from different residual concentrations (Cr).	45
Figure 33	Changes in pyrene polarity parameter from the TTAC adsorbed layer on alumina upon dilution from different residual concentrations and also in bulk solution. .	47
Figure 34	Adsorption isotherms of pentadecyl ethoxylated nonyl phenol (NP-15) on alumina: with preadsorbed amounts of tetradecyl trimethyl ammonium chloride (TTAC), and when added together with TTAC.	49
Figure 35	Adsorption of tetradecyl trimethyl ammonium chloride (TTAC) in the presence and absence of NP-15.	51
Figure 36	Adsorption of pentadecyl ethoxylated nonyl phenol (NP-15) on alumina in presence of varying amounts of tetradecyl trimethyl ammonium chloride (TTAC)	52
Figure 37	Total adsorption of surfactant mixtures at the alumina-water interface.	54
Figure 38	Zeta-potential of alumina after adsorption of TTAC:NP-15 mixtures of different composition.	55
Figure 39	Ratio of adsorption densities of TTAC:NP-15 for different surfactant mixtures.	56
Figure 40	Changes in surfactant ratios (TTAC:NP-15) after adsorption for an initial 4:1 mixing ratio	57
Figure 41	Changes in surfactant ratios (TTAC:NP-15) after adsorption at the alumina water interface for an initial mixing ratio of 1:1	58
Figure 42	Changes in surfactant ratios (TTAC:NP-15) after adsorption at the alumina-water interface for an initial mixing ratio of 1:4	59
Figure 43	Surface tension of solutions of TTAC, NP-15 and their mixtures.	60
Figure 44	Surface tension of TTAC:NP-15 surfactant mixtures after adsorption	61
Figure 45	Regular solution and ideal mixing theory for determining the interaction parameter for the tetradecyl trimethyl ammonium chloride (TTAC) and pentadecyl ethoxylated nonyl phenol (NP-15) system	65
Figure 46	Monomer concentrations of tetradecyl trimethyl ammonium chloride (TTAC) in mixtures with pentadecyl ethoxylated nonyl phenol (NP-15) calculated using	

	regular solution theory with an interaction parameter -1.5	66
Figure 47	Monomer concentrations of pentadecyl ethoxylated nonyl phenol (NP-15) in mixtures with tetradecyl trimethyl ammonium chloride (TTAC) calculated using regular solution theory with an interaction parameter = -1.5.	67
Figure 48	Desorption of tetradecyl trimethyl ammonium chloride (TTAC) from mixed adsorbed layer on alumina upon dilution from different residual concentrations of TTAC (C_r). TTAC:NP-15 = 4:1	68
Figure 49	Desorption of pentadecyl ethoxylated nonyl phenol (NP-15) from alumina upon dilution from different residual concentrations (C_r). TTAC:NP-15 ratio = 4:1.	69
Figure 50	Desorption of tetradecyl trimethyl ammonium chloride (TTAC) from alumina-water interface upon dilution from different residual concentrations (C_r) in presence of 1:1 pentadecyl ethoxylated nonyl phenol (NP-15).	70
Figure 51	Desorption of pentadecyl ethoxylated nonyl phenol (NP-15) upon dilution from different residual concentrations (C_r) in presence of 1:1 tetradecyl trimethyl ammonium chloride (TTAC).	71
Figure 52	Desorption of tetradecyl trimethyl ammonium chloride (TTAC) from alumina upon dilution from different residual concentrations (C_r). TTAC:NP-15 ratio = 1:4.	72
Figure 53	Desorption of pentadecyl ethoxylated nonyl phenol (NP-15) from alumina upon dilution from different residual concentrations (C_r). TTAC:NP-15 ratio = 1:4.	73
Figure 54	Monomer concentration of tetradecyl trimethyl ammonium chloride (TTAC) as the function of total concentration	75
Figure 55	Monomer concentration of pentadecyl ethoxylated nonyl phenol (NP-15) as the function of total concentration	76
Figure 56	Monomer concentrations of NP-15 as measured by ultrafiltration compared with those calculated using regular solution theory	79
Figure 57	Monomer concentrations of TTAC in mixtures with NP-15 as measured by ultrafiltration also calculated using regular solution theory	80
Figure 58	TTAC monomer concentrations in TTAC:NP-15 mixtures of different compositions. I.S. 0.03 M NaCl	81

Figure 59	NP-15 monomer concentrations in TTAC:NP-15 mixtures of different composition. I.S. = 0.03 M NaCl	82
Figure 60	Change in TTAC monomer concentrations before and after adsorption on alumina from a 4:1 TTAC:NP-15 mixture	85
Figure 61	Change in NP-15 monomer concentrations before and after adsorption on alumina from a 4:1 TTAC:NP-15 mixture	85
Figure 62	Relationship between TTAC monomer concentration and adsorption density for 4:1 TTAC:NP-15 mixture system	87
Figure 63	Relationship between NP-15 monomer concentration and adsorption density on alumina from 4:1 TTAC:NP-15 mixture	87
Figure 64	Correlation between adsorption density and monomer ratio after adsorption for TTAC from a 4:1 TTAC:NP-15 mixture	88
Figure 65	Correlation between NP-15 adsorption density and monomer ratio after adsorption for TTAC from a 4:1 TTAC:NP-15 mixture	89

LIST OF TABLES

Table I:	Surfactants used and their molecular structure	6
Table II:	Mineral and their principle properties	7
Table III:	Mixed CMC (C^*) at different mole fractions of TRITON X-100	22
Table IV:	Calculated results of X_1 and C^* by regular solution theory	25
Table V:	Surface coverage of kaolinite by nonionic surfactant (C_nEO_8)	29
Table VI:	Polarity parameter (I_3/I_1) values for surfactant micelles in aqueous solution	34
Table VII:	Aggregation number (N_{agg}) of Surfactant micelles, 0.03 M NaCl, 25°C	37
Table VIII:	Surfactant aggregation number (N_{agg}) for the adsorption of 1:1 SDS/ $C_{12}EO_8$ mixture on alumina: 0.03 M NaCl, pH 6.5, 25°C	39
Table IX:	Calculated results of x and C^* by regular solution theory	64

LIST OF SYMBOLS

- α : mole fraction of surfactant 1 in the mixed surfactant solution
- β : interaction parameter defined in the regular solution theory
- f_i : activity coefficient of surfactant i in mixed micelles
- N_A : Avogadro number
- w_{ij} : the energies of interaction between surfactant species i & j in the mixed micelles
- X_1 : mole fraction of surfactant 1 in mixed micelles
- C_i : CMCs of pure surfactant i
- C : total concentration of mixed surfactant
- C^* : CMC of mixed surfactant
- C_i^m : the monomer concentration of surfactant i
- I_3/I_1 : polarity parameter
- P : pyrene molecule in its ground state
- P^* : pyrene molecule in its excited state
- I_t : pyrene fluorescence emission intensity at desired wavelength at time t
- I_0 : pyrene fluorescence emission intensity at desired wavelength at time $t=0$
- k_0 : the monomer decay rate constant
- k_e : the excimer formation rate constant
- N_{agg} : the aggregation number of the surfactant aggregate (micelle or hemimicelle)
- C_t : the total initial surfactant concentration
- C_r : the total residual surfactant concentration
- $[Py]$: the pyrene concentration
- n : average number of pyrene molecule per surfactant aggregate

ABSTRACT

The aim of this research project was to investigate mechanisms governing adsorption and surface precipitation of flooding surfactants on reservoir minerals. Effects of surfactant structure, surfactant combinations, various inorganic and polymeric species, and solids mineralogy have been determined. A multi-pronged approach consisting of micro & nano spectroscopy, electrokinetics, surface tension and wettability is used in this study. The results obtained should help in controlling surfactant loss in chemical flooding and in developing optimum structures and conditions for efficient chemical flooding processes.

During the three years contract period, adsorption of single surfactants and select surfactant mixtures was studied at the solid-liquid and gas-liquid interfaces. Alkyl xylene sulfonates, polyethoxylated alkyl phenols, octaethylene glycol mono n-decyl ether, and tetradecyl trimethyl ammonium chloride were the surfactants studied. Adsorption of surfactant mixtures of varying composition was also investigated. The microstructure of the adsorbed layer was characterized using fluorescence spectroscopy. Changes in interfacial properties such as wettability, electrokinetics and stability of reservoir minerals were correlated with the amounts of reagent adsorbed. Strong effects of the structure of the surfactant and position of functional groups were revealed. Changes of microstructure upon dilution (desorption) were also studied. Presence of the nonionic surfactants in mixed aggregate leads to shielding of the charge of ionic surfactants which in turn promotes aggregation but reduced electrostatic attraction between the charged surfactant and the mineral surface. Strong consequences of surfactant interactions in solution on adsorption as well as correlations between monomer concentration in mixtures and adsorption were revealed.

EXECUTIVE SUMMARY

Loss of surfactants by adsorption and precipitation is a major problem in enhanced oil recovery by using micellar flooding processes. Clearly it is important to minimize the surfactant loss in these processes to make them more efficient. To elucidate mechanisms of adsorption and precipitation of surfactants on reservoir minerals, adsorption of selected individual surfactants and mixtures on oxide minerals was studied in this work. The aim was to determine the effect of structure on surfactant adsorption at the solid-liquid as well as at the liquid-gas interface and to characterize the microstructure of the adsorbed layers. Electrokinetic behavior was monitored along with the adsorption in order to establish the role of electrostatic forces in determining the adsorption. Adsorption of surfactants at the solid-liquid interface was correlated with changes in interfacial behavior such as wettability and zeta potential.

Anionic xylene sulfonates, nonionic polyethoxylated alkyl phenols, and cationic tetradecyl trimethyl ammonium chloride (TTAC) were the surfactants studied. Effect of pH was studied both because pH is a parameter with marked effects and the understanding of such effects can help in elucidating the overall mechanisms.

The effects of the variation in the positions of the sulfonate and methyl groups on the benzene ring of alkyl xylene sulfonate surfactants were systematically studied. The position of the sulfonate group was found to be very critical in relation to those of the methyl groups. Also shielding of the charged sulfonate groups by the methyl group is observed to influence the adsorption significantly.

The effect of the number of ethylene oxide groups on the adsorption of polyethoxylated alkyl phenols on silica and changes in silica-water interfacial properties was determined in detail since the

ethoxyl groups offer tolerance to deleterious species such as calcium and a unique opportunity to control the adsorption and the hydrophobicity of the surfactant. Wettability of silica after adsorption of nonyl phenyl polyethoxylated alcohols (with number of polyethylene oxide groups varying from 10-40) was measured using flotation technique to investigate the orientation of the adsorbed layer. Interestingly, the amount of silica floated after the nonionic surfactant adsorption was found to be independent of the ethylene oxide chain length within the range tested.

Several mixed surfactant systems were studied since most commercial surfactants are usually mixtures. First, the effect of the important variable, hydrocarbon chain length of one surfactant on the adsorption of another was studied by determining the adsorption of the anionic sodium dodecylsulfate (SDS) as a function of the chain length of a nonionic surfactant, octaethylene glycol mono-n-alkyl ether (C_nEO_8). The nonionic surfactant enhanced the adsorption of the anionic surfactant in certain concentration regions, but interestingly only when the hydrocarbon chain length was less than or equal to that of the latter. Results are discussed in terms of the hydrocarbon chain-chain interaction and shielding of the chains from hydrophilic environments. Such shielding was found to lead to an increase in the size of the adsorbed aggregates of 1:1 mixtures of SDS/ $C_{12}EO_8$ at the alumina-water interface as measured by fluorescence spectroscopy. Computation of individual aggregate size from the ratio of adsorption densities at the interface (and the total aggregate size) leads to the conclusion that the sodium dodecylsulfate (SDS) aggregate is smaller than the octaethylene glycol mono-n-dodecyl ether ($C_{12}EO_8$) aggregate. The above results suggest that by choosing suitable mixtures of surfactants the wettability of reservoir rock can be controlled since hydrophobicity will depend on the hydrophobic patch size.

Interactions between surfactants in their mixtures were studied also by determining surface

tension of such mixtures and their critical micelle concentrations at different mixing ratios. Mixed micellization of sodium dodecyl sulfate and dodecyl phenoxy polyethoxylated alcohol was found to be non-ideal and regular solution theory was found to adequately describe their interactions. The adsorption of sodium dodecyl sulfate (SDS) and octaethylene glycol mono n-decyl ether ($C_{12}EO_8$) on kaolinite was higher from their mixtures than from their single systems and this enhanced adsorption was accounted for by the hydrophobic chain-chain interactions. The effect of pH on the adsorption of single surfactant and surfactant mixtures on kaolinite was also investigated. The effect of such increased adsorption on wettability and oil displacement will depend upon the orientation of the molecules in the adsorbed layer and structure of hydrophobic and/or hydrophilic functional groups.

Next, cationic surfactants which have not been studied much in the past were investigated. The adsorption isotherm of a cationic surfactant, tetradecyl trimethyl ammonium chloride (TTAC), on alumina was determined at two pH values. Changes in the settling rate of alumina suspensions after TTAC adsorption were also followed to describe the evolution of the adsorbed layer. At high surface coverage the alumina was observed to become hydrophilic suggesting the formation of a TTAC bilayer at the surface. Desorption of the cationic tetradecyl trimethyl ammonium chloride from the alumina-water interface indicated that adsorption was reversible in the high concentration range, but in the low concentration range some hysteresis in desorption was found. Fluorescence spectroscopic measurements supported this observation. This information on desorption is important for micellar flooding process since there can be significant potentially useful desorption of surfactant upon subsequent dilution.

Adsorption/desorption of mixtures of TTAC and pentadecylethoxylatednonylphenol (NP-15)

at the alumina water interface was studied next. While NP-15 does not adsorb on alumina by itself, the presence of preadsorbed or coadsorbing TTAC forced the nonionic surfactant to adsorb. Interestingly coadsorbing TTAC had a higher influence on the adsorption of NP-15 than preadsorbed TTAC suggesting the importance of the dynamics of the adsorption process. With an increase in pentadecylethoxylatednonylphenol content in the mixtures, adsorption of TTAC was reduced possibly due to steric repulsion and competition for adsorption sites. In order to understand the dynamics and reversibility, desorption of the cationic TTAC from the alumina surface was studied in the presence and absence of nonionic NP-15. For the case of cationic TTAC alone, it was found that adsorbed aggregates reorganized at the alumina-water interface. In the presence of NP-15 it was observed that in TTAC rich mixtures, the desorption of TTAC is similar to that of TTAC alone. As the adsorption of NP-15 was dependent on the presence of TTAC, the desorption also was TTAC dependent except in the case of NP-15 rich mixtures. Regular solution theory was used to model interactions between NP-15 and TTAC in solutions and the model was extended to the adsorption behavior of the mixtures. It becomes clear that the adsorption and desorption behaviors of surfactant can be manipulated by simply adjusting mixing ratio and the order of addition of surfactant mixtures.

Interactions between surfactants can be exploited to monitor the adsorption/desorption behavior and the aggregation tendencies of the individual surfactants. In the case of anionic-nonionic as well as cationic-nonionic surfactant mixtures, hydrophobic interaction between the chains was the dominant mechanism which led to synergistic interactions. The presence of the nonionic surfactant in a surfactant mixture shields the charged ionic surfactant from each other thus promoting aggregation as well as reducing electrostatic attraction between the charged surfactant and the substrate.

To develop a model that can predict adsorption of both components as a function of their activity in the mixed surfactant system, monomer concentrations of TTAC and NP-15 in mixtures of different ratios were measured using ultrafiltration technique. The behavior of mixed micellization processes in solution was examined by considering various hydrophobic, electrostatic and steric forces involved. The relationship between monomer concentration and adsorption density was also discussed. It was found that the monomer concentrations of both TTAC and NP-15 do not remain constant above the mixed CMC of the system. Importantly, they are also different from that predicted by the regular solution theory. This result reveals the limitations of the regular solution theory for mixed surfactant systems. A more suitable model is needed to describe these systems.

From the results presented in this report, an improved understanding of adsorption/desorption mechanisms of surfactant systems and the effect of many important parameters, such as structure, mixing ratio and pH etc., on the controlling of surfactant behavior is obtained. It is clear that one can manipulate surfactant mixtures in different ways to design reagent schemes for high surface activity and at the same time low adsorption at solid-liquid interface for possible use in micellar flooding operations.

MATERIALS & METHODS

Materials

Surfactants: Several typical ionic and nonionic surfactants were selected for this study. Alkyl xylene sulfonates with different structures were obtained from ARCO Exploration and Technology Co. All these surfactants were specified to be at least 97% isomerically pure on the basis of NMR characterization. Sodium dodecyl sulfate (SDS) of greater than 99% purity purchased from Fluka chemicals was used as received. The nonionic surfactants covered a wide range of hydrophobic and hydrophilic chain lengths and were purchased from Nikko Chemicals. The ethoxylated alcohols were of the general structure $C_nH_{2n+1}(CH_2CH_2O)_mH$ or C_nEO_m . The homologues studied were $C_{10}EO_8$, $C_{12}EO_8$, $C_{14}EO_8$, and $C_{16}EO_8$ thus providing an opportunity for studying the effect of surfactant chain length on mixture adsorption. In addition to the alcohols, nonyl phenols obtained from Barnett Products, New Jersey with varying ethylene oxide groups were also studied. Cationic tetradecyl trimethyl ammonium chloride (TTAC) of greater than 99% purity purchased from TCI Chemicals, Japan was used as received. The surfactants which were studied in this work are listed in table I.

Table I. Surfactants used and their molecular structure

Surfactant	molecular structure	purity
Alkyl xylene surfonates	$C_{11}H_{23}(C_6H_2)(CH_3)_2 \cdot SO_3Na$	>97%
Sodium dodecyl sulfate	$C_{12}H_{23} \cdot SO_4Na$	>99%
Polyethoxylated alcohol	$C_nH_{2n+1}(CH_2CH_2O)_mH$	>97%
Polyethoxylated nonyl phenol	$C_9H_{19}(CH_2CH_2O)_nH$	>97%
Tetradecyltrimethylammonium chloride	$[CH_3(CH_2)_{13}N(CH_3)_3]Cl$	>98%

Minerals: Minerals used are listed below along with their surface area and particle size.

Table II Minerals and their principle properties

Mineral	Supplier	Surface area (m ² /g)	Particle size (μm)
Kaolinite	Univ. of Missouri	8.2	--
Alumina	Linde (Union Carbide)	15.0	0.3
Silica	Spherosil	25.0	40 - 100

Other Chemicals: Pyrene was obtained from Aldrich Chemicals and recrystallized from ethanol. NaCl, HCl and NaOH used were of ACS reagent grade. All solutions were prepared in triply distilled water and at constant ionic strength as indicated in later sections.

Methods

Analytical Techniques: Sodium dodecyl sulfate (SDS) concentration was determined using a two-phase titration method¹. Tetradecyl trimethyl ammonium chloride (TTAC) concentration was determined by complexing the surfactant with excess SDS and measuring the non-complexed SDS using the two-phase titration. The concentration of ethoxylated alcohol (C_nEO_m) was determined using high pressure liquid chromatography (HPLC) with a C₁₈ bonded silica column and a refractive index detector. The solvent used was a 90:10 mixture of acetonitrile and water. Pentadecylethoxylated nonyl phenol concentration was determined by UV absorption at 223 nm. This is the wavelength at which NP-15 solution has maximum absorption of UV light.

Adsorption: Adsorption experiments were conducted in 25 cc Teflon capped scintillation vials. One gram of the solid was brought in contact with 5 cc of solution of desired ionic strength for 2 hours. Next, 5 cc of salt solution containing surfactant or surfactant mixture of desired concentration was

added. The system was conditioned on a wrist action shaker 15 hours in the case of silica, 24 hours in the case of alumina and 72 hours in the case of kaolinite. The suspensions were then centrifuged at 3000-4000 rpm and the supernatant analyzed for residual concentration. Adsorption was calculated based upon surfactant depleted from solution.

Surface tension: Surface tension of surfactant solutions was measured using a Wilhelmy plate or a du Nuoy ring tensiometer.

Flotation test: A modified Hallimond tube was used for flotation tests. Hallimond test procedure consisted of mixing 1 gram sample in desired surfactant solution. The pH of the pulp supernatant was measured and the pulp was then transferred to the Hallimond tube. Flotation was conducted for twenty seconds at a nitrogen flow rate of 50ml/minute.

Zeta potential: Zeta potential of mineral particles before and after adsorption was measured using a Zeta Meter Model D system.

Fluorescence spectroscopy: A Photon Technology International PTI LS-100 was used for fluorescence experiments. The samples containing pyrene dissolved to its maximum solubility in water ($\approx 2 \times 10^{-7}$ kmol/m³) were excited at 335 nm and emission between 365 and 500 nm was recorded.

Ultrafiltration: The filtrations were carried out in stirred cell (model 8050) purchased from Amicon Inc.. All experiments were done at room temperature (22-25°C) and at a pressure of about 850 mm Hg absolute. The membranes (YM-1 and YM3) with the molecular weight cut-off 1000 and 3000 that were used in the study were also obtained from Amicon Inc..

RESULTS & DISCUSSION

Effect of surfactant structure on adsorption of xylene sulfonates

The structures of the surfactants studied are shown below:

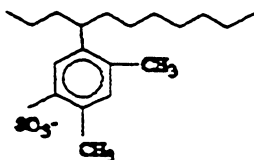


Figure 1 4C11 2,4 Meta xylene sulfonate (Meta)

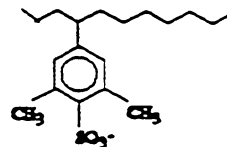


Figure 2 4C11 3,5 Paraxylene sulfonate (Para1)

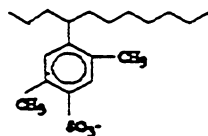


Figure 3 4C11 2,5 Paraxylene sulfonate (Para2)

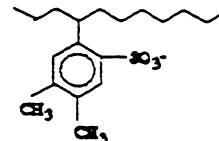


Figure 4 4C11 4,5 Orthoxylene sulfonate (OXS)

The adsorption behavior of these xylene sulfonates on alumina is illustrated in figure 5. The position of the functional groups has a significant effect on the adsorption of alkyl xylene sulfonates: when the sulfonate was in the meta position with respect to the methyl groups (124 MXS), surfactant adsorption on alumina was lower than with the sulfonate in the para position (135 PXS - Para 1). But when the position of the methyl group was changed with the sulfonate kept in the para position (125 para xylene sulfonate - Para 2), the adsorption isotherm was identical to that of the para1². This suggested that the position of the methyl groups does not play as important a role as the position of the sulfonate. The adsorption isotherm of OXS is different from that of the meta and para xylene

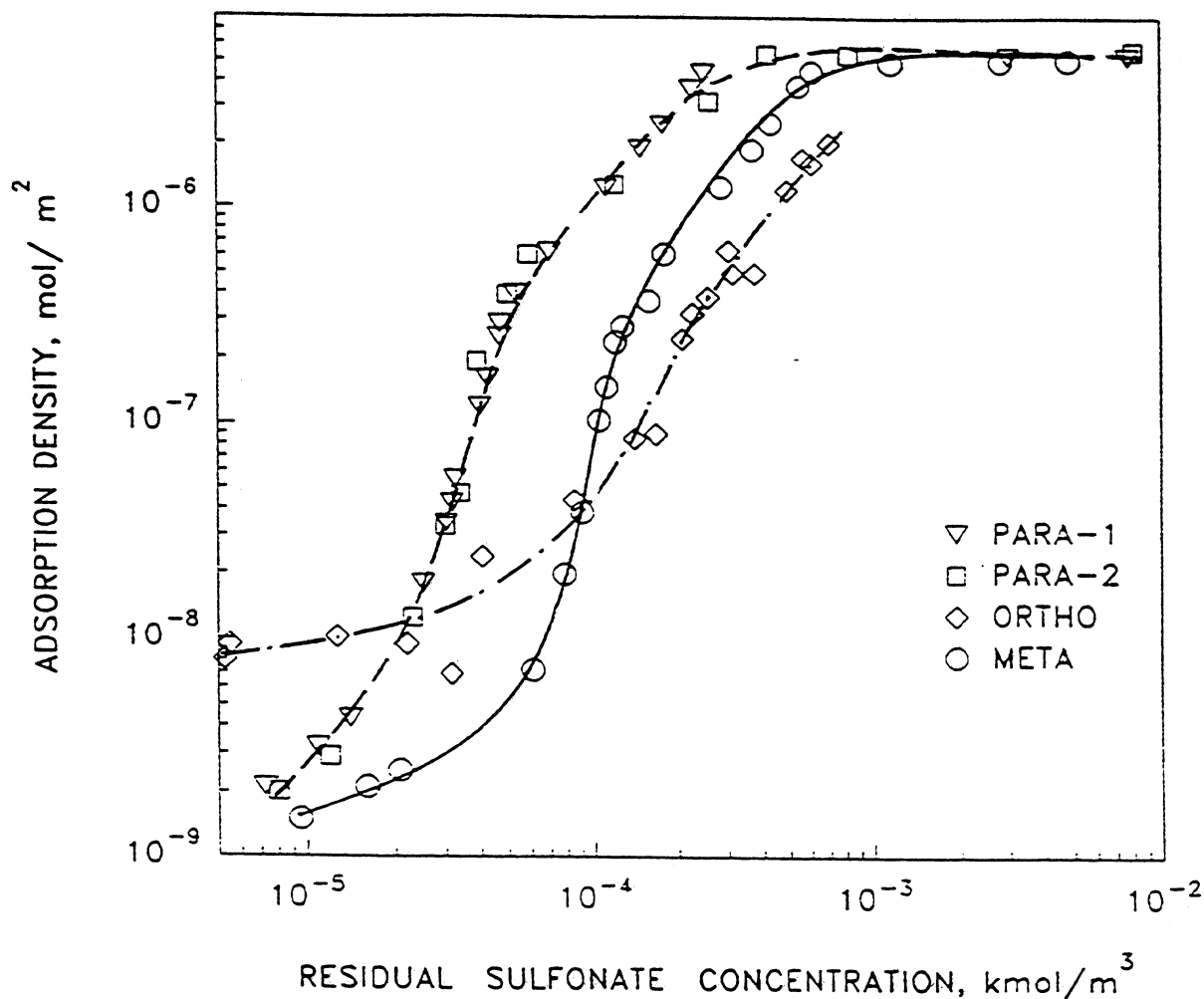


Figure 5 Adsorption of xylene sulfonates on alumina

sulfonates. The results in figure 5 indicate that the adsorption density of OXS on alumina is higher in low concentration region. At higher concentrations the adsorption of OXS is consistently lower than that of MXS, Para 1 as well as Para 2. Lower electrostatic attraction in the high concentration region due to the shielding of the sulfonate group by methyl groups could be a possible reason for the lower adsorption.

Interfacial behavior of nonionic surfactants

Adsorption:

The effect of the number of ethylene oxide (EO) groups on the adsorption behavior of polyethoxylated alkyl phenols on silica was studied. The number of EO groups on the surfactants, 10, 15, 20 and 40, offered a wide range. The generic structure of the surfactants is shown below:

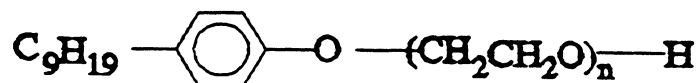


Figure 6 Polyethoxylated nonyl phenol (NP) surfactant (N: 10, 15, 20, 40).

The purity of the surfactants used is evident from the surface tension behavior of the surfactants shown in figure 7; these measurements were performed on the Fisher du Nuoy ring tensiometer. The surface tension of the commercial grade polyethoxylated nonyl phenol with 40 ethylene oxide groups (NP-40) is also shown for comparison. The minimum in surface tension which is indicative of impurities is detected only for the commercial NP-40.

It can be concluded from the results in figure 7 that as the number of ethylene oxide groups is increased the surface activity decreases and the critical micellization concentration (CMC) increases. These agree with our earlier results on the behavior of the nonionic surfactants³.

The adsorption isotherms for some polyethoxylated nonyl phenols (NP) on silica are shown in figure 8. With an increase in the number of ethylene oxide groups on the surfactant, the

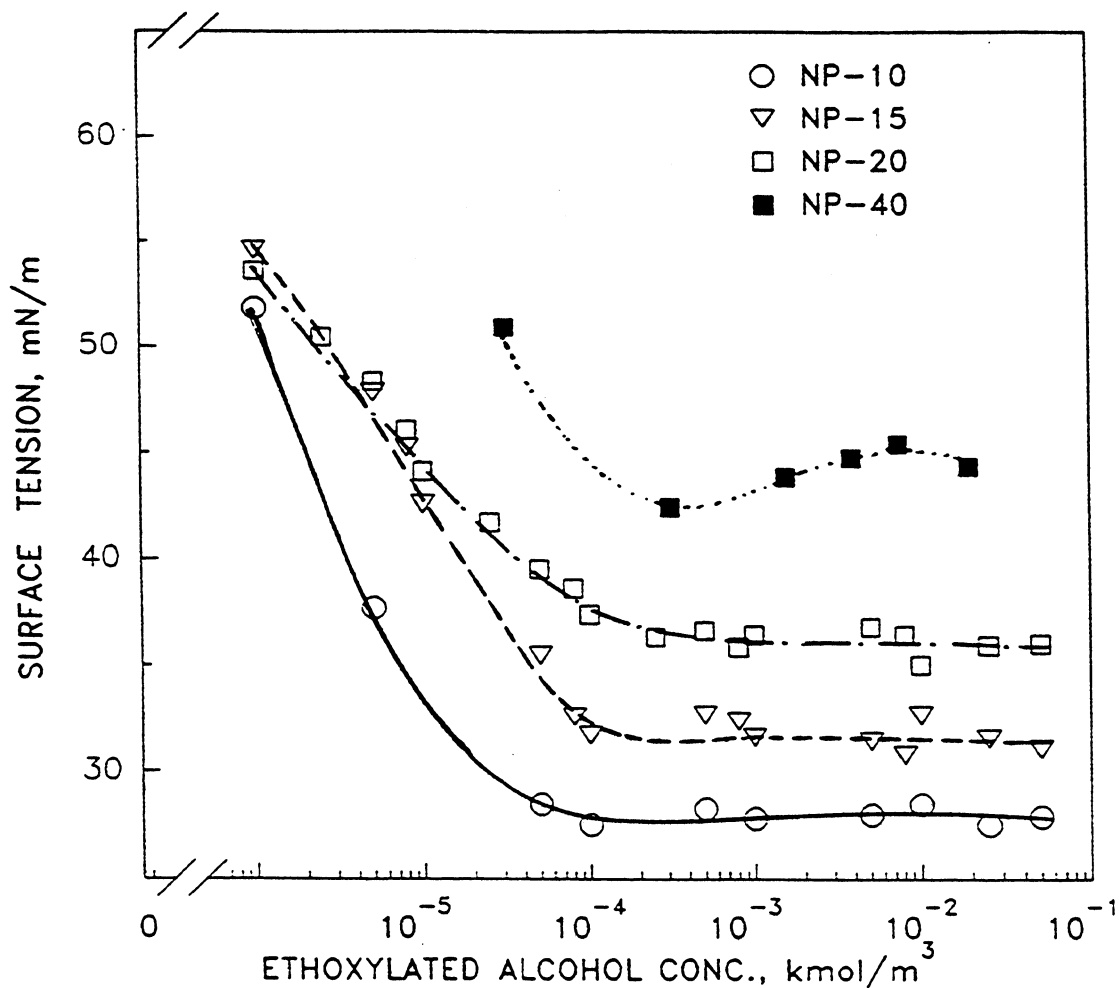


Figure 7 Surface tension of polyethoxylated nonyl phenols with 10, 15, 20 & 40 ethylene oxide groups adsorption density at the silica water interface is decreased.

The slope of the curve in the pre-adsorption maximum region, which is an indication of the cooperative association behavior of the hydrocarbon chains at the solid-liquid interface, decreases with the increase in number of EO groups. An increase in the number of EO groups on the surfactant causes the molecule to become bulky. This will provide steric hindrance to the packing of the molecules into aggregates and, as a result, the adsorption density will be lower.

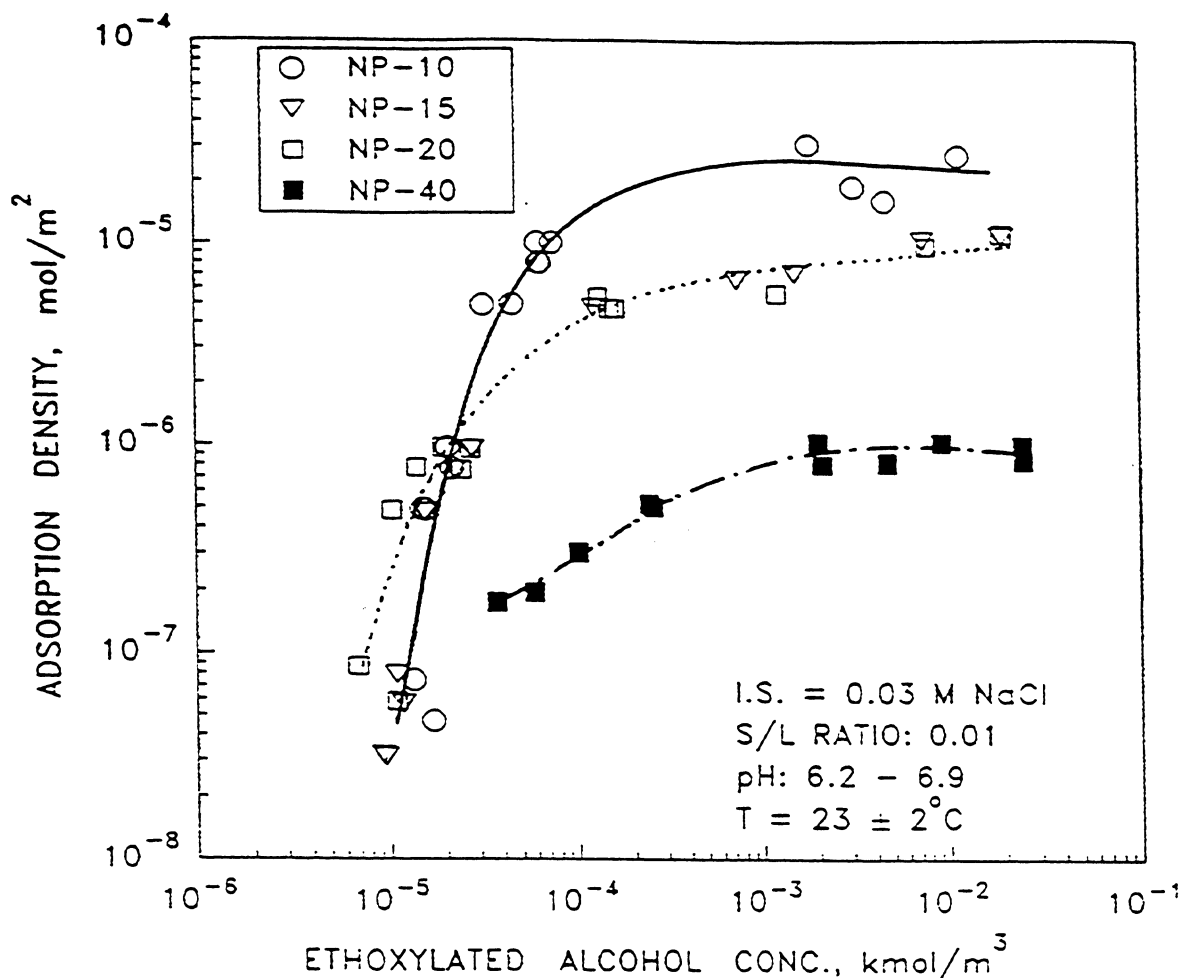


Figure 8 Effect of change in number of ethylene oxide groups on the adsorption of polyethoxylated nonyl phenols on silica

The effect of pH on the adsorption of polyethoxylated nonyl phenol with 10 ethylene oxide groups (NP-10) is shown in figure 9. Three different concentrations were studied, and the pH was varied from 2.5 to 11.

Interestingly, there was no effect of pH on the adsorption of NP-10 on silica in the range studied. The mechanism of adsorption of ethoxylated surfactants on silica is considered to be hydrogen bonding between the ether oxygen of the ethylene oxide group and the surface silanol groups⁴. As the pH is raised, the number of silanol groups on the silica surface will decrease and the

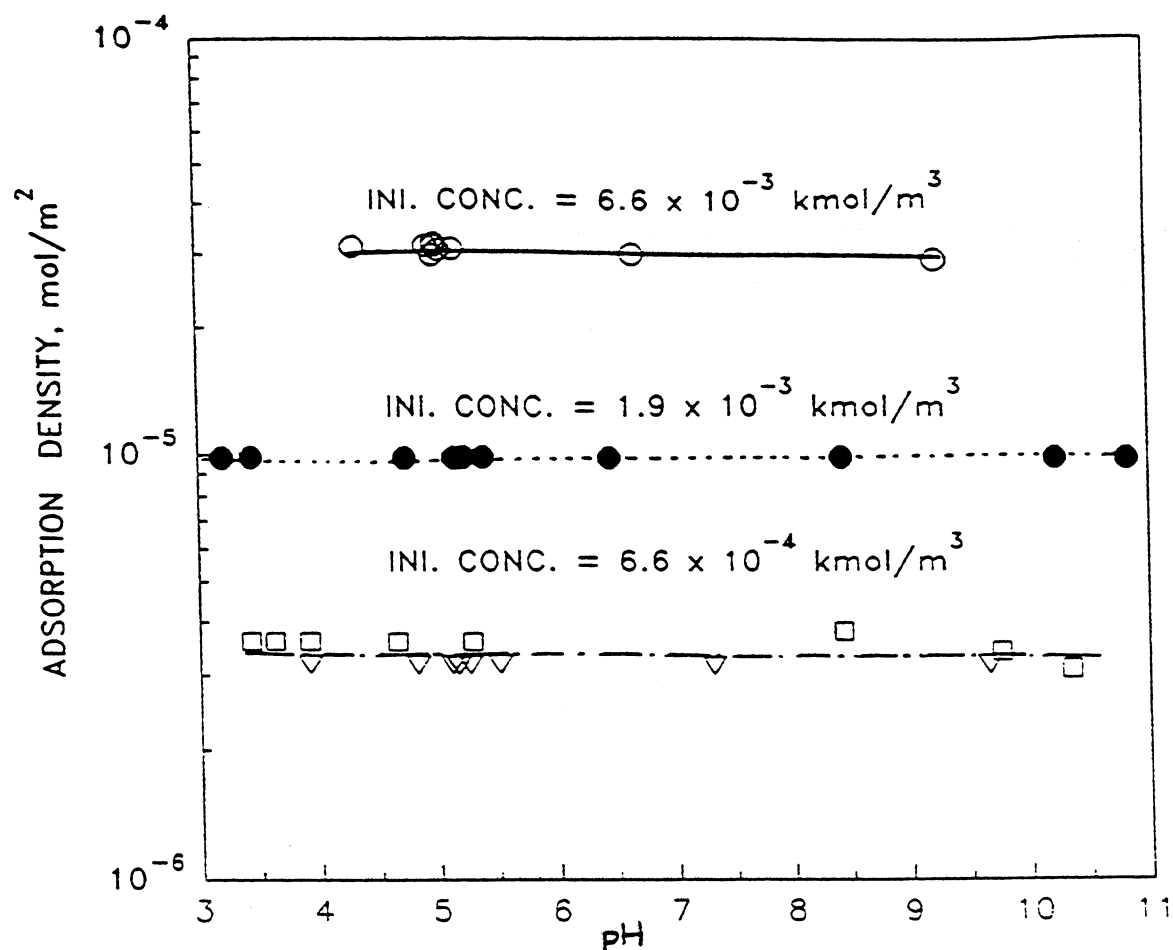


Figure 9 Effect of pH on the adsorption of polyethoxylated nonyl phenol (NP-10) on silica

adsorption of NP-10 could have decreased if the mechanism of adsorption was via hydrogen bonding. To understand this behavior, the electrokinetic behavior of silica was determined, and the results are given in figure 10.

Silica is negatively charged in the entire pH range studied. By extrapolation, the iso-electric point (IEP) is < 2 . Above pH 4.5 the zeta potential of silica is constant suggesting that there is no change in the number of charged surface groups above this pH value for this sample. On the basis of this, pH will be expected to have no effect on the adsorption of NP-10 on silica above pH 4.5. But from figure 9, it can be seen that the adsorption of NP-10 is constant even down to a pH value of 3.

We propose that at pH values higher than the IEP the number of silanol groups (-SiOH) on the surface are very few, and there is no significant change in their number to affect adsorption.

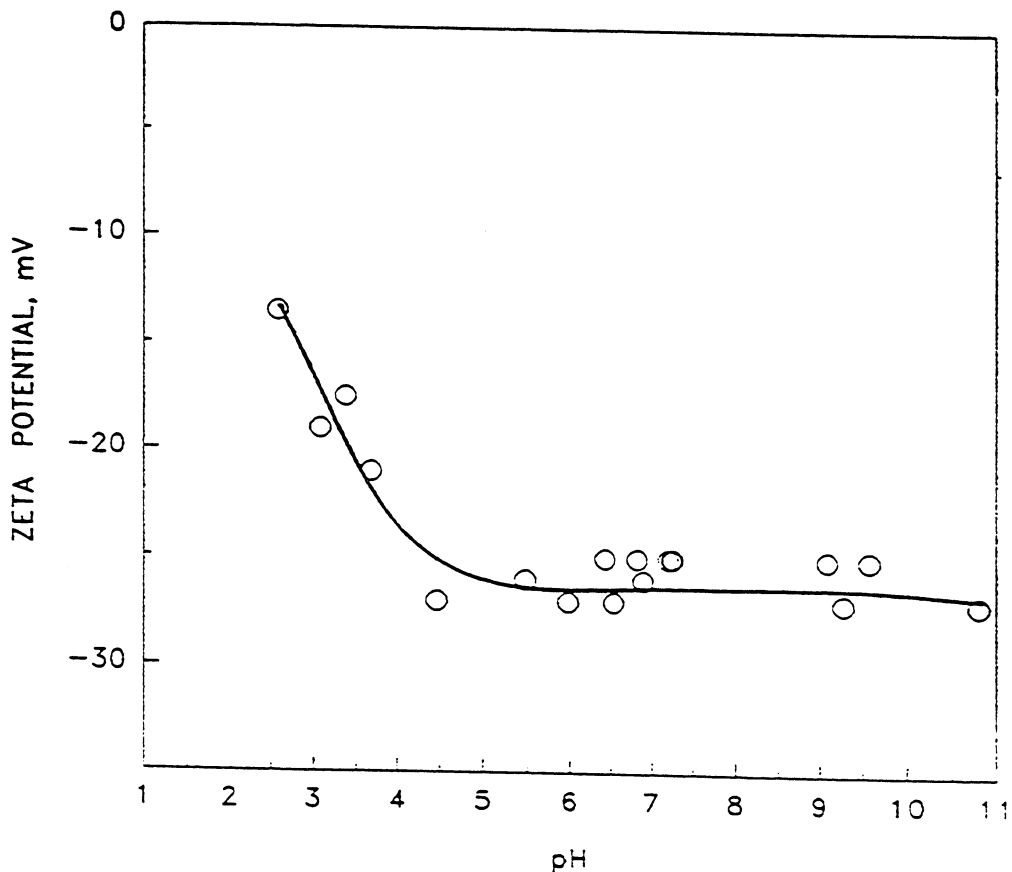


Figure 10 Zeta potential of silica

Electrokinetics:

Changes in the electrokinetic properties of silica after adsorption of NP-10 and NP-15 are shown in figures 11 and 12 along with the adsorption isotherms. In both cases, adsorption of the nonionic surfactant decreases the surface charge of silica.

It is proposed that the adsorbed layers of NP-10 and NP-15 cause a shift in the shear plane resulting in a decrease in the magnitude of the zeta potential. There seems to be no significant difference in the adsorbed layer thickness for NP-10 and NP-15 since their effect on the surface

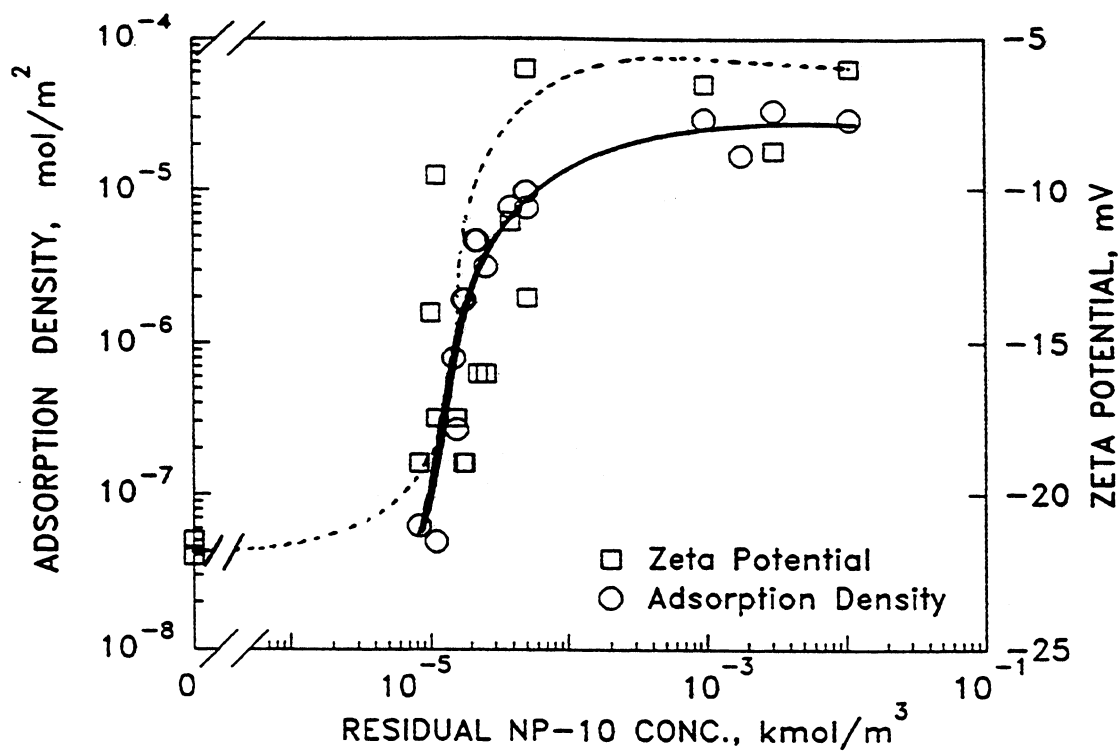


Figure 11 Effect of NP-10 adsorption on the zeta potential of silica (pH=6)

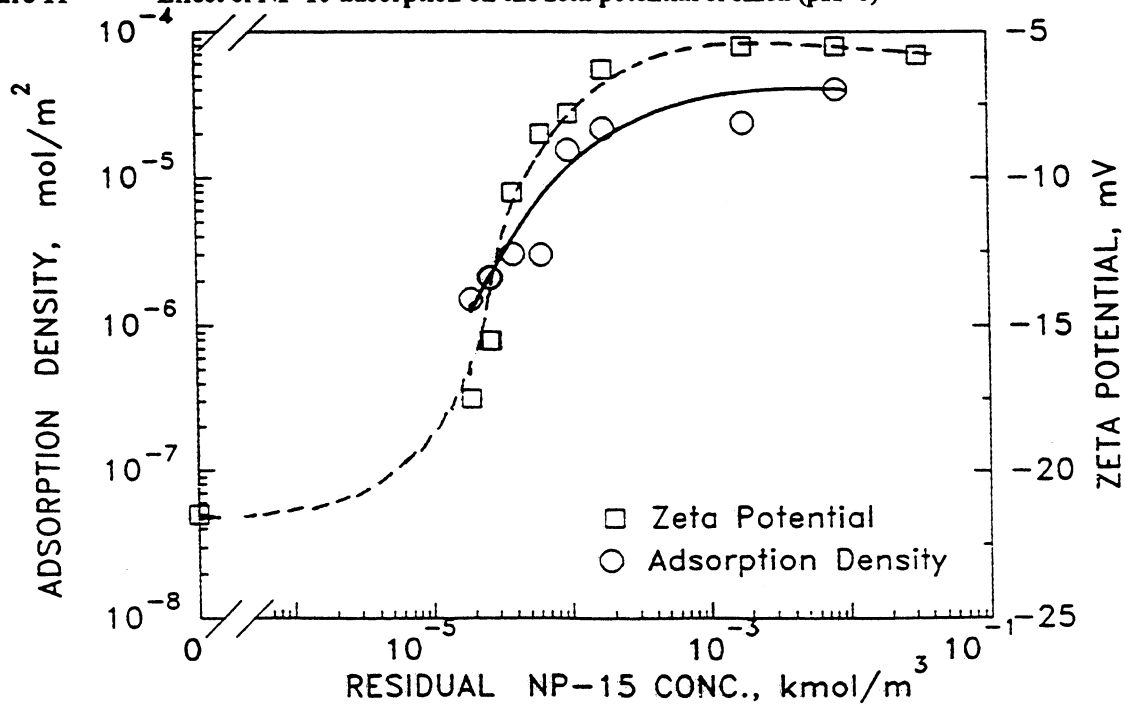


Figure 12 Effect of NP-15 adsorption on the zeta potential of silica (pH=6)

charge of silica is identical.

Wettability:

The wettability of silica after adsorption of nonionic surfactant was measured by determining flotation using a modified Hallimond tube and the results are shown in figures 13 and 14. The surfactants chosen were nonyl phenols with 10 and 40 ethylene oxide groups. Based on adsorption results it is proposed that NP-10 formed aggregates at the silica-water interface whereas the bulky NP-40 did not. Presence of such aggregates at the interface can be expected to affect the wettability to a different extent.

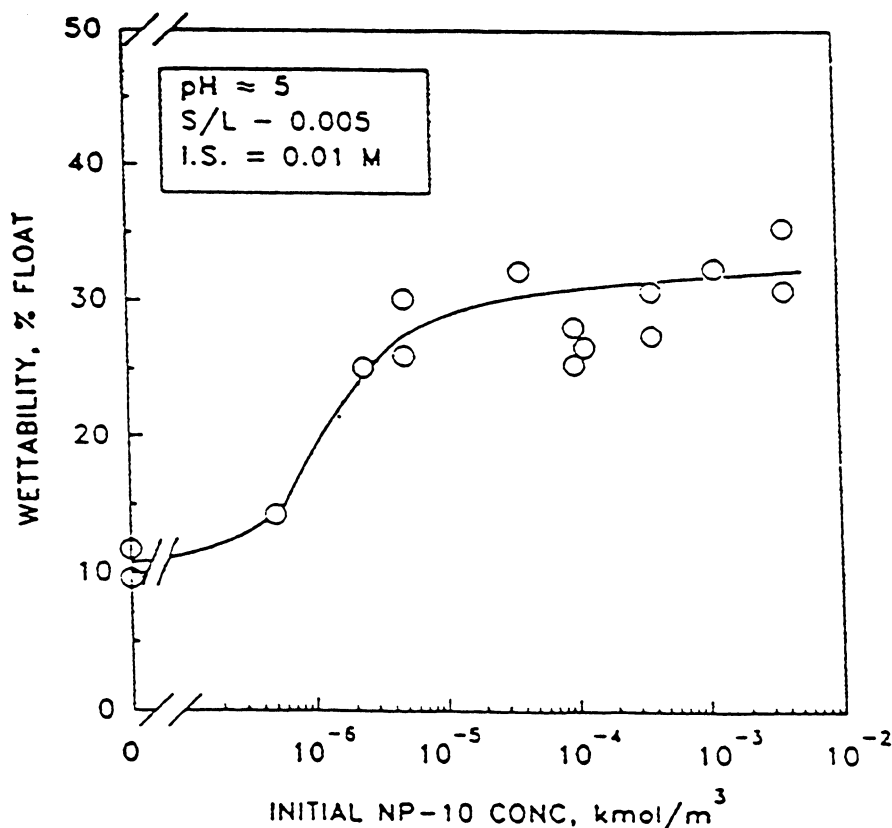


Figure 13 Wettability of silica after NP-10 adsorption

From figures 13 and 14 it is seen that in the absence of surfactant, silica is hydrophilic and

floats very little. Surfactant adsorption via hydrogen bonding between the ether oxygens of the EO group and surface silanol groups will expose the hydrocarbon chain to the aqueous phase which renders the silica surface hydrophobic thereby increasing the floatability. Interestingly, the maximum hydrophobicity achieved in the presence of each surfactant is identical. It is to be noted that the flotation results in figures 13 and 14 are plotted as a function of the initial surfactant concentration.

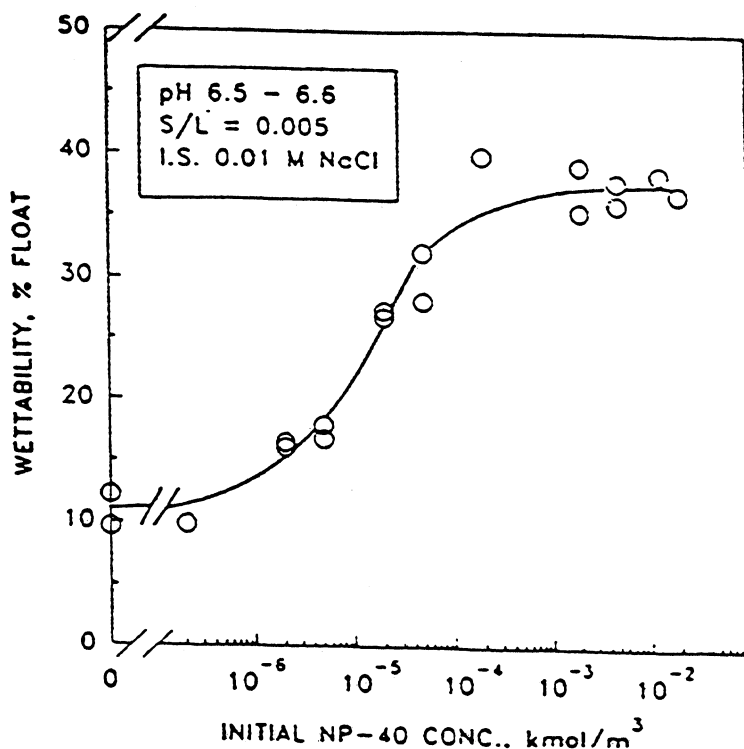


Figure 14 Wettability of silica after NP-40 adsorption

Since the adsorption of NP-10 is significantly higher than NP-40 it is likely that the adsorbed layers for similar initial concentrations will be very different. The residual concentrations could not be measured at the time of flotation. Nevertheless, it is to be noted that the flotation recovery reaches a maximum and does not decrease at higher surfactant concentrations. This suggests that these surfactants do not form bilayer at the interface: formation of a bilayer at the interface would create

a hydrophilic surface and reduce flotation.

Microstructural studies:

Fluorescence spectroscopy was used to characterize the adsorbed layer in terms of micropolarity. Pyrene monomer fluorescence is used for determining the polarity of unknown environments. The ratio of intensities of the third to the first peaks on the pyrene emission spectrum is sensitive to the polarity of the medium in which the pyrene resides⁵. In polar solvents such as water the value of this ratio (I_3/I_1) is ~ 0.6 but in nonpolar solvents and hydrocarbons it varies from 1 to 1.7; I_3/I_1 for sodium dodecylsulfate micelles is ~ 1.0. The value of the polarity parameter when pyrene is solubilized in NP-40 micelles is around 0.8. Since this ratio characterizes the polarity it is termed here the *polarity parameter*.

Adsorption of NP-40 on silica was determined in the presence of low concentrations of pyrene. There was no effect of the pyrene on the amount of surfactant adsorbed. Fluorescence emission spectra were recorded from the suspension as well as the supernatant to determine the presence of hydrophobic aggregates. The results obtained are shown in figure 15. At low values of adsorption density (low residual concentration) the value of the I_3/I_1 ratio is ~ 0.6 indicating an aqueous environment. Only above 10^{-3} kmol/m³, does the value of the I_3/I_1 ratio increase to ~ 0.8. At this concentration there are micelles in the supernatant, and they are detected by pyrene. Since the emissions from the suspension and the supernatant are similar, it is proposed that there are no hydrophobic aggregates at the solid-liquid interface in this case. The long ethylene oxide chain is proposed to prevent aggregation between the hydrocarbon chains.

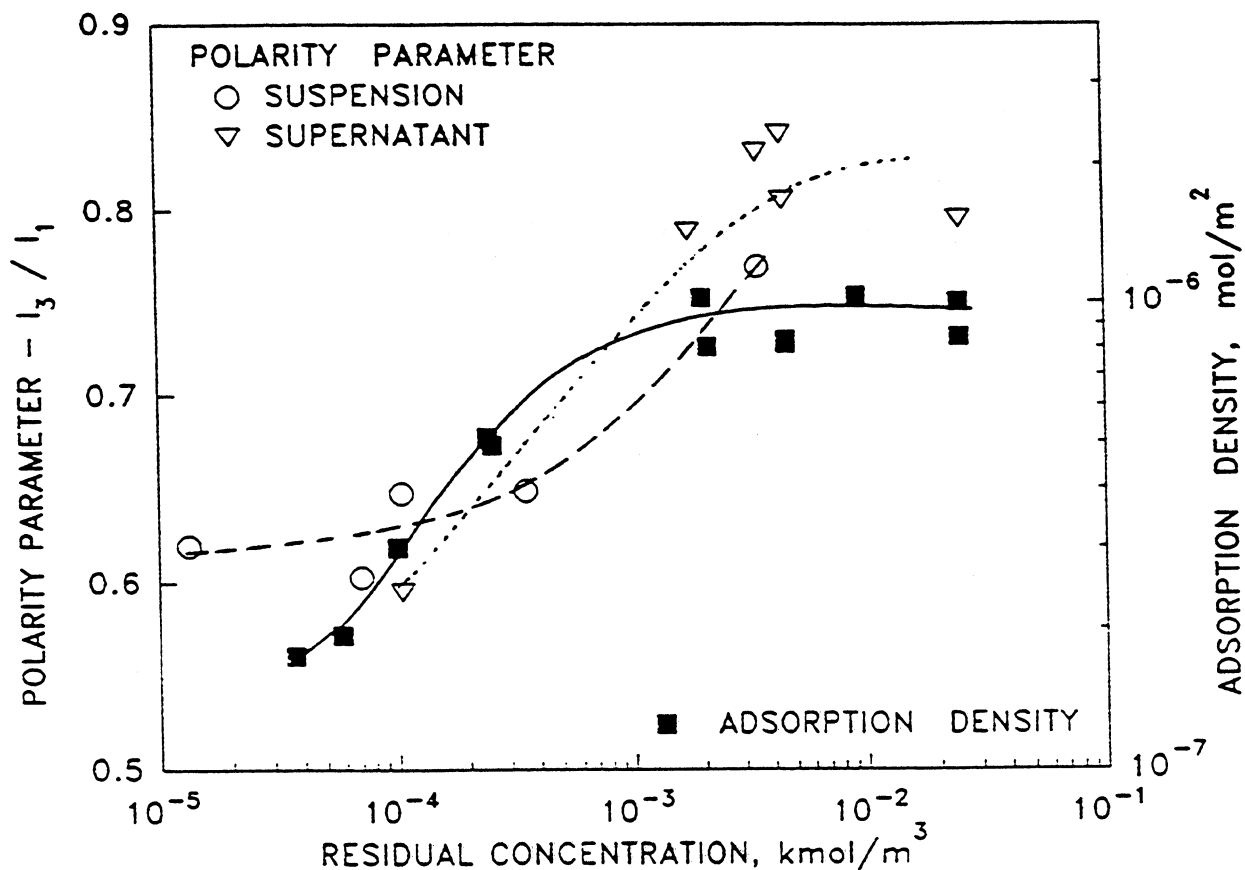


Figure 15 Adsorption of NP-40 on silica and characterization of the adsorbed layer using pyrene

Interfacial and solution behavior of anionic - nonionic surfactant mixtures

Mixtures of anionic and nonionic surfactants offer improved solution and interfacial properties as compared to those of the individual components. The interactions between two commonly used surfactants, anionic sodium dodecyl sulfate (SDS) and nonionic dodecyl phenoxy polyethoxylated alcohol with some polydispersity in the number of ethylene oxide groups (TRITON X-100) were studied using surface tension, and the interactions were modeled using regular mixing theory. Understanding the activity of the surfactants at the air-water interface will help to explain the differences in the behavior of the surfactants at the solid-liquid interface. The surface tension of mixtures of SDS and TRITON X-100 of varying compositions are shown in figure 16. The

measurements were made with a Wilhelmy Plate tensiometer using a sand-blasted platinum plate as the sensor. Upon the nonionic surfactant addition to SDS, the surface tension of the mixture is drastically reduced.

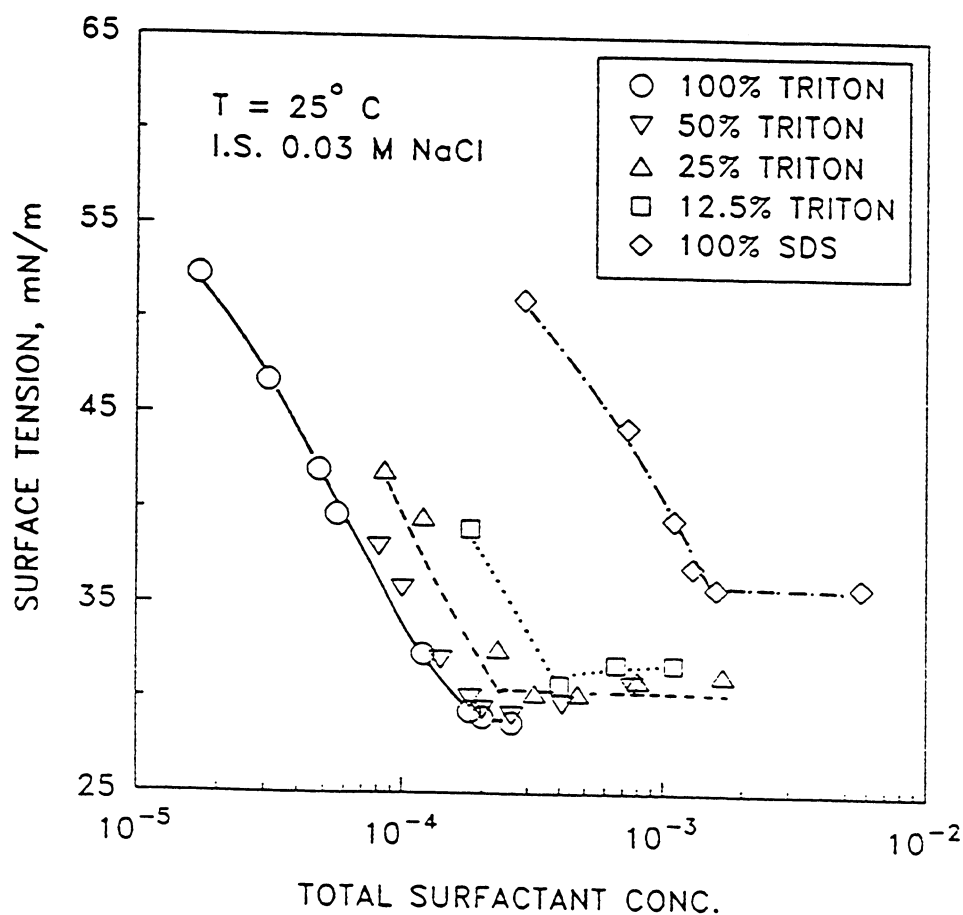


Figure 16 Surface tension of mixtures of sodium dodecyl sulfate (SDS) and polyethoxylated dodecyl phenol (TRITON)

Table III lists the results obtained for critical micellization concentration (CMC) at different mole fractions (α) of the nonionic surfactant, TRITON X-100.

Table III: Mixed CMC (C^*) at different mole fractions of dodecyl phenoxy polyethoxylated alcohol

α	0	0.125	0.25	0.50	1.00
C^* (kmol/m ³)	1.6×10^{-3}	4×10^{-4}	3.4×10^{-4}	2.0×10^{-4}	1.8×10^{-4}

Regular mixing theory is based on the assumption that the excess Gibbs free energy of mixing is given by:

$$\Delta G_{mix} = X_1 X_2 \beta R T \quad (1)$$

where X_1 and X_2 are the mole fractions of the two surfactants in the mixed micelle, β the interaction parameter, R the gas constant and T the temperature. Regular solution also assumes that the excess entropy and volume of mixing are zero and hence the excess enthalpy of mixing is given by:

$$\Delta H_{mix} = X_1 X_2 \beta R T \quad (2)$$

The interaction parameter β can be evaluated as an experimental parameter from CMC measurements and used to interpret subsequent experiments. If C_1 and C_2 are the CMC values of the pure surfactants and C^* that of the mixed system, the following relationships⁶ permits estimation of β in terms of C_1 , C_2 and C^* :

$$\frac{X_1^2 \ln \left(\frac{C^* \alpha}{C_1 X_1} \right)}{(1-X_1)^2 \ln \left[\frac{C^*(1-\alpha)}{C_2 (1-X_1)} \right]} = 1 \quad (3)$$

$$\beta = \frac{\ln \left(\frac{C \cdot \alpha}{C_1 X_1} \right)}{(1-X_1)^2} \quad (4)$$

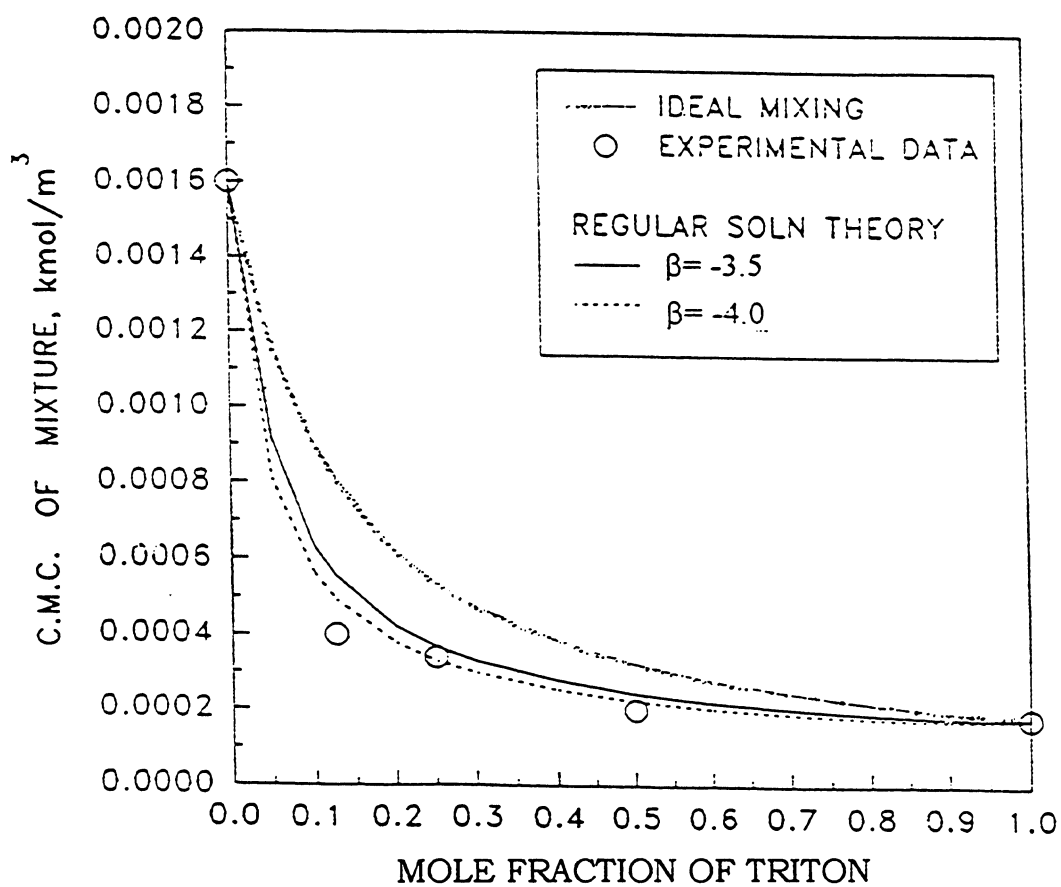


Figure 17 Correlation of CMC of a mixture of SDS and TRITON with mole fraction of TRITON

where X_1 is the mole fraction of surfactant 1 in the mixed micelle and α is the mole fraction of surfactant 1 in the total mixed solute. Equation (3) must be solved iteratively for X_1 , and substitution of this X_1 into equation (4) results in a solution for β . C_1 and C_2 in this case are 1.8×10^{-4} and 1.6×10^{-3} respectively and results obtained using the values of -3.5 and -4.0 for β , are shown in Table IV.

Experimental data and calculated results for CMC are plotted in figure 17. It can be seen that the experimental data show negative deviation from ideal mixing predictions. The effectiveness of regular solution theory can be seen from the fit using $\beta = -4.0$. The negative values of β result in CMC and monomer concentration values which are less than that predicted by the ideal solution theory. When the two surfactants with dissimilar polar heads form micelles, electrostatic repulsion between the SDS molecules is reduced by the presence of TRITON X-100 molecules.

Adsorption of surfactant mixtures at solid-liquid interfaces

The adsorption of ionic-nonionic surfactant mixtures at the kaolinite-water interface was systematically studied. The system studied was a 1:1 mixture of anionic sodium dodecyl sulfate (SDS) and nonionic octaethylene glycol mono-n-decyl ether ($C_{12}EO_8$). Isotherms obtained for the adsorption of the anionic sodium dodecyl sulfate (SDS) on kaolinite are shown in figure 18 (a). The adsorption of SDS decreases as the pH is increased from 5 to 10. Both positive and negative sites coexist on the kaolinite surface and the number of positive sites will decrease with increasing in pH. As a result it can be stated that the adsorption mechanism prevalent here is purely electrostatic. At pH 5, the saturation adsorption is $\approx 1.6 \times 10^{-6}$ mol/m²: using a cross-sectional area of 53 Å² for an SDS molecule, this translates into a surface coverage of roughly 56% which suggests that roughly

Table IV: Calculated results of X_1 and C^* by regular solution theory

α	$\alpha/(1-\alpha)$	$\beta = -3.5$		$\beta = -4.0$	
		X_1	$C^* (10^{-4})$	X_1	$C^* (10^{-4})$
0.05	0.053	0.538	9.16	0.538	8.09
0.10	0.111	0.605	6.31	0.597	5.60
0.125	0.143	0.628	5.56	0.617	4.94
0.20	0.25	0.677	4.22	0.662	3.78
0.25	0.333	0.701	3.69	0.685	3.32
0.30	0.428	0.722	3.31	0.705	2.99
0.40	0.67	0.759	2.78	0.739	2.53
0.50	1	0.791	2.44	0.769	2.24
0.60	1.5	0.821	2.2	0.799	2.04
0.80	4	0.886	1.9	0.863	1.8
0.90	9	0.928	1.82	0.908	1.76
0.95	19	0.957	1.8	0.941	1.76

half the surface is covered by positive sites.

As in the case for the adsorption of sodium dodecyl sulfate (SDS), $C_{12}EO_8$ adsorption on kaolinite decreases with an increase in pH (figure 18b). A hydrogen bonding mechanism has been proposed for the adsorption of ethylene oxide (EO) groups on oxide surfaces, and it can be expected that a similar effect predominates here. Reduced adsorption at higher pH values can be attributed to the deprotonation of the surface hydroxyl groups which will result in a decrease in the number of hydrogen bonding sites available for $C_{12}EO_8$ adsorption. Using a molecular cross-sectional area of 65 \AA^2 for $C_{12}EO_8$ in the adsorbed state, the surface coverage at saturation can be estimated to be 12%

at pH 5.

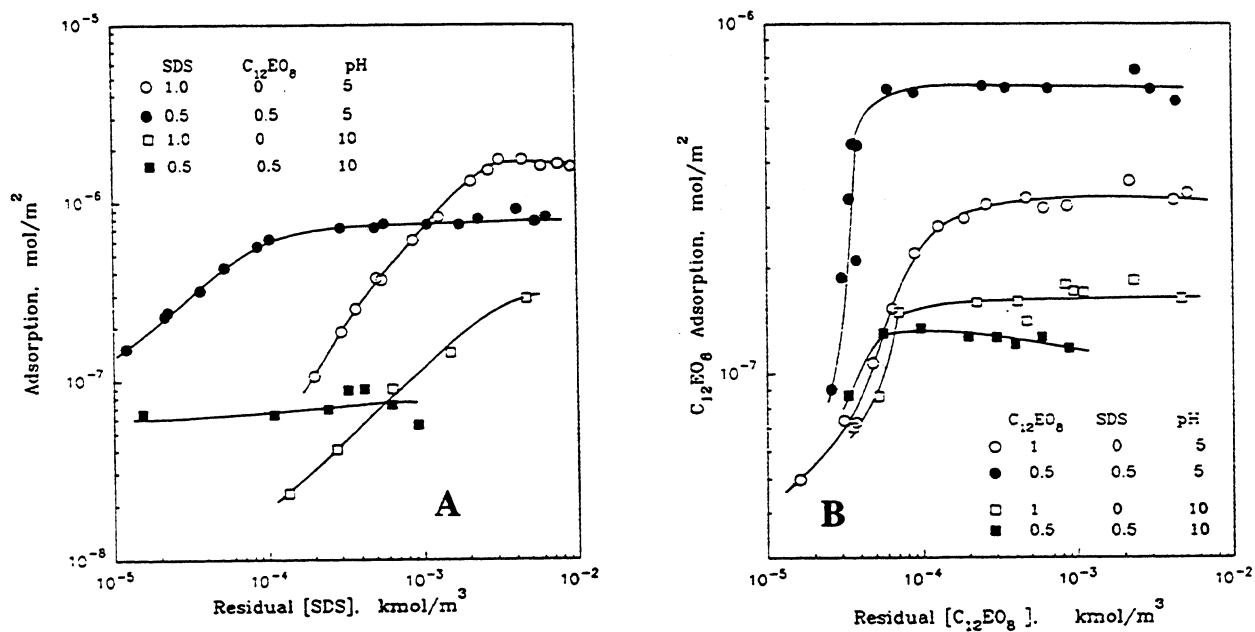


Figure 18 Effect of pH on the adsorption on kaolinite of (a) SDS and (b) C₁₂EO₈ from SDS/C₁₂EO₈

Unlike alumina which does not adsorb ethoxylated alcohols and silica which adsorbs ethoxylated alcohols but not sodium dodecyl sulfate (SDS), kaolinite adsorbs both SDS and C₁₂EO₈ in the same order of magnitude suggesting that the kaolinite surface exhibits the characteristics of both alumina and silica with respect to the adsorption of these two surfactants.

Adsorption of SDS/C₁₂EO₈ mixtures on kaolinite was also conducted at different pH values. The adsorption of sodium dodecyl sulfate (SDS) from the mixtures is shown in figure 18 (a) and that for octaethylene glycol mono-n-decyl ether (C₁₂EO₈) in figure 18 (b). At pH 5, the adsorption of the

nonionic $C_{12}EO_8$ is markedly enhanced by the presence of the anionic sodium dodecylsulfate (SDS) suggesting cooperative adsorption through hydrocarbon chain-chain interactions in the adsorbed layer. At pH 10, adsorption of the nonionic $C_{12}EO_8$ is suppressed by the presence of SDS, indicating competition between the anionic SDS and the nonionic $C_{12}EO_8$ for the limited number of common adsorption sites available.

The mechanisms of the pH effect on surfactant mixture adsorption are schematically presented in figure 19. While hydrocarbon chain-chain interaction between the adsorbed surfactant species is predominant at low pH it is not likely to be as significant at high pH because the adsorbed surfactant species cannot be close to each other due to lack of adjacent adsorption sites for both surfactant species. Instead competition from the anionic sodium dodecylsulfate (SDS) for limited common adsorption sites leads to the suppression of $C_{12}EO_8$ adsorption.

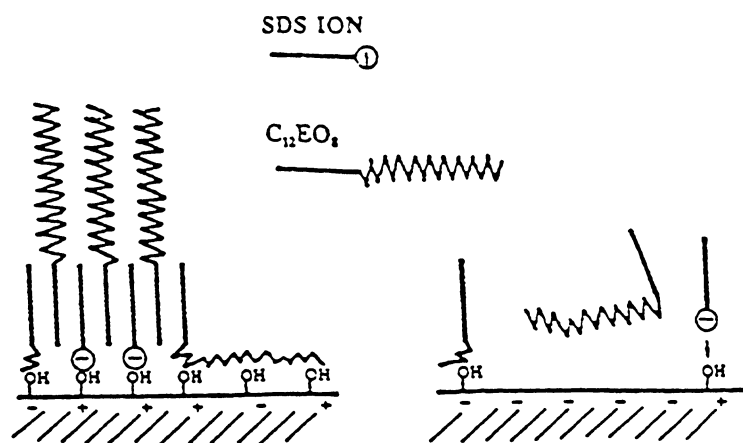


Figure 19 Schematic representation of pH effect on the adsorption of SDS/ $C_{12}EO_8$ mixtures on kaolinite

Effect of hydrocarbon chain length of nonionic surfactant on its adsorption

Figure 20 shows the isotherms for the adsorption of the nonionic surfactants C_nEO_8 with different hydrocarbon chain length ($n=10, 12, 14, 16$) on kaolinite.

The isotherms are consistently shifted to the lower concentration region as the hydrocarbon chain length is increased from C_{10} to C_{16} . It can be seen that the plateau adsorption tends to increase slightly with increase in hydrocarbon chain length. Using a parking area of 9.2 \AA^2 per $(-O-CH_2CH_2-)$ group based upon adsorption on silica, it can be calculated that the kaolinite surface is only partly covered by the nonionic surfactant. These data are given in Table V.

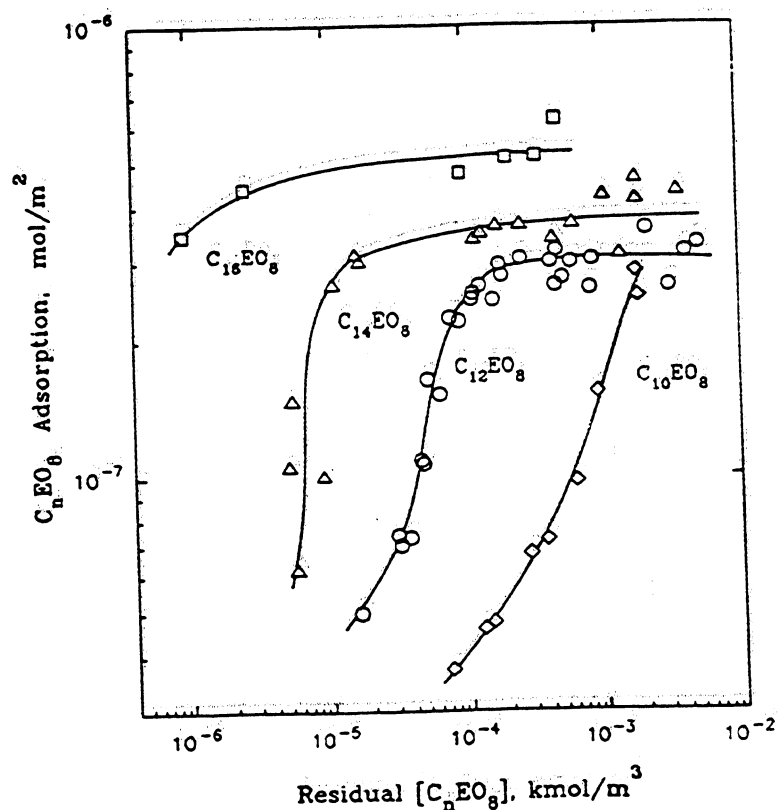


Figure 20 Effect of hydrocarbon chain length of nonionic surfactant on its adsorption on kaolinite

Table V: Surface coverage of kaolinite by nonionic surfactant (C_nEO_8)

Surfactant	Plateau Adsorption mol/m^2	Surface Coverage Θ
$C_{12}EO_8$	2.5×10^{-7}	0.11
$C_{14}EO_8$	3.1×10^{-7}	0.14
$C_{16}EO_8$	4.4×10^{-7}	0.19

Sodium dodecyl sulfate (SDS)/Octaethyleneglycol mono-n-alkyl ether (C_nEO_8) mixture adsorption

The adsorption of 1:1 mixtures of sodium dodecyl sulfate (SDS) and octaethylene glycol mono n-alkyl ether (C_nEO_8) mixtures at the kaolinite-water interface was studied in detail and the results are given in figure 21. It is noted that the isotherms for the adsorption of SDS are identical

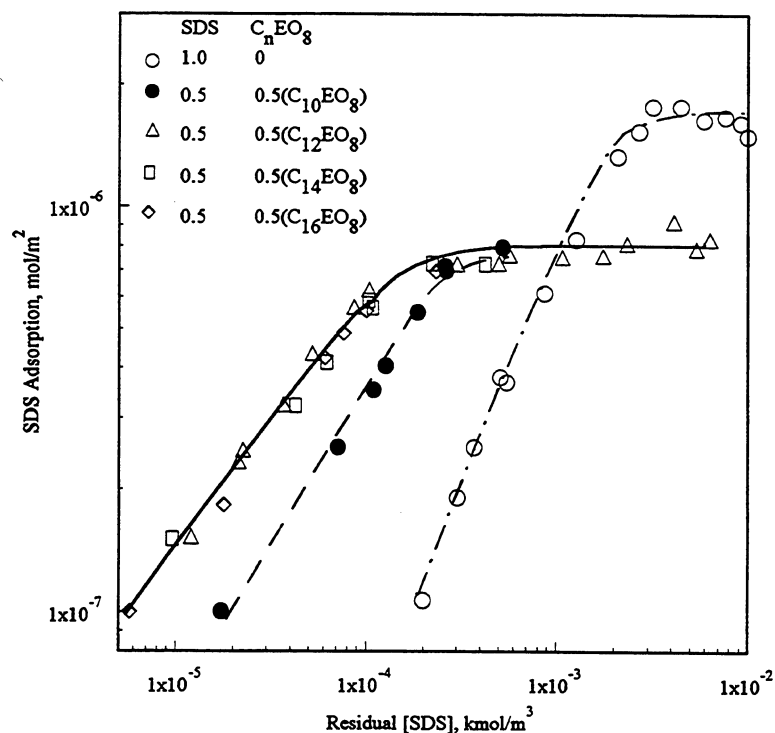


Figure 21 Effect of nonionic surfactant hydrocarbon chain length on the adsorption of sodium dodecyl sulfate (SDS) on kaolinite from 1:1 SDS/ C_nEO_8 mixtures. 0.03 M NaCl, pH 5.

to each other when the hydrocarbon chain length of the nonionic surfactants, octaethylene glycol mono n-alkyl ethers ($C_{12}EO_8$, $C_{14}EO_8$, $C_{16}EO_8$), is equal to or longer than that of the anionic SDS (C_{12}), but markedly different from that of the isotherm in the absence of the C_nEO_8 . When the hydrocarbon chain length of the nonionic surfactant is shorter ($C_{10}EO_8$) than that of the anionic SDS, however, a different isotherm is obtained.

The role of chain length of the nonionic surfactants on kaolinite is illustrated in figure 22.

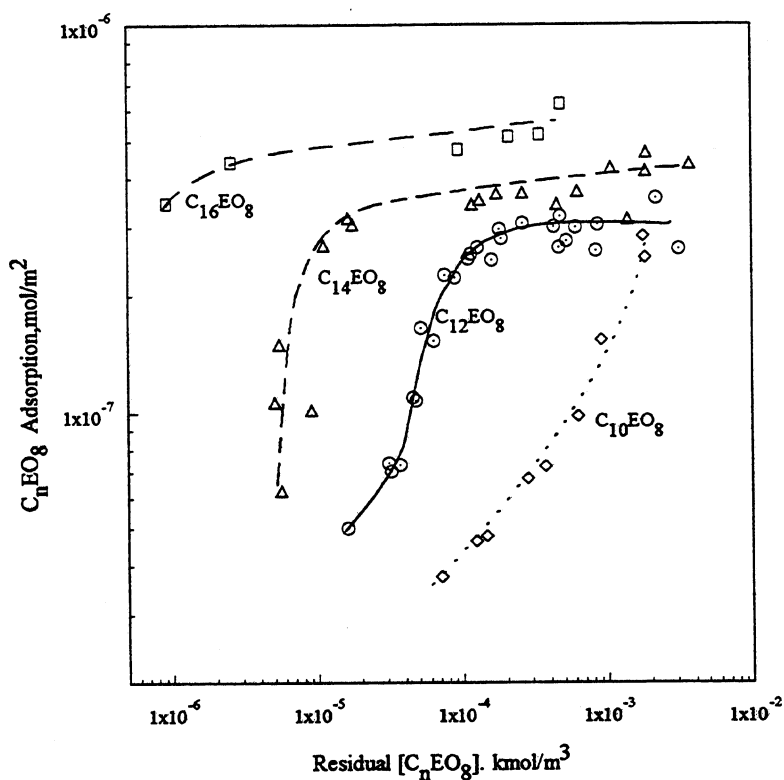


Figure 22 Effect of hydrocarbon chain length (C_nEO_8) on the adsorption of nonionic surfactant on kaolinite. 0.03 M NaCl, pH 5.

It is clear that the chain length has drastic effect on the adsorption. The presence of the anionic SDS enhances the adsorption of the nonionic C_nEO_8 (figure 23) and the isotherms are shifted to lower concentration region as compared to the adsorption isotherms of C_nEO_8 in the absence of any SDS.

These results show that the hydrophobic interaction between the coadsorbing surfactants is very strong and a schematic description of the interactions is provided in figure 24.

When the hydrocarbon chain length of the nonionic surfactant is equal to or longer than that of the anionic SDS, the hydrocarbon chains of SDS are equally shielded from the hydrophilic environment by the hydrophobic chains of the coadsorbing nonionic surfactant. The identical residing environment then leads to a common SDS adsorption isotherm (figure 21). When the hydrocarbon chain of the nonionic surfactant is shorter than that of the anionic sodium dodecyl sulfate (SDS), part of the SDS hydrocarbon chain is exposed to the hydrophilic environment (aqueous solution of the hydrophilic ethylene oxide chain of the nonionic surfactant). The environment for SDS hydrocarbon chain is then less hydrophobic and therefore the isotherm is

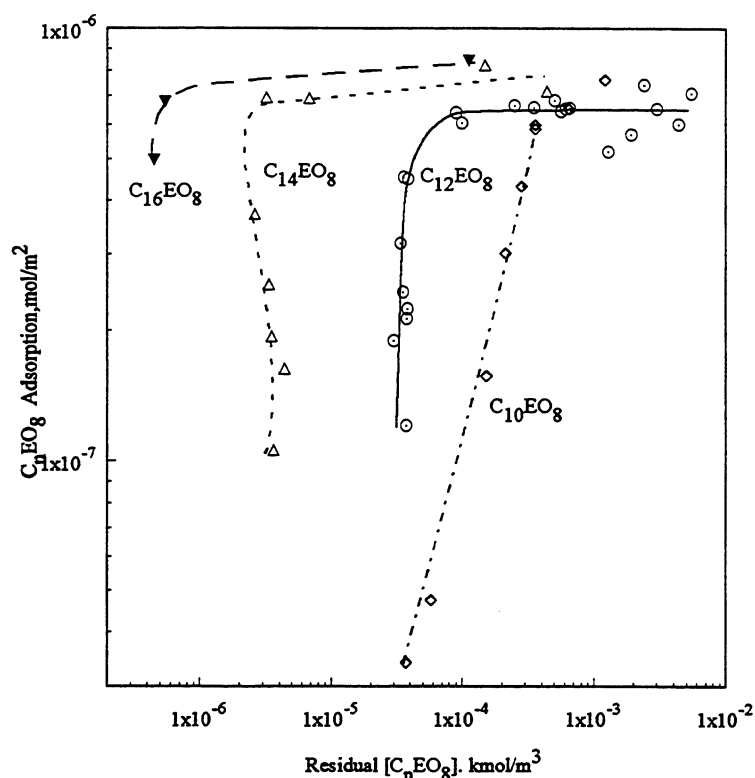


Figure 23 Effect of nonionic surfactant hydrocarbon chain length on the adsorption of C_nEO_8 ($n=10,12,14,16$) on kaolinite from its 1:1 mixtures with SDS. 0.03 M NaCl, pH 5

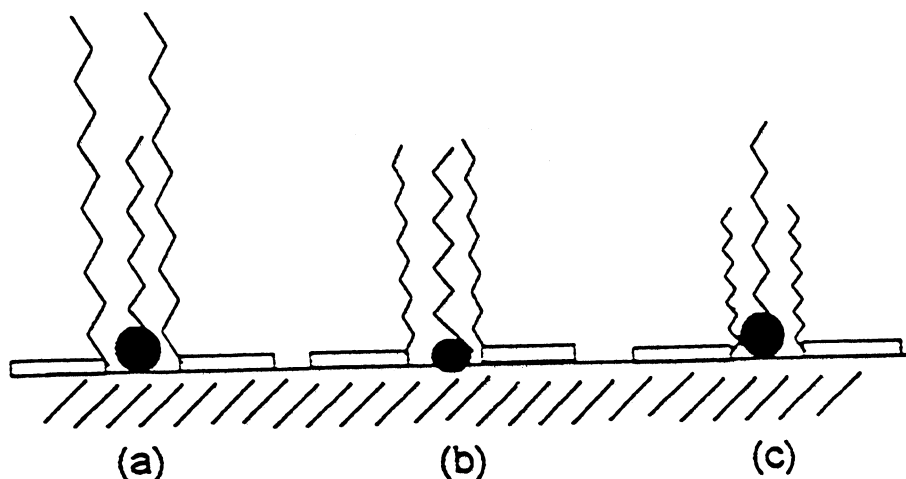


Figure 24 **Schematic representation of the effect of nonionic surfactant hydrocarbon chain length on the adsorption of the anionic surfactant SDS when the nonionic surfactant hydrocarbon chain is (a) longer than SDS, (b) equal to SDS and (c) shorter than SDS.**

shifted less to the lower concentration region than in the former case.

This modification in adsorption characteristics of both surfactants should have a direct impact on the size of the surfactant aggregates bound at the solid-liquid interface and the related interfacial properties. The size of the bound aggregate was determined using fluorescence spectroscopy.

Fluorescence probing of mixed-surfactant adsorbed layers

Fluorescence probing of the adsorbed layer was performed for alumina and surfactant system. Fluorescence spectroscopy could not be conducted at the kaolinite-water interface since kaolinite quenched the fluorescence signal from pyrene. The I_3/I_1 values of pyrene obtained for the mixed adsorbed layers of sodium dodecyl sulfate (SDS) and octaethylene glycol mono-n-decyl ether ($C_{12}EO_8$) on alumina are given in figure 25 along the isotherms.

Table VI: Polarity parameter (I_3/I_1) values for surfactant micelles in aqueous solution

Surfactant	Concentration studied (kmol/m ³)	C.M.C. (kmol/m ³)	I_3/I_1
SDS	3×10^{-2}	1.5×10^{-3}	0.88
C ₁₂ EO ₈	1.0×10^{-3}	1.0×10^{-4}	0.80
1:1 SDS/C ₁₂ EO ₈	2.6×10^{-3}	1.1×10^{-4}	0.85

However, the values obtained for the mixed micelle of SDS and C₁₂EO₈ is close to that obtained for the adsorbed layer at the alumina-water interface suggesting that the presence of the ethoxyl chains of the nonionic C₁₂EO₈ could be a key factor in determining the polarity in mixed surfactant aggregates.

As we mentioned earlier, fluorescence spectroscopy could not be conducted at the kaolinite-water interface since kaolinite quenched the fluorescence signal from pyrene. Fluorescence probing of the adsorbed layer was hence performed for adsorption on alumina assuming that the interactions between the surfactants at a different interfaces would be altered slightly but the trend would be the same. In addition, alumina is a constituent of kaolinite.

In prior studies, pyrene monomer fluorescence was used to determine the micropolarity of the adsorbed layer. In addition to the monomer fluorescence, another aspect of pyrene fluorescence, viz. excimer formation, was exploited to determine the size of surfactant aggregates (micelles, hemimicelles, etc). An excimer is formed when a pyrene molecule in its excited state (P^*) interacts with a pyrene molecule in its ground state (P) according to the reaction:



The excimer formed $(PP)^*$ decays to the ground state by emitting a photon:



In the presence of pyrene molecules in a fragmented media (such as when surfactant micelles, hemi-micelles, etc. are present) the decay of pyrene fluorescence can be fitted to the following model⁷ based upon a Poisson distribution of probes in surfactant (or hydrophobic) aggregates:

$$I_t = I_0 \exp \left[-k_o \cdot t + n \left(\exp \{-k_e \cdot t\} - 1 \right) \right] \quad (7)$$

where I_0 is the fluorescence emission intensity at the desired wavelength at time $t=0$, k_o the monomer decay rate constant, k_e the excimer formation rate constant, and n the average number of pyrene molecules in a surfactant aggregate. At long times, there is no excimer formation and the fluorescence decay profiles represent decay due to monomeric emission. Therefore equation 7 reduces to:

$$\ln \left(\frac{I_t}{I_0} \right) = -n - k_o \cdot t \quad (8)$$

and extrapolation to $t=0$ gives n . With a knowledge of n , the aggregation number of the hydrophobic aggregate in which the pyrene molecules reside can be calculated from the following:

$$\begin{aligned} N_{\text{agg}} &= \frac{n \cdot [C_i - \text{CMC}]}{[\text{Py}]} && \text{for micelles} \\ &= \frac{n \cdot [C_i - C_r]}{[\text{Py}]} && \text{for adsorbed layer} \end{aligned} \quad (9)$$

where C_i is the initial total surfactant concentration, CMC the critical micelle concentration, $[\text{Py}]$ the

pyrene concentration and C_r , the total residual surfactant concentration.

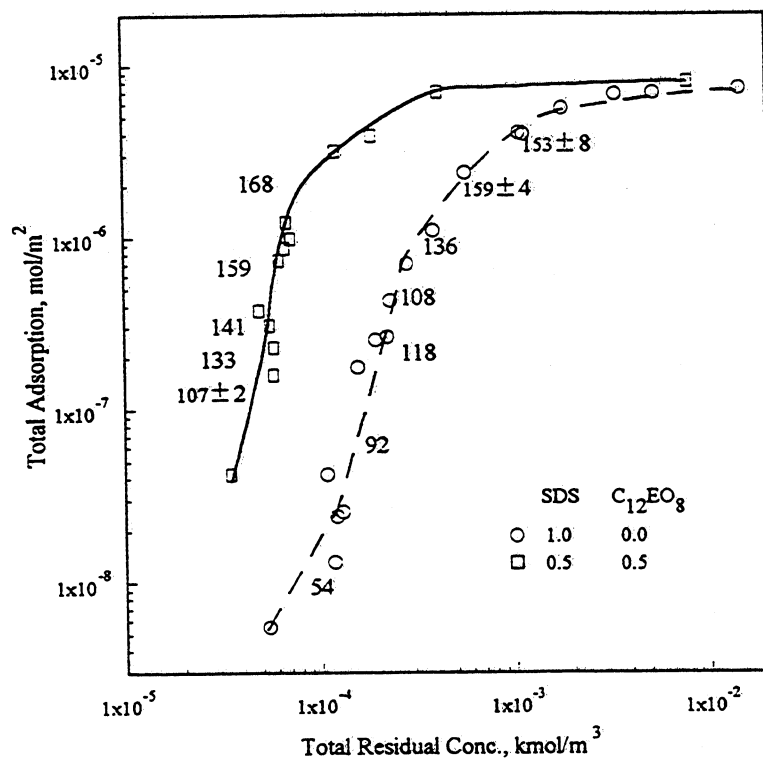


Figure 26 Total adsorption of sodium dodecyl sulfate (SDS) and 1:1 SDS/ $C_{12}EO_8$ mixtures on alumina and aggregation numbers of surfactant.

Using this procedure the aggregation number of a 1:1 SDS/ $C_{12}EO_8$ mixed adsorbed layer was determined and the numbers obtained are given in figure 26 along the adsorption isotherms. It is seen that for SDS adsorption, the aggregation number initially increases and then remains relatively constant. Most importantly, the aggregation number for the adsorption of a 1:1 SDS/ $C_{12}EO_8$ mixture is larger than that for pure SDS adsorption at a similar adsorption density. It is also seen from Table VII that the aggregation number for a 1:1 SDS/ $C_{12}EO_8$ micelle is larger than that of SDS micelles.

Table VII Aggregation number (N_{agg}) of Surfactant micelles, 0.03 M NaCl, 25°C

SURFACTANT	CONC. (kmol/m ³)	k_o ns ⁻¹	k_c ns ⁻¹	n	N_{agg}
Sodium dodecyl sulfate (SDS)	8.0×10^{-2}	0.0064	0.024	0.88	91
Octaethylene glycol mono n-decyl ether (C ₁₂ EO ₈)	2×10^{-3}	0.0059	0.015	0.53	109±9
1:1 SDS/C ₁₂ EO ₈	8.6×10^{-3}	0.0066	0.012	0.84	165±3

Clearly, the aggregates of the mixed surfactants are larger than the aggregates of the single components, and this is proposed to be due to a reduction in the electrostatic repulsion between sodium dodecyl sulfate (SDS) ions due to the presence of the nonionic C₁₂EO₈ for 1:1 SDS/C₁₂EO₈ mixtures in the adsorbed layer or in micelles. As a result of the screening of the electrostatic repulsion, the adsorption of sodium dodecyl sulfate (SDS) should be energetically enhanced. This is indeed seen in figure 27.

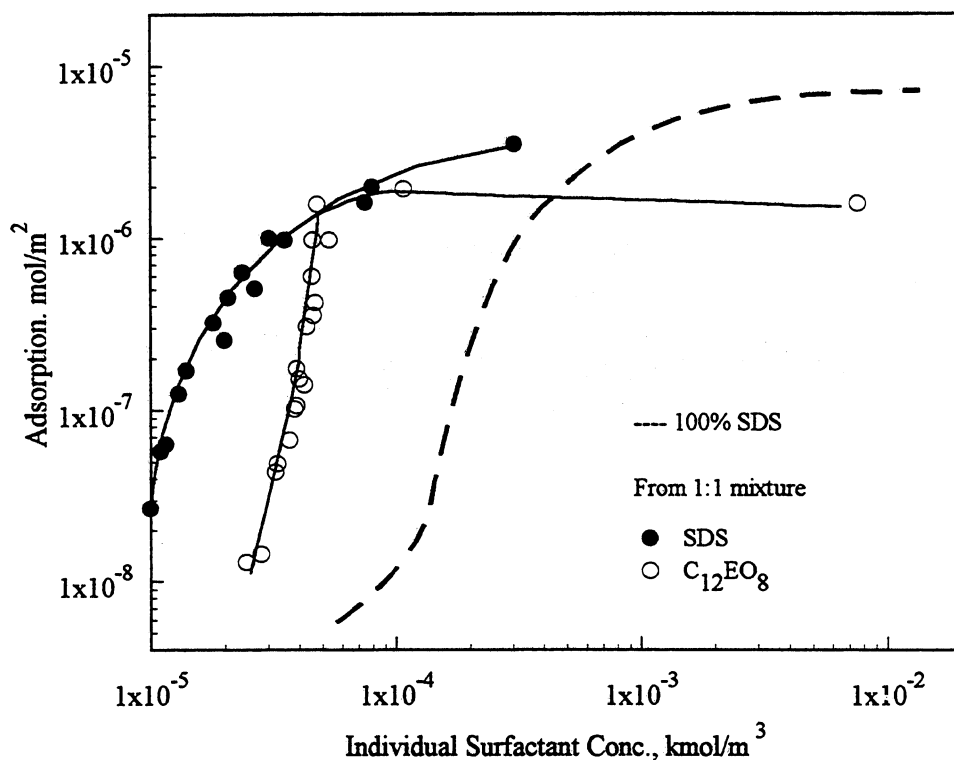


Figure 27 Isotherms for individual surfactant adsorption on alumina from 1:1 SDS/ $C_{12}EO_8$ mixtures.

Since the mixed aggregates consist of both the anionic sodium dodecyl sulfate (SDS) and the nonionic octaethylene glycol mono n-decyl ether ($C_{12}EO_8$), it is useful to determine the aggregation number of each surfactant in the mixed aggregates. This can be done by knowing the adsorption density of each component in the mixed adsorbed layer. It is seen from Table VIII that at low adsorption densities, the aggregation number of the nonionic octaethylene glycol mono n-decyl ether ($C_{12}EO_8$) species is lower than that of the anionic SDS. As the adsorption increases, however, the hydrophobic chain-chain interaction becomes more important and the aggregation number of each surfactant becomes similar to each other.

Table VIII Surfactant aggregation number (N_{agg}) for the adsorption of 1:1 SDS/ $C_{12}EO_8$ mixture on alumina: 0.03 M NaCl, pH 6.5, 25°C

ADS. (kmol/m ³)	SURF./PY	k_o	k_c ns ⁻¹	n ns ⁻¹	SDS	N_{agg} $C_{12}EO_8$	TOTAL
1.1×10^{-7}	157	0.015	0.18	0.68	61	46	107
2.3×10^{-7}	173	0.013	0.055	0.77	72	61	133
3.2×10^{-7}	179	0.01	0.015	0.79	74	67	141
6.2×10^{-7}	187	0.0079	0.011	1.60	82	77	158
1.9×10^{-6}	194	0.0071	0.0055	0.86	85	83	168

It is to be noted that the aggregation number for SDS in the mixed adsorbed layer is lower than that for pure sodium dodecyl sulfate (SDS) adsorption. This is proposed to be due to surface heterogeneity. Since the surface consists of energetic patches⁸ for SDS adsorption and since the nonionic $C_{12}EO_8$ does not adsorb on alumina by itself, the aggregate size should be largely limited by the finite size of the energetic patches for SDS adsorption. In the case of 1:1 SDS/ $C_{12}EO_8$ adsorption, part of the SDS ions will be displaced by the nonionic $C_{12}EO_8$ in order to co-adsorb and as a result the aggregation number of SDS is decreased.

Adsorption/Desorption of cationic surfactant at the alumina-water interface

The adsorption/desorption behavior of a cationic surfactant (tetradecyltrimethylammonium chloride - TTAC) at the alumina water surface was studied in the presence and absence of a cosurfactant, nonionic pentadecylethoxylatednonylphenol (NP-15). Adsorption behavior was correlated with changes in interfacial properties such as zeta potential and stability. The microstructure of the adsorbed layers was probed using fluorescence spectroscopy.

The adsorption isotherm of TTAC on alumina at pH 10 is shown in figure 28. At this pH the alumina surface is negatively charged and the electrostatic attraction with the cationic TTAC will be dominant. There is a sharp increase in the adsorption density at around $5 \times 10^{-4} \text{ kmol/m}^3$ which is attributed to the formation of surfactant aggregates (hemimicelles) at the solid-liquid interface.

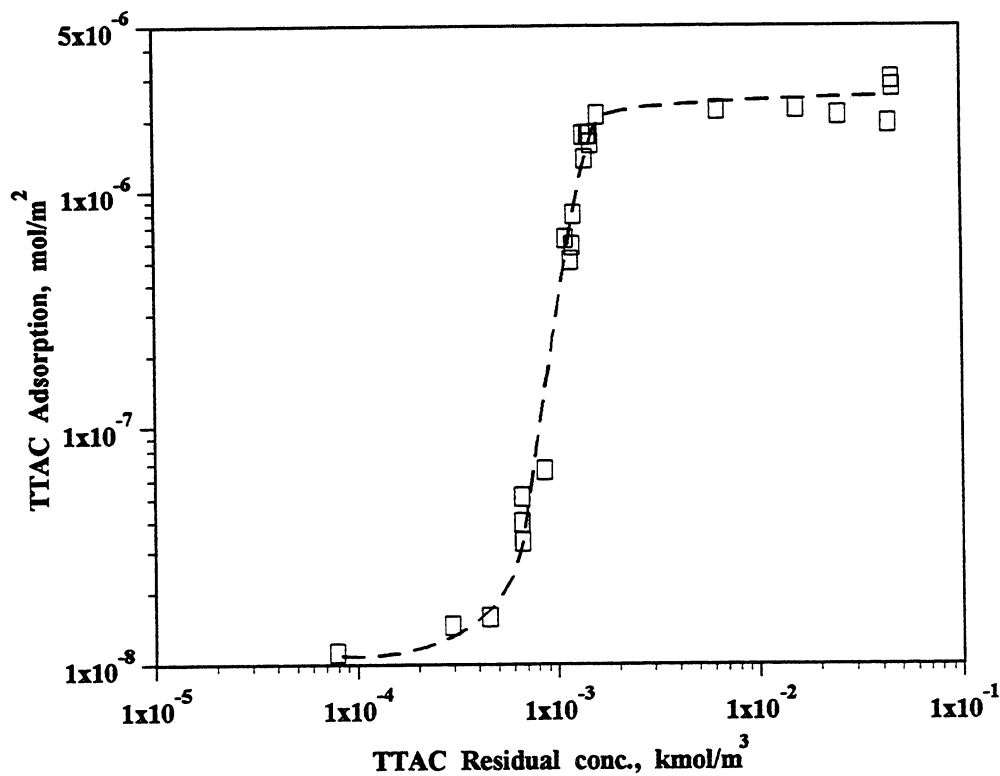


Figure 28. Adsorption isotherm of tetradecyl trimethylammonium chloride (TTAC) on alumina at pH 10.

The maximum adsorption density of tetradecyltrimethylammonium chloride (TTAC) on alumina at pH 10 is about $2.5 \times 10^{-6} \text{ mol/m}^2$. This translates to roughly $66 \text{ \AA}^2/\text{molecule}$ which is similar to the reported molecular area at the air/solution interface (61 \AA^2)⁹. Comparing the zeta potential to the adsorption at the same residual concentrations, it can be seen that the charge of alumina is neutralized at a very low adsorption density of TTAC (figure 29). The fact that adsorption of the cationic tetradecyltrimethylammonium chloride (TTAC) continues to take place leading to monolayer coverage even after the particles have become similarly charged suggests the predominating role of hydrophobic interactions between the hydrocarbon tails in causing the adsorption.

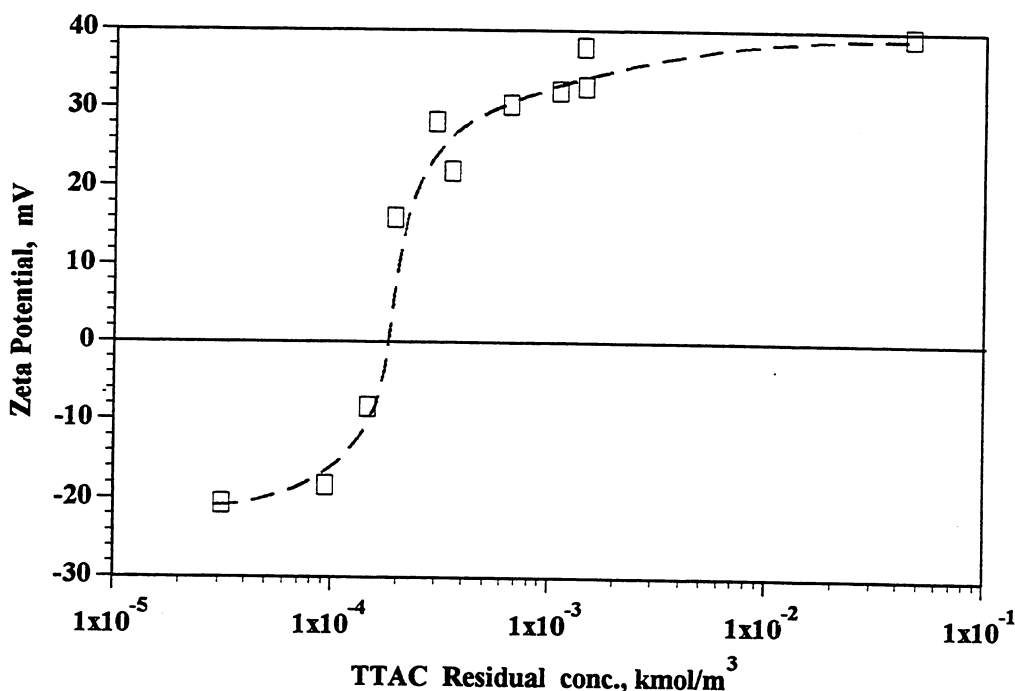


Figure 29 Zeta potential of alumina after adsorption of tetradecyl trimethyl ammonium chloride (TTAC) at pH 10.

The settling rate of the alumina suspensions after TTAC adsorption at pH 10 was measured and the results obtained are shown in figure 30. In the absence of and at low surfactant adsorption densities, the alumina suspension in water is dispersed and the settling rate is low. Once the surfactant

forms aggregates at the interface, the alumina surface becomes hydrophobic and the settling rate is markedly increased which upon correlation with figures 28 and 29 can be attributed to hydrophobic bridging between particles¹⁰.

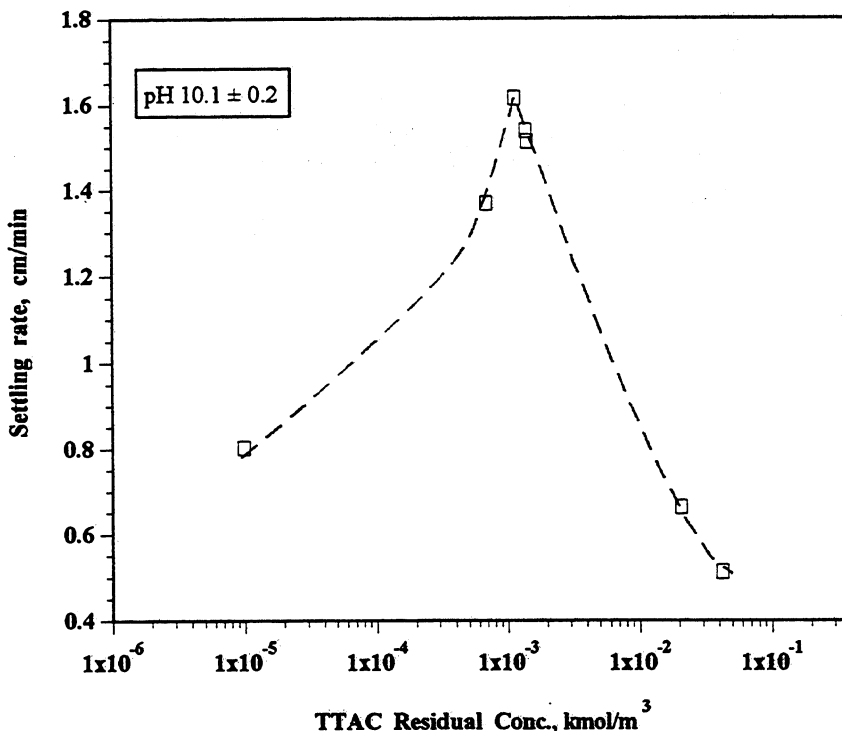


Figure 30 Settling rate of alumina suspensions after tetradecyl trimethyl ammonium chloride (TTAC) adsorption at pH 10.

With further increase in the TTAC adsorption, the settling rate decreases; this can be attributed to the increase of the positive charge of alumina at higher surfactant concentration (figure 29) causing repulsion between the alumina particles. As a result of the balance between the hydrophobic bridging force and the electrical repulsion force, the settling rate reaches a maximum at a concentration of about $1 \times 10^{-3} \text{ kmol/m}^3$. At higher concentrations the electrostatic forces dominates in this system and the settling rate decreases.

Changes in the microstructure of the adsorbed layer were probed using fluorescence

spectroscopy. The adsorption isotherm of TTAC on alumina is plotted in figure 31 along with changes in the polarity parameter of pyrene at the alumina-water interface and in the supernatant. It is observed that pyrene goes to the alumina-water interface in a narrow TTAC concentration range which corresponds to the sharp increase in adsorption isotherm. From this it is evident that pyrene is solubilized in TTAC aggregates at the alumina-water interface. However once TTAC micelles form in the supernatant, pyrene is preferentially solubilized into the micelles and does not go to the alumina-water interface in spite of the presence of TTAC hemimicelles. This result is interesting considering that in the alumina-SDS system, pyrene is preferentially solubilized in hemimicelles at the alumina-water interface rather than SDS micelles in the supernatant¹¹. It is proposed that aggregates of TTAC at the alumina-water interface are not as tightly packed. The solubilizing power of the TTAC hemimicelles at the alumina-water interface is not very high. The removal of the surfactant from the solid-liquid interface, a process of important consequence in enhanced oil recovery, depends upon the packing of the surfactant in the aggregates and on the strength of interaction between the surfactant and the solid. The role of the latter was investigated by diluting the suspensions and studying the desorption.

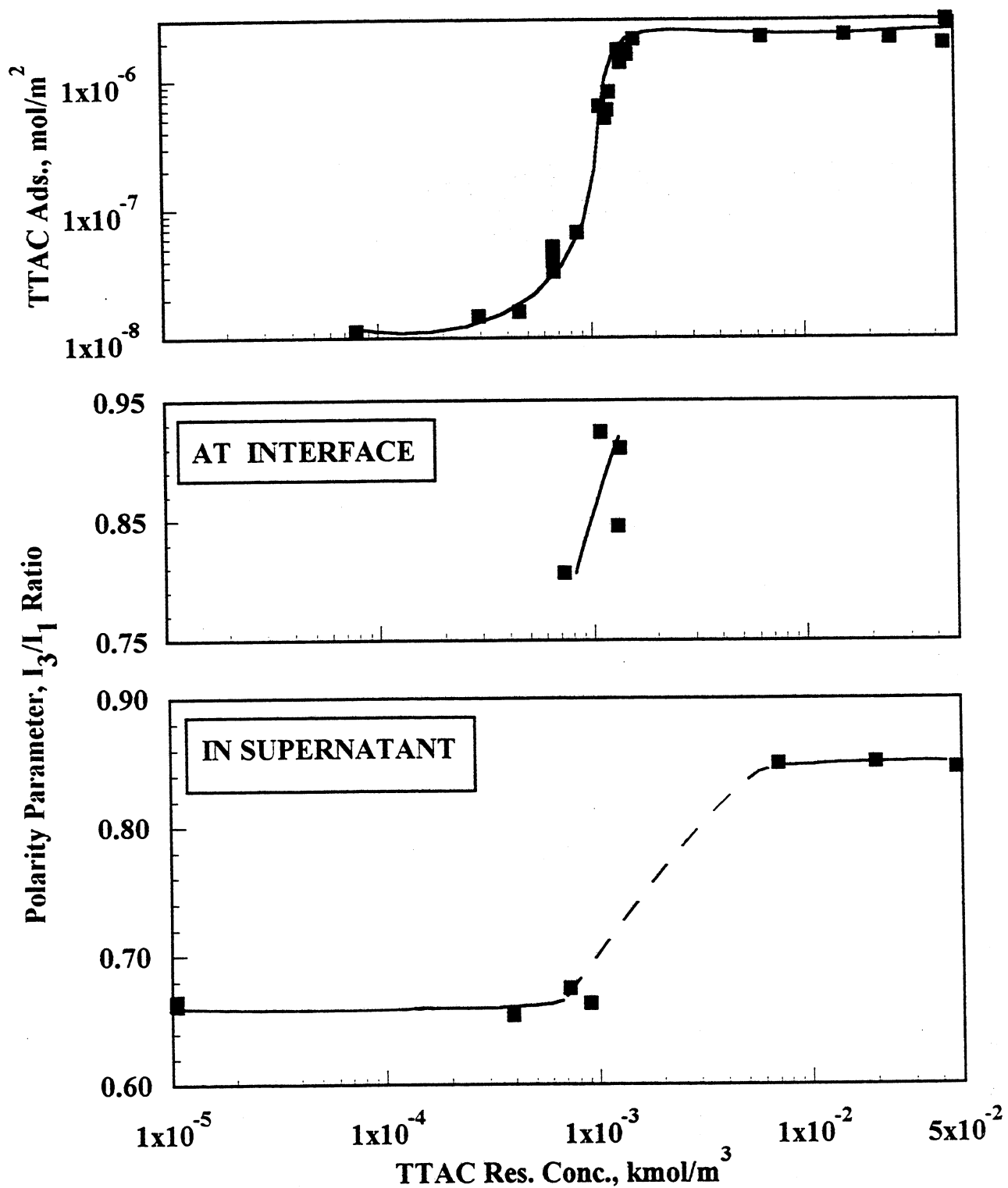


Figure 31 Adsorption isotherm of tetradecyl trimethylammonium chloride (TTAC) on alumina and corresponding changes in pyrene monomer fluorescence from the alumina water interface and the supernatant.

Desorption of cationic surfactant from alumina-water interface

The adsorption isotherm of tetradecyltrimethylammonium chloride on alumina was determined first and then supernatant solutions of different residual concentrations (C_r) along the isotherm were diluted with 0.03 kmol/m^3 sodium chloride solution and the slurry mixed for 15 hours. This procedure was repeated several times depending upon the concentration, and the material balance was monitored during the dilution. The results obtained are shown in figure 32. The solid line represents the initial adsorption isotherm. It is observed that adsorption is reversible in most cases, but interestingly it is irreversible in the low concentration range where significant changes in wettability normally occur. In low concentrations, there is some hysteresis with measurable differences in adsorption and desorption amounts.

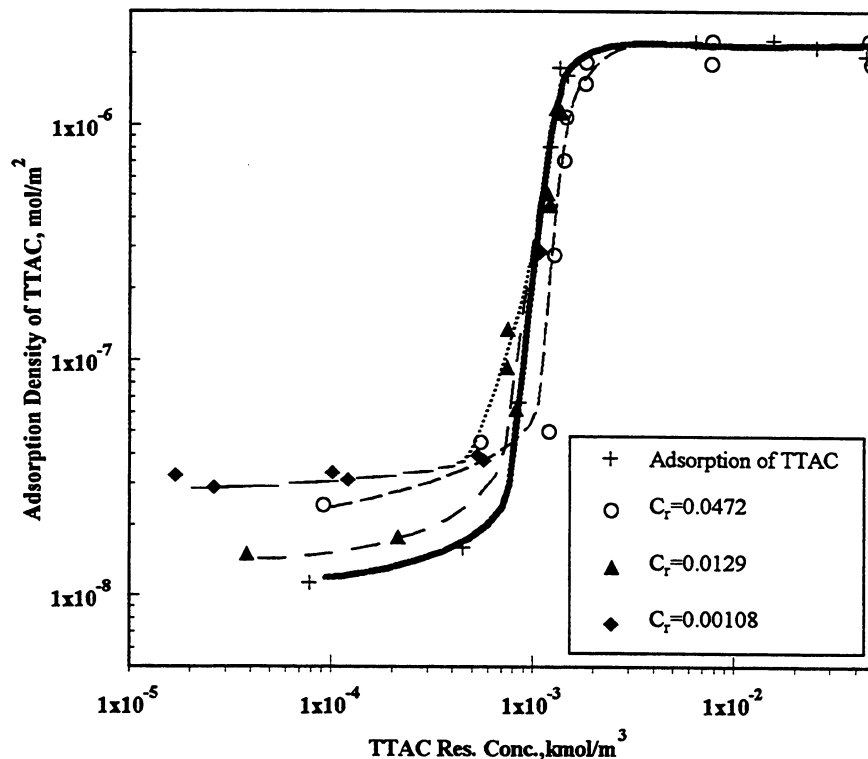


Figure 32 Desorption of TTAC from alumina upon dilution from different residual concentrations (C_r).

Fluorescence spectroscopy was used to probe changes in aggregation of surfactants at the solid-liquid interface upon dilution. Supernatant solutions of different residual concentrations along the isotherm were diluted with pyrene solutions at the desired ionic strength and the slurry conditioned for 15 h. The procedure was repeated several times. Pyrene emission spectra from the alumina-water interface were then obtained to gain an insight into the microstructural changes of the adsorbed layer upon dilution. The results are plotted in figure 33 along with the polarity parameter for pyrene dissolved in TTAC solutions of similar concentrations. Pyrene reports the presence of hydrophobic aggregates at the alumina-water interface. The value of the I_3/I_1 ratio decreases with decreases in concentrations but it is to be noted that hydrophobic aggregates are detected at concentrations lower than those at which they were first detected during adsorption (see figure 31). It should be mentioned that there will be some contribution to the spectrum by pyrene in the supernatant since a slurry was used in the sample cell. However for the residual concentrations discussed there will be no aggregates in solution as it is clear from the results in figure 33. Aggregates form in solution only above a concentration of 1.5×10^{-3} kmol/m³. Thus the hydrophobic environment reported by pyrene must be from the interface.

The results obtained so far show that tetradecyltrimethylammonium chloride adsorbs strongly on alumina at pH 10, and dilution causes a rearrangement in the aggregate state at the alumina-water interface. Changes in this behavior in the presence of a cosurfactant were studied next using a mixture of a cationic surfactant and a nonionic surfactant.

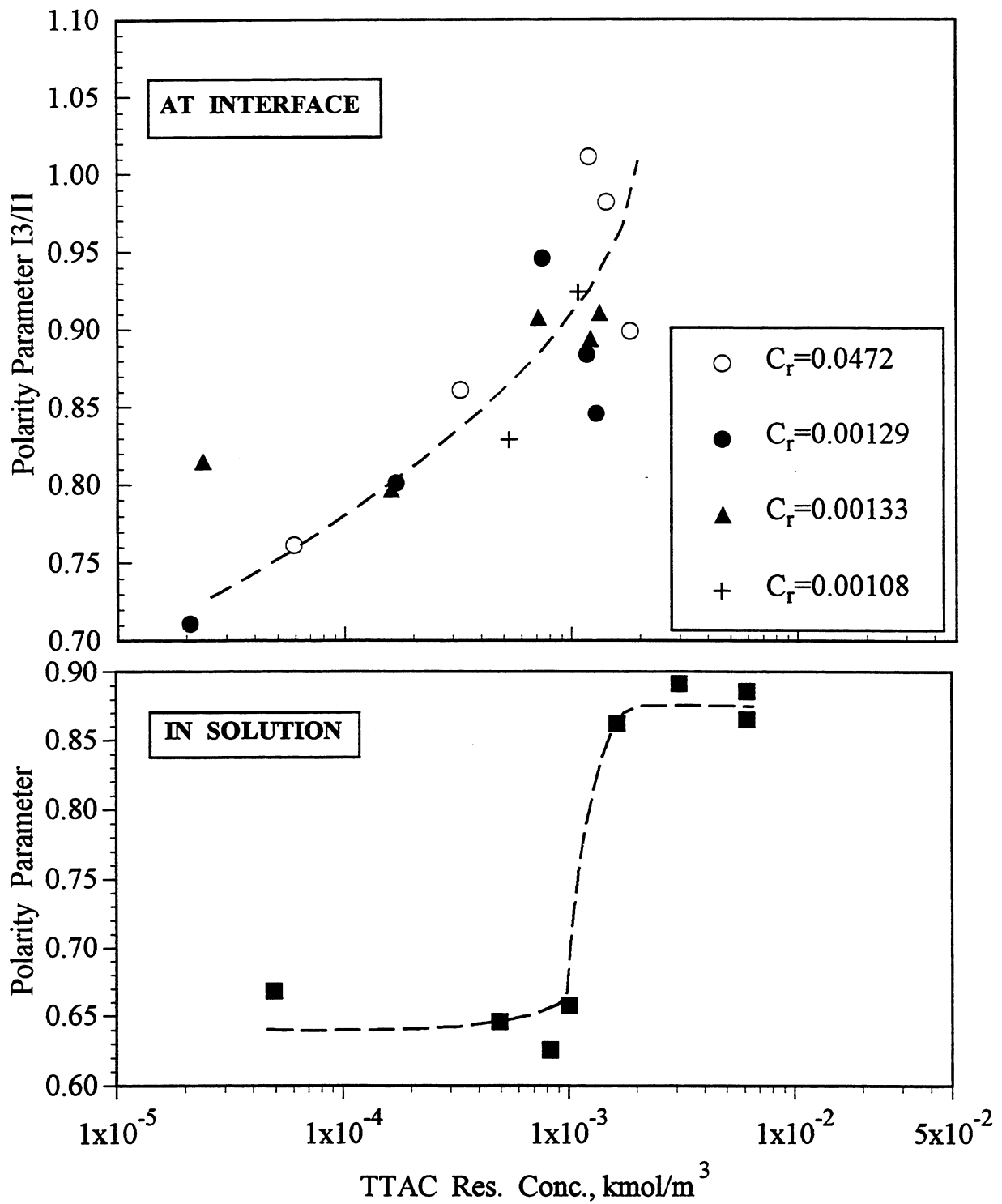


Figure 33 Changes in pyrene polarity parameter from the TTAC adsorbed layer on alumina upon dilution from different residual concentrations and also in bulk solution.

Adsorption of cationic-nonionic surfactant mixtures

Adsorption of tetradecyltrimethylammonium chloride and pentadecylethoxylated nonyl phenol surfactant mixtures at the alumina-water interface was studied as a function of relevant variables. The experiments showed NP-15 not to adsorb by itself on alumina. In a study on the adsorption of polyethoxylated monolaurate and polyethoxyl lauryl ether on titania, Fukushima and Kumagai¹² concluded that for adsorption on polar surfaces it is necessary that the nonionic surfactant have a radical which has sufficient adsorption force to overcome the strong interaction between water and the ethylene oxide groups. This observation is similar to our results on the adsorption of polyethylene oxide (PEO) on different minerals⁴. In this work we found PEO to adsorb on silica but not on alumina or hematite. It was proposed that for PEO to adsorb on oxide surfaces, the polymer has to displace enough water molecules bonded to the solid surface and create a strong entropic effect. In the case of the strongly hydrated alumina surface the polymer cannot displace sufficient water molecules necessary for adsorption of polymer. We propose similar reasons for the fact that NP-15 does not adsorb at the alumina-water interface.

Figure 34 shows the adsorption isotherms of NP-15 on alumina in the presence of pre-adsorbed TTAC and when added together with TTAC. In all these experiments the initial concentration of TTAC was fixed, and the pH was maintained at 10.

It is to be noted that tetradecyltrimethylammonium chloride does cause the adsorption of NP-15 on alumina. Pre-adsorbed TTAC functions as anchors for the adsorption of NP-15. With an increase in TTAC addition, the adsorption of NP-15 increased with the adsorption isotherms shifting to lower NP-15 concentrations. It is also observed that above the TTAC concentration at which it

forms hemimicelles at the alumina-water interface, there is no further effect on the adsorption of NP-15.

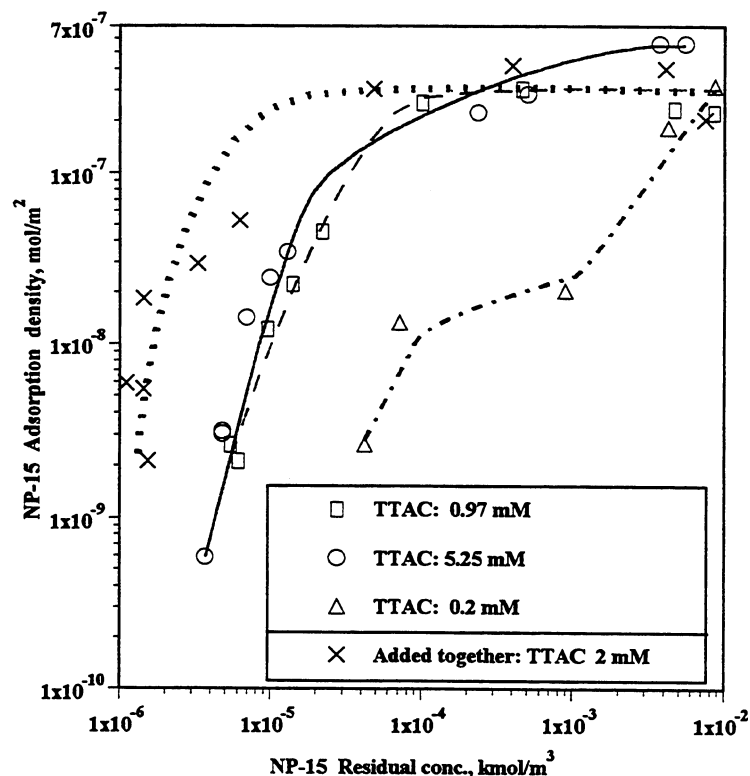


Figure 34 Adsorption isotherms of pentadecylethoxylated nonyl phenol (NP-15) on alumina: with preadsorbed amounts of tetradecyl trimethylammonium chloride (TTAC), and when added together with TTAC.

It is interesting to note the implication that TTAC hemimicelles are impermeable by the NP-15 even though there is synergism between the two species. It will be important to test this and investigate the reasons for this behavior. Desorption and reorientation of the surfactants adsorbed in the form of aggregates will depend to large extent on the activation barrier involved in dehemimicellisation.

The results also show that the order of addition of the surfactants has a marked effect on the adsorption of NP-15. If NP-15 and TTAC were pre-mixed and added to the alumina suspension together, the adsorption density of NP-15 is higher in the low concentration range. This indicates that

NP-15 adsorption with TTAC is not completely reversible, but is controlled by the nature of molecules packed at the alumina-water interface. Particle wettability and dispersion can also be expected to be affected by this markedly. It is important to note the lack of adsorption of the nonionic polyethoxylated nonyl phenol without the synergistic interaction of the cationic TTAC which shows the essential role of the electrostatic interaction in initiating the adsorption.

Since it is seen that the adsorption of the pentadecylethoxylated nonyl phenol from its mixtures with tetradecyl trimethyl ammonium chloride is higher than when TTAC was preadsorbed, adsorption from mixtures with different TTAC:NP-15 ratios was studied. Total adsorption as well as adsorption of the components are given in figures 35 through 37. In all the experiments TTAC and NP-15 were pre-mixed in 0.03 M sodium chloride solution and mixed with Linde A alumina for 15 hours at pH 10, and this pH was maintained constant during experiments. Under this pH conditions the alumina surface is originally negatively charged. Results reported in this project have shown that the adsorption of TTAC on alumina is higher at pH 10 than at lower pH values. Figure 35 shows the adsorption isotherms of TTAC in the presence of different amounts of NP-15. Zeta potential of alumina particles after adsorption under the above conditions are given in figure 38.

With the addition of the NP-15, TTAC adsorption rises in the low concentration range due to earlier onset of hemimicelle aggregation for both 4:1 and 1:1 TTAC:NP-15 ratios. For the 1:4 ratio no such trend is clear in the concentration range studied. At high concentrations, adsorption density decreases markedly with the addition of the nonionic surfactant. This is attributed to the competitive adsorption provided by NP-15. To quantitatively derive the adsorption mechanism governing the individual adsorption, it is necessary to determine the variation in the monomer concentration of each component in the system.

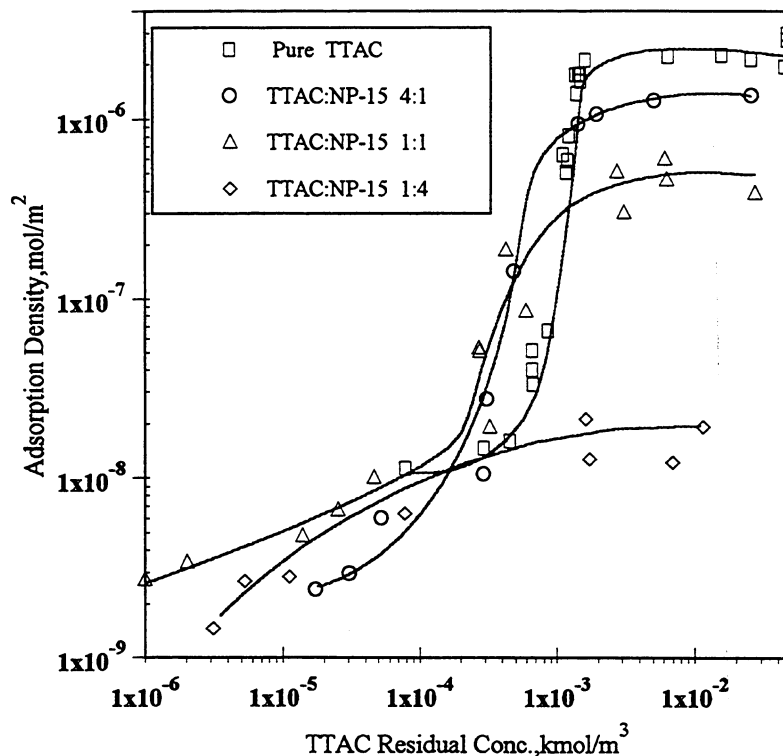


Figure 35 Adsorption of tetradecyl trimethyl ammonium chloride in the presence and the absence of NP-15.

With respect to the adsorption of nonionic NP-15 from the mixed system, while the nonionic surfactant NP-15 does not adsorb by itself on alumina, significant adsorption of the NP-15 occurs even at a ratio of 1:4 TTAC:NP-15.

With an increase in TTAC ratio in the mixtures, the adsorption of NP-15 is further enhanced significantly, and the adsorption isotherms are shifted to the lower concentration range. The residual surfactant concentration at which maximum (or plateau) adsorption density is attained usually corresponds to the critical micelle concentration (CMC) of the surfactant. The isotherm normally shifts to lower concentrations if the CMC and hemimicelle concentration (HMC) of the surfactant decrease. But in the present system, the onset of the plateau of the adsorption isotherm of NP-15 from mixtures with TTAC does not correspond to the CMC of the mixtures.

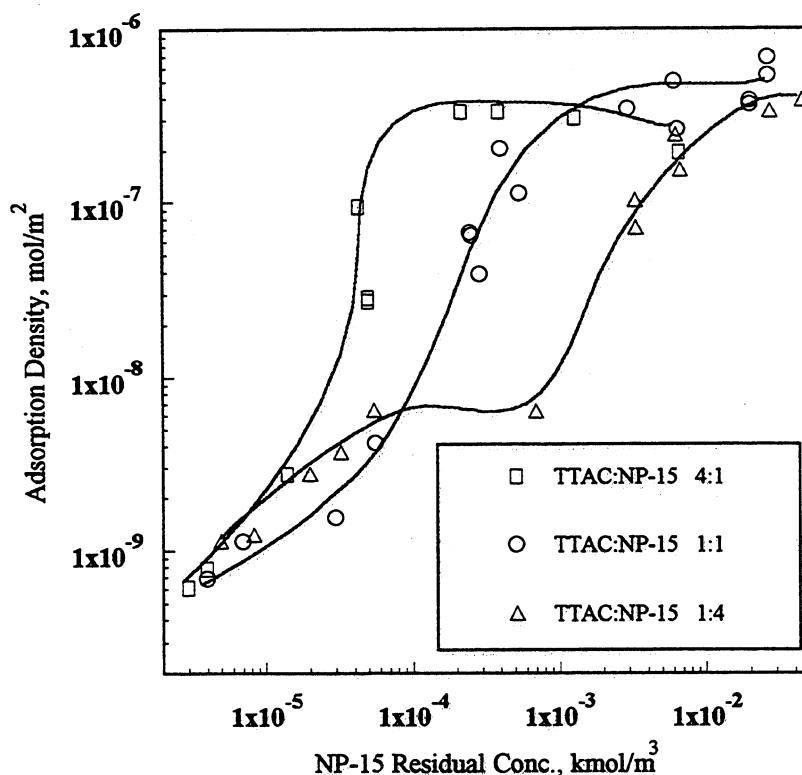


Figure 36 Adsorption of pentadecylethoxylated nonyl phenol (NP-15) on alumina in presence of varying amounts of tetradecyltrimethylammonium chloride (TTAC).

For example, the CMC of the 4:1 mixture solution is the highest of all mixtures (see figure 43), but the isotherm of NP-15 from this mixture is located in the lowest concentration range. This implies that the adsorption of NP-15 is controlled not by the micelle formation alone, but also by the adsorption of TTAC, the change in monomer composition, and the structure of adsorbed layer. The above factors warrant an investigation in order to fully understand the mechanism and to develop the capability to manipulate the adsorption behavior of mixtures.

The peculiar S-shape isotherm obtained for NP-15 adsorption as a function of NP-15 residual concentration should be noted and is in agreement with our previous work¹³. This is attributed to the more effective coadsorption of NP-15 inside the aggregates as the number of TTAC hemimicelles at the alumina-water interface increases. It is to be noted that the residual concentration of tetradecyl

trimethylammonium chloride varies from point to point along the NP-15 adsorption isotherm.

The total adsorption density of tetradecyltrimethylammonium chloride and pentadecylethoxylated nonyl phenol on alumina are plotted in figure 37 as a function of total surfactant concentration. It can be seen that with an increase in NP-15 in the mixtures the total adsorption density in moles/m² decreases, and this is suggested to be due to large size of NP-15 and the steric hinderance caused by it. Since the NP-15 molecules are much larger than the TTAC molecules, the adsorbed NP-15 will occupy more area thus reducing the area available for TTAC. Another plausible reason is the alteration in the structures of hemimicelles and micelles in the system with some screening of TTAC charge by the NP-15 with the increase of NP-15 in the mixtures. This will reduce the net electrostatic attractive forces between the alumina surface and the TTAC molecules which in turn can decrease also the adsorption of NP-15, since the adsorption of NP-15 depends upon the coadsorbed TTAC for anchoring. The remarkable effect of structure features of the surfactants in mixed system is clearly seen here.

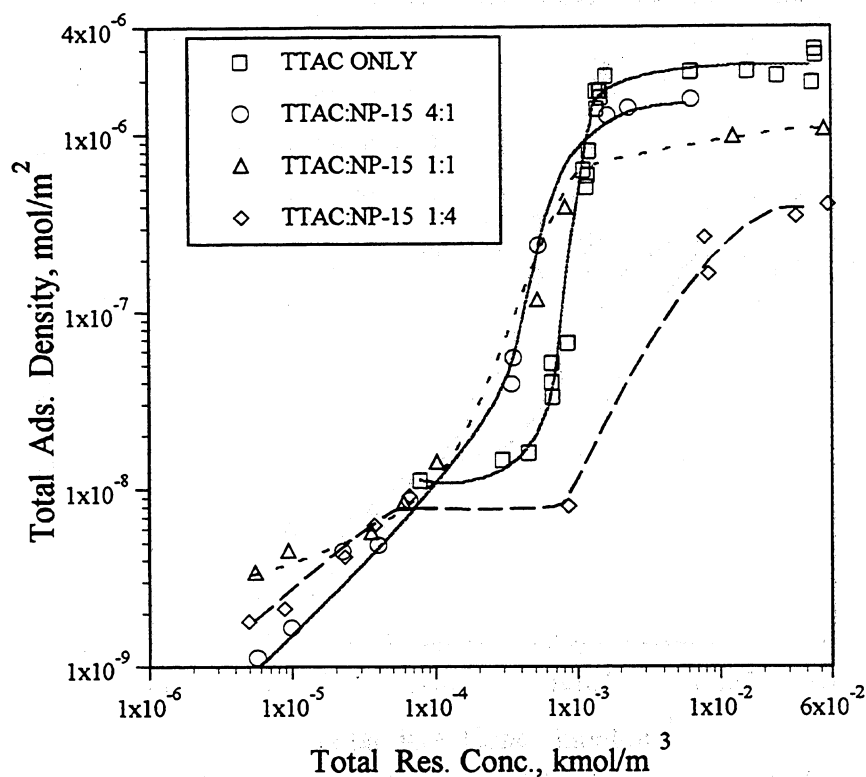


Figure 37 Total adsorption of surfactant mixtures at the alumina-water interface.

This hypothesis was tested by studying the zeta potential change due to adsorption and the results obtained are shown in figure 38. In this system, the zeta potential of alumina particles is decided mainly by the adsorption of the oppositely charged TTAC. From figure 38 it can be seen that with an increase of NP-15 in the mixture, the zeta potential of alumina decreases drastically, especially in the high concentration range. This is in agreement with the adsorption isotherms of TTAC and NP-15 in figures 35 & 36 respectively. Comparing the isoelectric point (IEP) for alumina in the presence of mixtures to that in the presence of TTAC alone it can be seen that with an increase in the NP-15 the IEP is shifted to higher TTAC concentrations. Upon examining the adsorption density of TTAC at IEP, it can be seen that the adsorption density of TTAC in mixtures is higher than that for TTAC alone. This means that the effect of TTAC in mixtures on zeta potential reduction is

less than that of TTAC when present alone. It can be concluded that the positive charge of the TTAC ionic head is partially screened by the co-adsorbed nonionic NP-15 molecule. These changes in the structure of the adsorbed layer can also affect the position of the shear plane. This is a possible reason for the observed change of zeta potential.

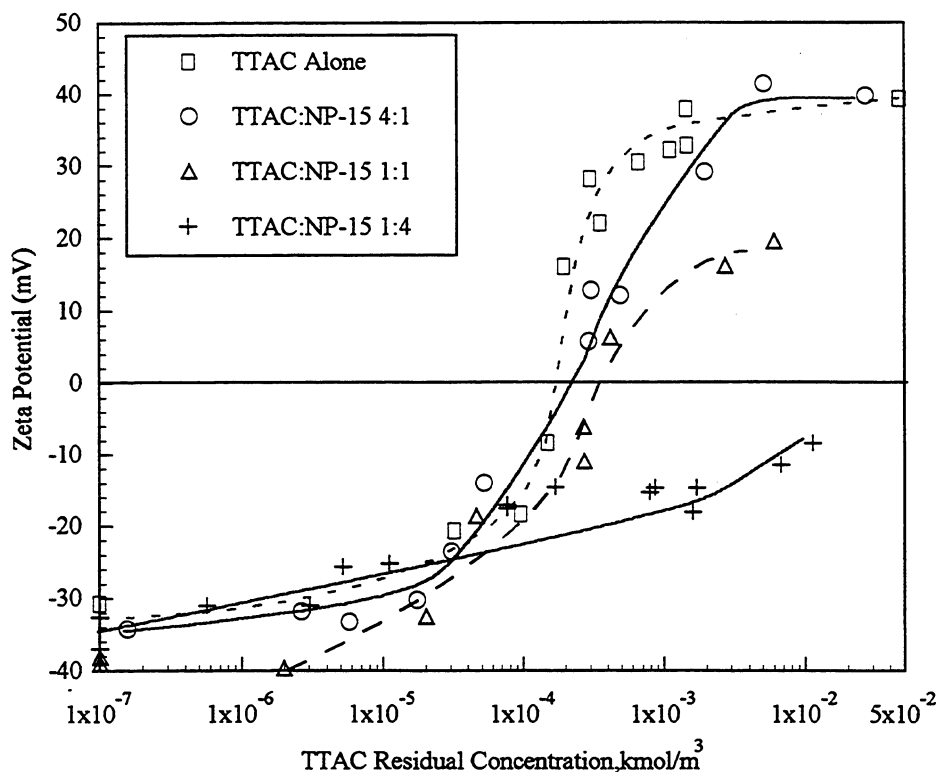


Figure 38 Zeta-potential of alumina after adsorption of TTA:NP-15 mixtures of different composition.

Changes in surfactant ratios of tetradecyl trimethyl ammonium chloride (TTAC) to pentadecylethoxylated nonyl phenol(NP-15) after Adsorption

It will be useful to examine the ratio of adsorption densities of TTAC to NP-15 as a function of total residual concentration. Such a plot is given in figure 39. The shapes of the plots of the ratio vs concentration changes drastically with the cationic/nonionic surfactant ratio exhibiting an intriguing set of interactions between the two components and suggesting ways to probe them. It can be seen

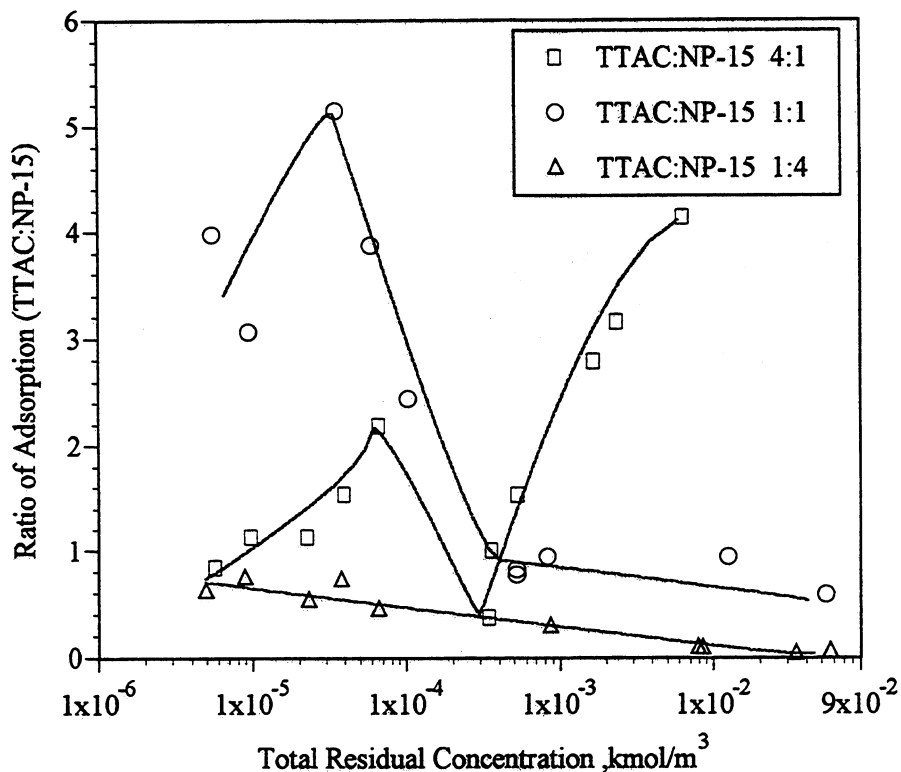


Figure 39 Ratio of adsorption densities of TTAC:NP-15 for different surfactant mixtures.

that the ability of the two surfactants to cooperate/compete at the alumina-water interface changes over the entire concentration range. This suggests the monomer compositions and adsorption mechanism to be changing over the concentration range studied. Clearly it becomes interesting to investigate these issues and develop a model that determines adsorption of both components as a function of their activities in solution and synergies/competitions involved.

Changes in surfactant ratio for an initial tetradecyl trimethyl ammonium chloride to pentadecylethoxylated nonyl phenol mixture of 4:1 are plotted in figure 40. It is seen that the ratios of TTAC:NP-15 both at the alumina-water interface and in the supernatant after adsorption are constantly changing over the concentration range studied.

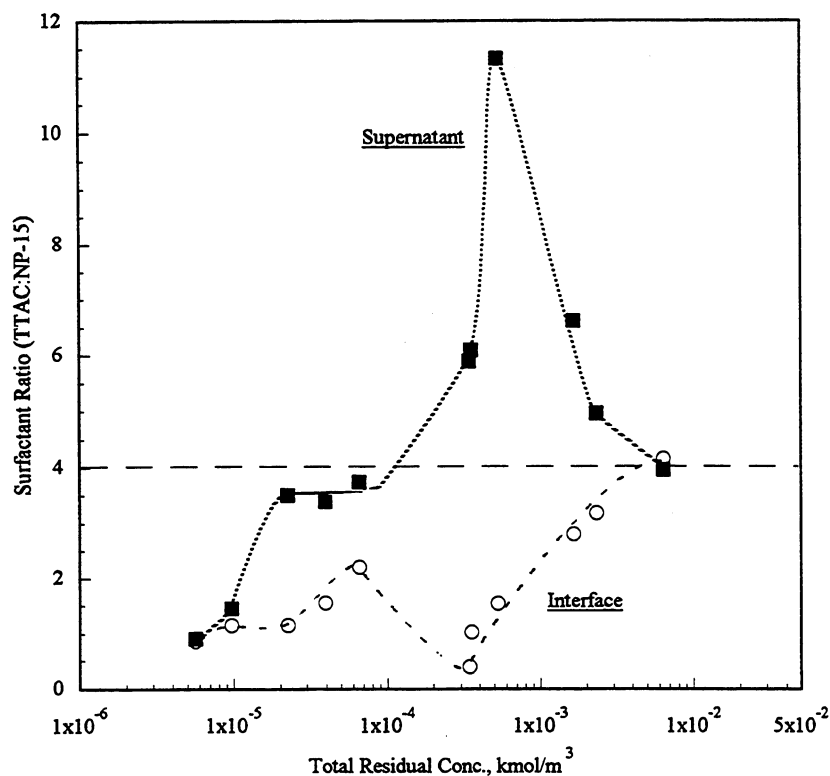


Figure 40 Changes in surfactant ratios (TTAC to NP-15) after adsorption for an initial 4:1 mixing ratio.

TTAC adsorbs first on alumina through electrostatic interaction. As a result of this preferential adsorption the ratio of TTAC to NP-15 is lower than 4.0 in the initial stages. Once sufficient TTAC adsorbs at the interface, NP-15 is coadsorbed through interactions between the hydrocarbon chains. Preadsorbed TTAC will function as anchors and induce the adsorption of NP-15 leading to formation of mixed surfactant aggregates at the interface. The activity of NP-15 is higher than that of the TTAC which results in excess TTAC in the supernatant leading to a high ratio of TTAC to NP-15 in the supernatant. This is also seen as a decrease of the surfactant ratio at the interface. The NP-15 molecule is larger than the TTAC molecule hence the steric hinderance to the further adsorption of TTAC leads to depression of TTAC adsorption. Once adsorption of NP-15 is complete, TTAC adsorption continues and eventually equilibrium is attained. At high concentrations of surfactant the initial mixing ratio is reflected both at the interface and in bulk solution after adsorption. Thus it is

seen that partitioning of surfactant to the interface does not depend upon the initial mixing ratio particularly at low concentrations. A combination of electrostatic and hydrophobic interactions is responsible for the observed phenomena.

Similar changes for a 1:1 TTAC:NP-15 mixture are shown in Figure 41. The adsorption

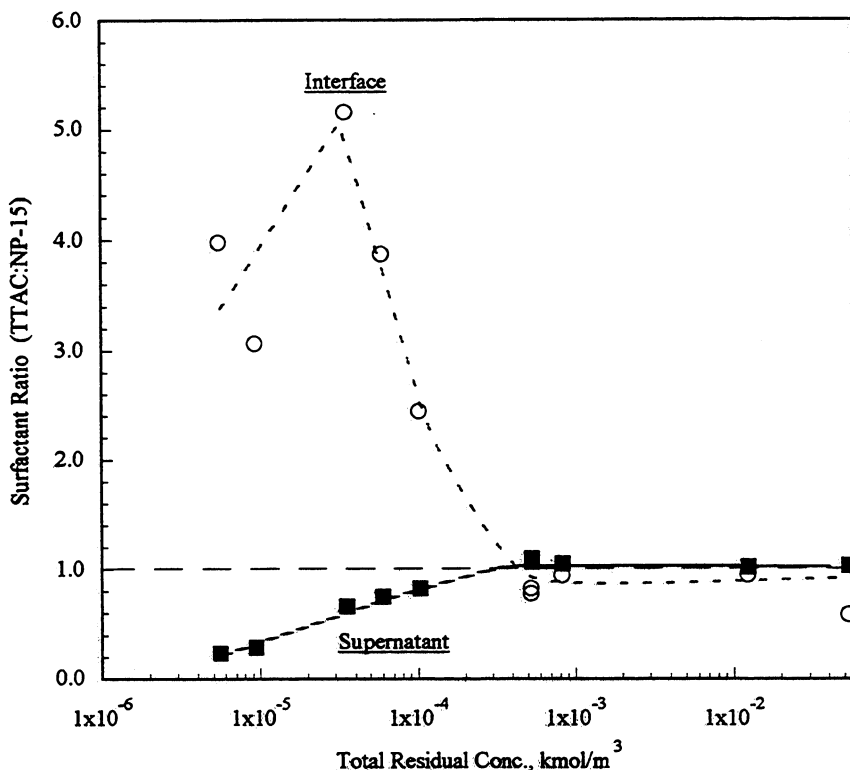


Figure 41 Changes in surfactant ratios (TTAC to NP-15) after adsorption at the alumina water interface for an initial mixing ratio of 1:1.

behavior in this system is similar to that in 4:1 TTAC:NP-15 mixture system. At low concentrations more TTAC molecules will be adsorbed at the alumina-water interface by electrostatic attraction, and the mixing ratio in supernatant is lower than 1.0 but the ratio at the interface is far greater than 1.0. It is interesting to note that the maximum surfactant ratio at the interface is higher than that in the 4:1 TTAC:NP-15 system (figure 40). This indicates that the synergism between these two surfactants is stronger in the 1:1 TTAC:NP-15 system than in the 4:1 TTAC:NP-15 system. The behavior in the

supernatant is however not very complicated and at high concentrations the initial mixing ratio is reflected both in the bulk and at the interface.

For a 1:4 TTAC:NP-15 mixture the changes in mixing ratio indicate similar interactions particularly at low concentrations (figure 42).

Since the TTAC content is very low, adsorption of TTAC also will be low leading to lower

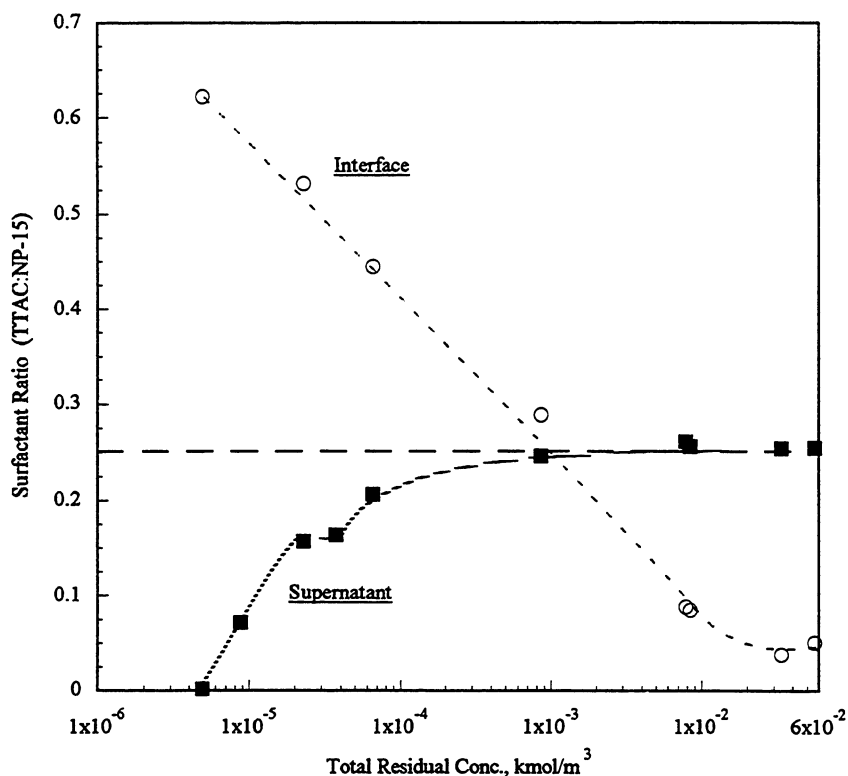


Figure 42 **Changes in surfactant ratios (TTAC to NP-15) after adsorption at the alumina-water interface for an initial mixing ratio of 1:4.**

NP-15 adsorption as well. There was no maximum or minimum observed for the ratios either in the supernatant or at the interface. The concentration of preadsorbed TTAC molecules is not enough to induce significant coadsorption of NP-15.

Comparing the changes in mixing ratios after adsorption for the different mixtures it is seen that the adsorption behavior in this system depends on both the relative mixing ratio and the absolute

concentration ranges. Considering the synergism and steric hindrance in these systems, it can be concluded that adsorption of TTAC will be decided by the relative and absolute quantity of NP-15 in the mixture. If the relative and absolute quantity of NP-15 is low, synergism between these two surfactants can be seen. At high concentrations, the absolute quantity of NP-15 is significant and steric hindrances will be dominant thus suppressing the adsorption of TTAC. On the other hand, the adsorption of NP-15 will simply depend on the mixing ratio of TTAC:NP-15 in the mixtures. With the increase of TTAC ratio the adsorption of NP-15 will be enhanced.

Surface tension of different mixtures was measured before and after adsorption to investigate the partitioning of the two surfactants to the alumina-water interface and the results obtained are shown in figures 43 and 44. Surface activity of the nonionic NP-15 is greater than that of the TTAC,

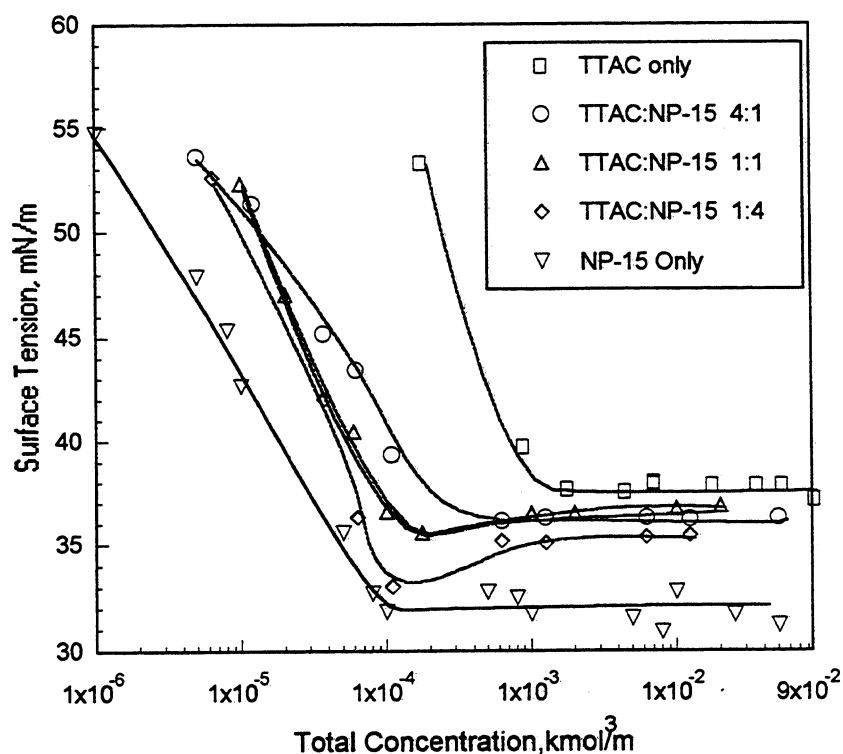


Figure 43 Surface tension of solutions of TTAC, NP-15 and their mixtures.

and the total activity decreases with an increase of TTAC in the mixtures. Comparison of results in

figure 43 to those in figure 44 shows that there is not much change in the surface tension behavior due to adsorption. Any change should correspond to the relative adsorption of the two surfactants.

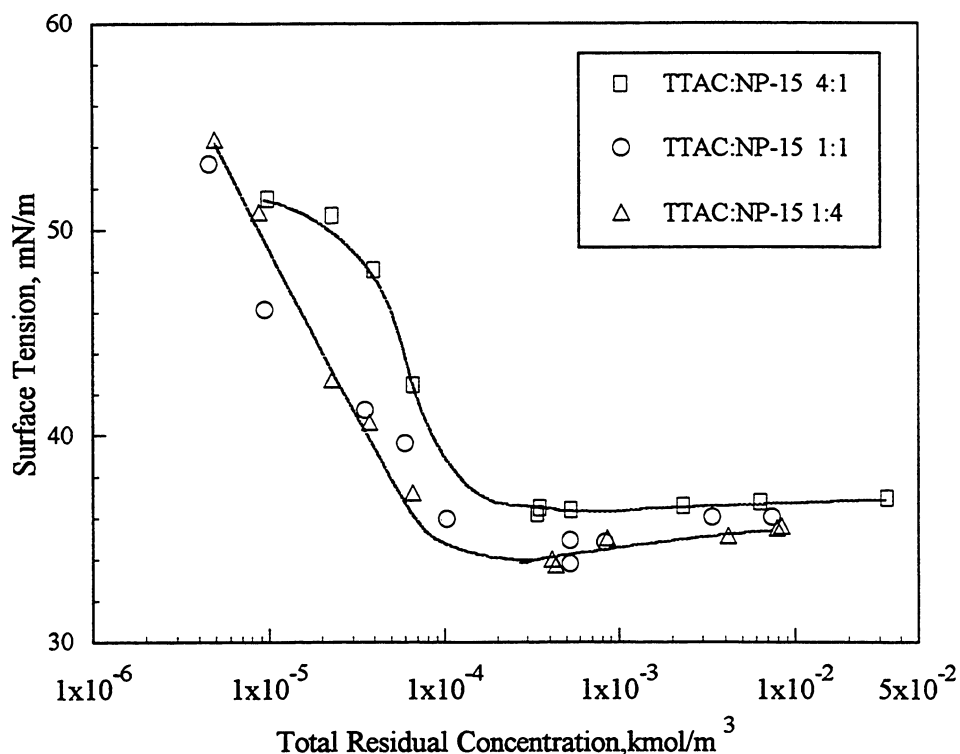


Figure 44 Surface tension of TTAC:NP-15 surfactant mixtures after adsorption.

If TTAC adsorbs more than NP-15 (compared to the ratio in the initial mixture) surface activity of the mixed solution can be expected to increase, whereas, if NP-15 adsorbs more, surface activity can decrease. For example, in the 4:1 mixed system the NP-15 adsorbed significantly in the low concentration range, and this caused the surface tension to shift to higher values in this range.

It has been shown very clearly in this work that interactions between the two surface active components in a mixture can lead to drastic alterations in the adsorption behavior of the system

reinforcing the need to understand such behavior since, as mentioned earlier, surfactant systems used in practice are invariably of the mixed type. It is important to investigate the microstructure of the adsorbed layer and changes in it as well as to elucidate the effects of the mechanisms involved and the variation in the adsorption process on interfacial properties such as wettability.

Theoretical and thermodynamic modelling of cationic - nonionic surfactant interactions

In an attempt to interpret adsorption and desorption behavior of mixed surfactant systems, regular solution theory was used to model the interactions between tetradecyltrimethylammonium chloride and pentadecylethoxylated nonyl phenol. The interaction parameter β and the monomer concentrations were calculated for different mixtures. One can determine β and C^* by means of Eq. (3) and (4). The concentrations of the monomers in the mixture can be calculated using the following equations:

$$X_1 = \left[\frac{- (C - \Delta) + [(C - \Delta)^2 + 4\alpha C \Delta]^{1/2}}{2\Delta} \right] \quad (10)$$

$$C_1^m = \left[\frac{- (C - \Delta) + [(C - \Delta)^2 + 4\alpha C \Delta]^{1/2}}{2 \cdot (f_2 C_2 / f_1 C_1 - 1)} \right] \quad (11)$$

where $(\Delta = f_2 C_2 - f_1 C_1)$

$$C_2^m = \left(1 - \frac{C_1^m}{f_1 C_1} \right) \cdot f_2 C_2 \quad (12)$$

where X_1 is the mole fraction of surfactant 1 in mixed micelles. β is a measure of the deviation of the mixture from ideality and the activity coefficients f_i for binary mixtures can be expressed by the following equations:

$$f_1 = \exp [\beta \cdot (1 - x)^2] \quad (13)$$

$$f_2 = \exp [\beta \cdot x^2] \quad (14)$$

Although the regular solution theory has been criticized by some researchers, it has provided a very tractable way to describe the behavior of mixed surfactant aggregates. The calculated results of X_1 and C^* are shown in Table IX.

Table IX **Calculated results of x and C^* by regular solution theory**

α	$\beta = - 1.5$		$\beta = - 1.0$	
	x_1	$C^*(10^{-4}M)$	x_1	$C^*(10^{-4}M)$
0.05	0.4374	5.33	0.4271	6.03
0.10	0.5439	3.90	0.5512	4.42
0.125	0.5795	3.49	0.5925	3.93
0.20	0.6567	2.69	0.6808	3.01
0.25	0.6974	2.37	0.7232	2.63
0.30	0.7267	2.12	0.7580	2.34
0.40	0.7793	1.78	0.8135	1.92
0.50	0.8229	1.54	0.8571	1.65
0.60	0.8613	1.37	0.8932	1.44
0.70	0.8968	1.24	0.9244	1.29
0.80	0.9308	1.13	0.9520	1.16
0.90	0.9647	1.05	0.9770	1.06
0.95	0.9821	1.01	0.9887	1.02
0.99	0.9964	0.99	0.9978	0.99

Critical micelle concentrations of the mixtures determined by the surface tension measurement are plotted in figure 45 as a function of NP-15 mole fraction. Regular solution theory has been used to fit these data.

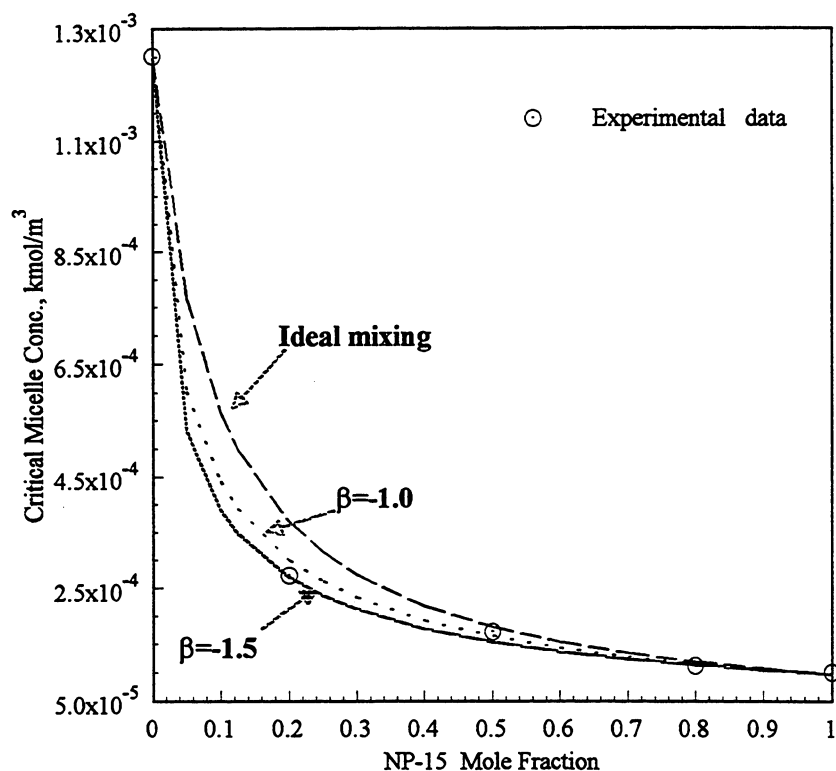


Figure 45 Regular solution and ideal mixing theory for determining the interaction parameter for the tetradecyl trimethylammoniumchloride pentadecylethoxylated nonyl phenol system.

It was found that the interaction parameter β for this system is between -1.5 and -1.2. A considerable number of binary mixed micellar systems have been studied using regular solution theory. Generally, the strength of interaction in mixed systems with cationic surfactants increases in the order of cationic-cationic, cationic-zwitterionic, cationic-nonionic, and cationic-anionic. For cationic-anionic system the value of the interaction parameter β can be about -25, for cationic-nonionic, -4.6 to -1.0, for cationic-cationic, about -0.2 to 0. In addition to the nature of the components in the mixture, the interaction parameter is affected by the structure of the surfactants and the ionic strength of the mixed system. The interaction parameter observed for the TTAC:NP-15 system is not very large. This indicates that the interaction between TTAC and NP-15 in 0.03 M NaCl solution is not very strong.

To better understand the adsorption/desorption mechanisms the monomer concentrations of different mixtures in this system were calculated using the regular solution theory with an interaction parameter of -1.5. The results obtained are shown in figures 46 and 47.

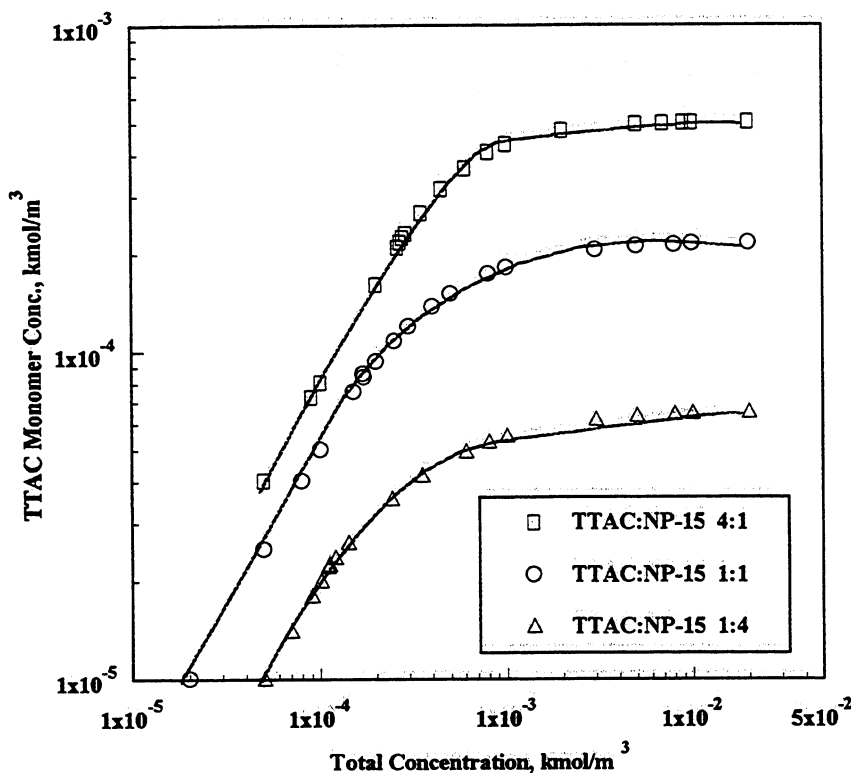


Figure 46 Monomer concentrations of tetradecyl trimethylammoniumchloride in mixtures with pentadecylethoxylated nonyl phenol calculated using regular solution theory with an interaction parameter -1.5

Comparing these monomer concentrations with the adsorption isotherms (figures 35 and 36) it can be found that the adsorption of NP-15 does not depend upon its monomer concentration in the mixtures. For example, the adsorption of NP-15 in 4:1 TTAC:NP-15 mixture is the most significant in all these mixtures, but its monomer concentration is the lowest. This result is in agreement with the fact that the adsorption of NP-15 depends on the pre-adsorbed TTAC acting as anchors. For the adsorption of TTAC, the adsorbed amount corresponds to the monomer concentrations in the mixtures. The higher the monomer concentration, the higher is the adsorption

density.

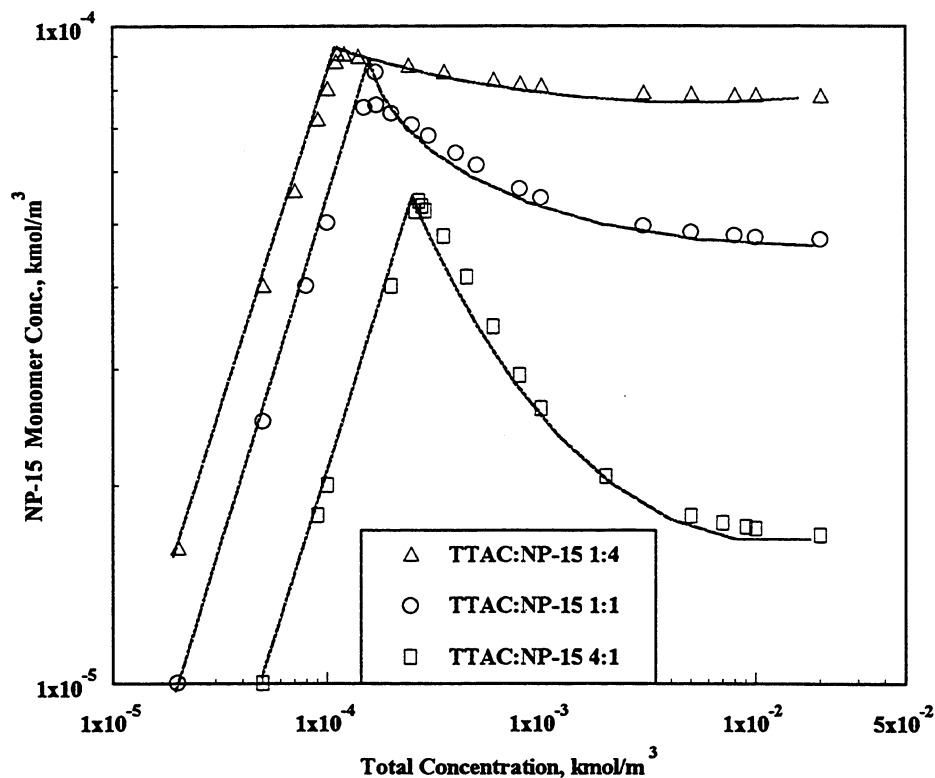


Figure 47 Monomer concentrations of pentadecylethoxylated nonyl phenol (NP-15) in mixtures with tetradecyl trimethylammonium chloride (TTAC) calculated using regular solution theory with an interaction parameter = -1.5.

Since these monomer concentrations are the concentrations calculated before adsorption, it is not directly related to changes in the monomer composition upon adsorption and during desorption. It is therefore necessary to determine the variation of the monomer concentration of each component during the adsorption and desorption directly by some suitable experimental methods.

Whereas adsorption of TTAC is greatly affected by the presence of NP-15 the adsorption of the latter depends solely upon the presence of TTAC, we suspect the aggregate size and structure to be affected and this in turn should also control the desorption process. In the next section the desorption behavior of the mixed system is discussed.

Desorption of surfactant mixtures from alumina-water interface

Interactions between surfactants and solids can be understood better by studying desorption along with adsorption. It has been shown earlier in this report that the desorption of TTAC from alumina-water interface was reversible at high concentrations but was irreversible at lower concentrations. This was attributed to changes in the structure of the adsorbed layer upon dilution. Similar studies were conducted next with the mixed adsorbed layer.

The desorption tests consisted of mixing of supernatants of slurries from adsorption tests for 15 hours with the desired amounts of diluents adjusted for pH and ionic strength. This procedure was repeated several times. The results obtained for the desorption of a 4:1 TTAC:NP-15 mixture are shown in figures 48 & 49. It is noted that the desorption of TTAC from a 4:1 mixture (figure 48) is

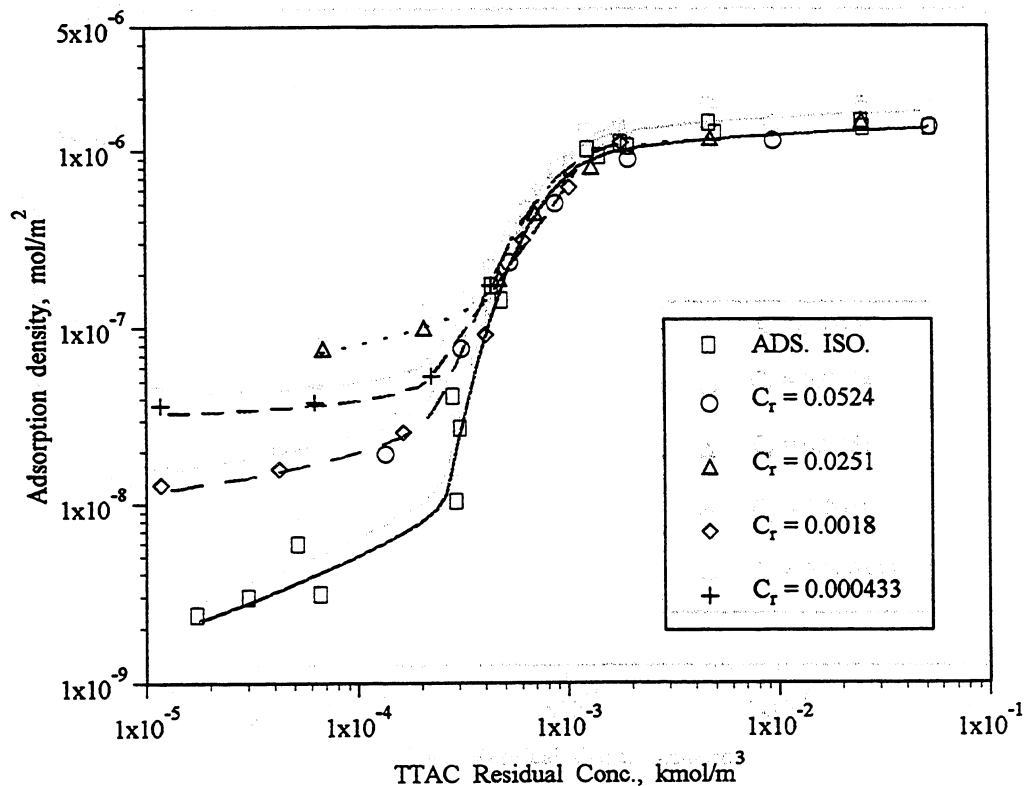


Figure 48 Desorption of tetradecyl trimethyl ammonium chloride (TTAC) from mixed adsorbed layer on alumina upon dilution from different residual concentrations of TTAC (C_r). TTAC:NP-15 = 4:1

similar to that for TTAC alone (figure 32).

At high concentrations the adsorption of TTAC is reversible, but at low concentrations the desorption shows some positive hysteresis, i.e. at same residual concentrations, the adsorption density is higher after desorption than that after adsorption. This is attributed to the hysteresis involved in the deaggregation of the hemimicelles from the interface. Interestingly, the fully grown hemimicelles come off the surface easily upon dilution whereas the incipient ones do not. Similar isotherms for the desorption of NP-15 is shown in figure 49. As reported earlier, the adsorption of NP-15 on alumina requires the tetradecyl trimethyl ammonium chloride (TTAC) to coadsorb and act as an anchor. It is the reasonable to expect the desorption behavior of the NP-15 to be controlled by the desorption of TTAC.

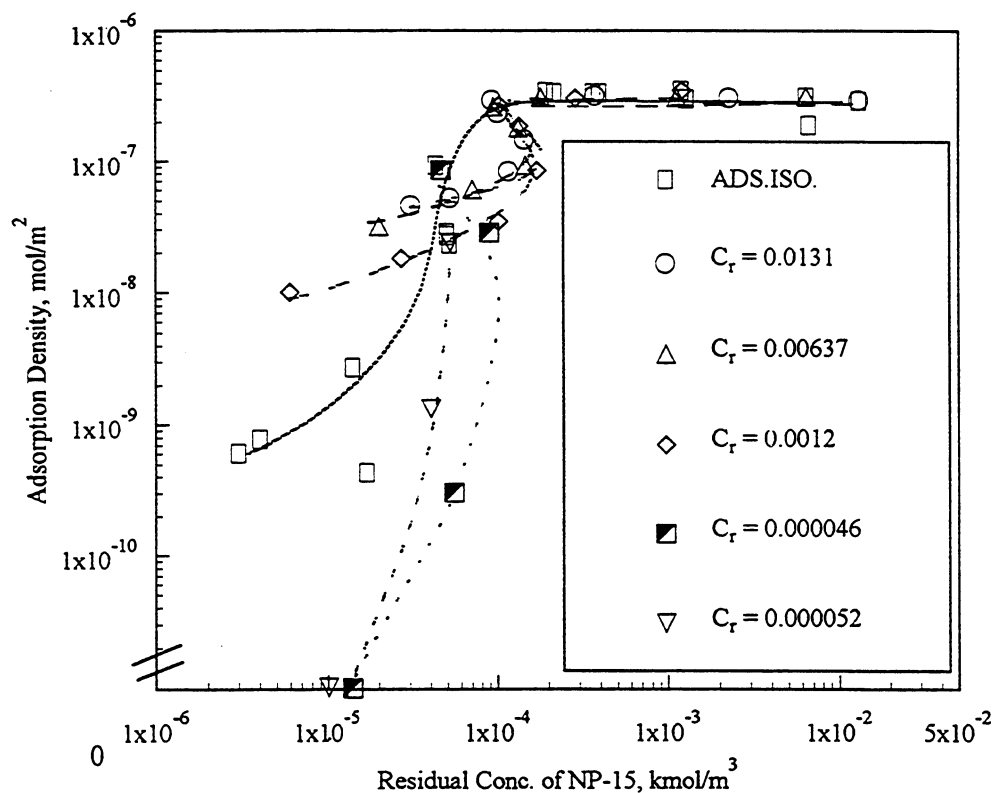


Figure 49 Desorption of pentadecyl ethoxylated nonyl phenol (NP-15) from alumina upon dilution from different residual concentrations (C_r). TTAC:NP-15 ratio = 4:1.

At high concentrations the adsorption density of TTAC does not change much upon dilution, neither does NP-15 desorb from the interface under these conditions. However in cases where TTAC desorbs from the interface, desorption of NP-15 is significant and S-shape desorption isotherms are obtained. The desorption of NP-15 is facilitated in this case by the desorption of TTAC. For dilutions from high concentrations, the desorption of NP-15 shows some positive hysteresis (similar to the positive hysteresis of TTAC) but only when the residual concentration becomes low due to dilution.

The desorption isotherms for a 1:1 TTAC:NP-15 mixture are shown in figures 50 & 51. It can be seen that at this ratio both TTAC and NP-15 desorb significantly and the desorption isotherms show negative hysteresis, i.e. the surfactant adsorption at the interface is less during desorption than that during adsorption at the same residual concentration.

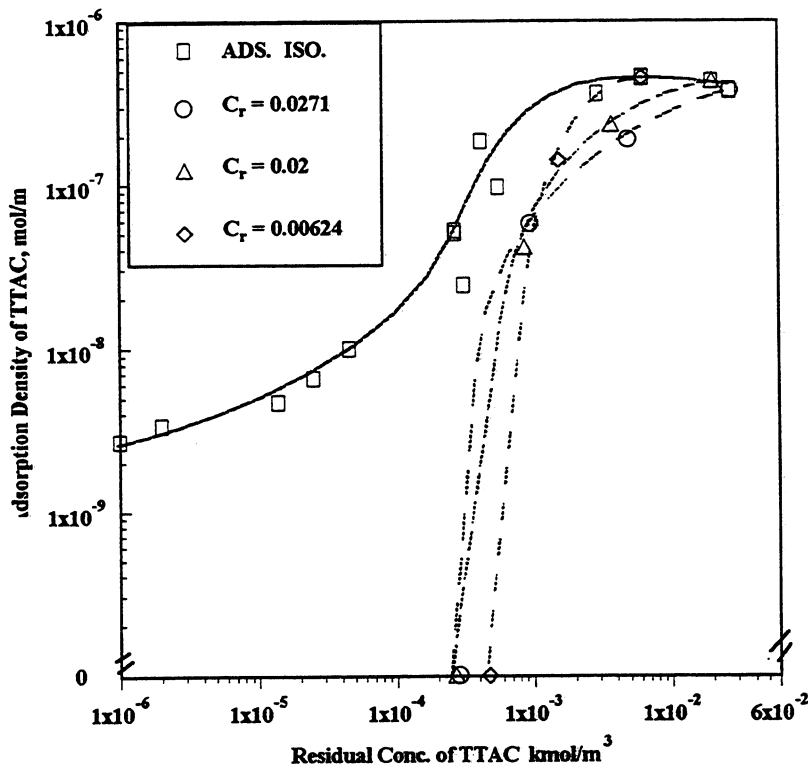


Figure 50 Desorption of tetradecyl trimethylammonium chloride from alumina-water interface upon dilution from different residual concentrations (C_r) in presence of 1:1 pentadecyl ethoxylated nonyl phenol.

As the NP-15 content of the mixture increases, the positively charged head of the TTAC will be partially shielded from each other by the co-adsorbed nonionic NP-15 molecules. This will decrease the electrostatic interaction between the cationic TTAC molecules and the negatively charged alumina surface and facilitate desorption.

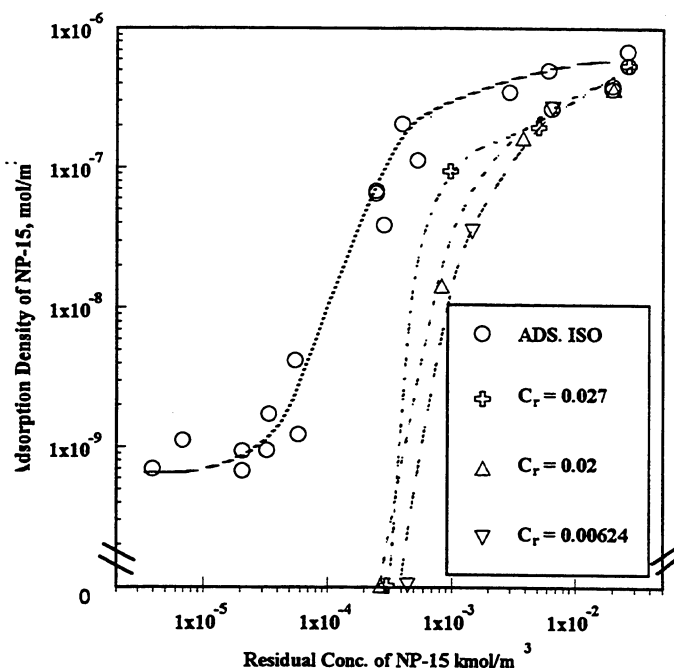


Figure 51 Desorption of pentadecylethoxylated nonyl phenol (NP-15) upon dilution from different residual concentrations (C_r) in presence of 1:1 tetradecyl trimethylammonium chloride (TTAC).

The desorption of 1:4 TTAC:NP-15 mixed system is shown in figures 52 & 53. At this ratio the adsorption of TTAC is very low. Nevertheless, the desorption of TTAC in this system still shows some negative hysteresis. The desorption of NP-15 shows some positive hysteresis. The mechanisms of desorption in this mixed system are evidently complex.

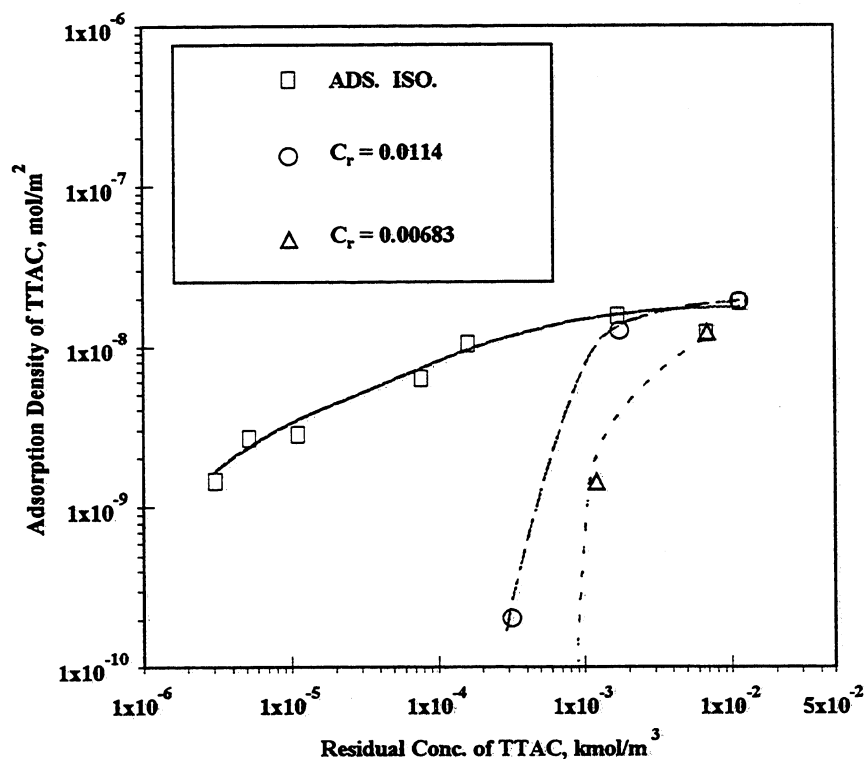


Figure 52 Desorption of tetradecyl trimethyl ammonium chloride (TTAC) from alumina upon dilution from different residual concentrations (C_r). TTAC:NP-15 ratio = 1:4.

From the above results it is evident that the desorption behavior of this mixed system depends upon the ratio of surfactants in the mixture. With an increase of NP-15 in the mixture the desorption of TTAC becomes easy. The desorption of both surfactants show significant negative hysteresis at a ratio of 1:1.

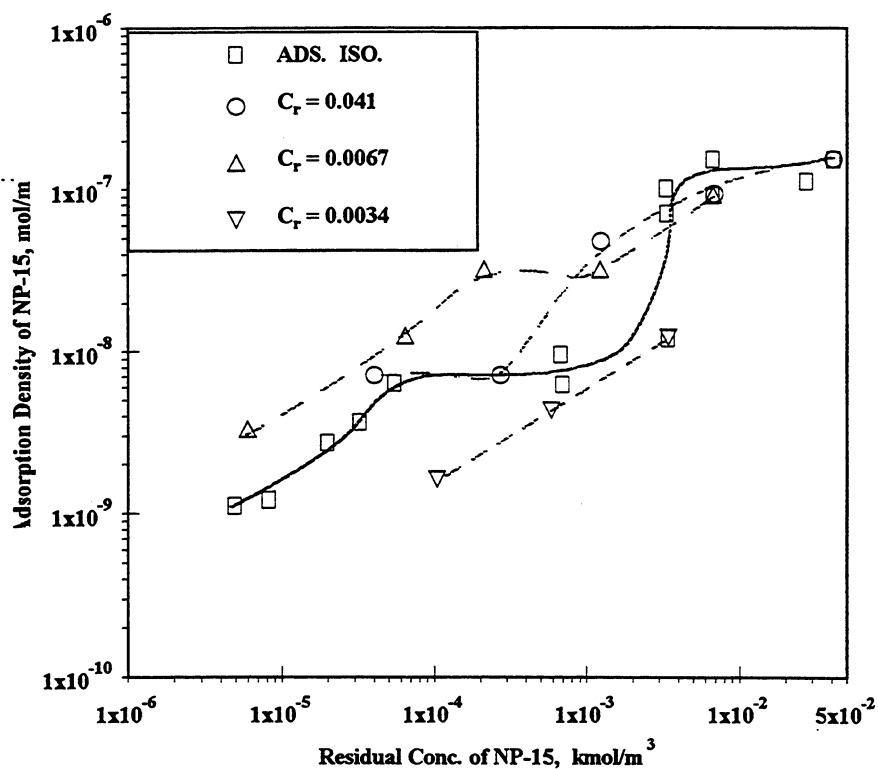


Figure 53 Desorption of pentadecyl ethoxylated nonyl phenol (NP-15) from alumina upon dilution from different residual concentrations (C_r). TTAC:NP-15 ratio = 1:4.

It is shown that the interactions between surfactant mixtures can be exploited to control and alter the adsorption and desorption behavior of the individual surfactants. Thermodynamic models can be used to calculate the monomer concentrations and predict adsorption behavior but only if the adsorption is not contingent upon the adsorption of a coadsorbing species.

Measurement of monomer concentration by ultrafiltration

As suggested earlier in this report, information on changes in the monomer concentration of individual surfactants in mixtures during the adsorption is vital since these changes are usually directly related to the mechanisms of adsorption in the mixtures. Ultrafiltration is a method which can be used to separate the monomer and micelles directly and was used for determining tetradecyltrimethylammonium chloride (TTAC) and pentadecylethoxylated nonylphenol (NP-15) monomer concentrations.

The cell and membrane used in this study were obtained from Amicon Company (model 8050 and YM-3 membrane). The membrane chosen was specified to exclude molecules with molecular weight greater than 3000. Since the micelles of both TTAC and NP-15 will be considerably larger than this molecular weight cutoff, this membrane was considered satisfactory for separating monomers from micelles. A constant pressure of 870 mm mercury was exerted on the mother liquor using compressed nitrogen and the effluent was collected at atmospheric pressure. All these experiments were performed at an ionic strength of 0.2 M or 0.03 M NaCl .

The results obtained from ultrafiltration experiments are shown in figures 54 and 55. It is observed that when the mother liquor concentration is lower than the CMC of the surfactants, monomer concentration (or filtrate concentration) is the same as the mother liquor concentration and increases linearly with mother liquor concentration. Above the CMC, the monomer concentrations obtained by ultrafiltration are relatively constant. This indicates that micelles of both TTAC and NP-15 can not go through the membranes.

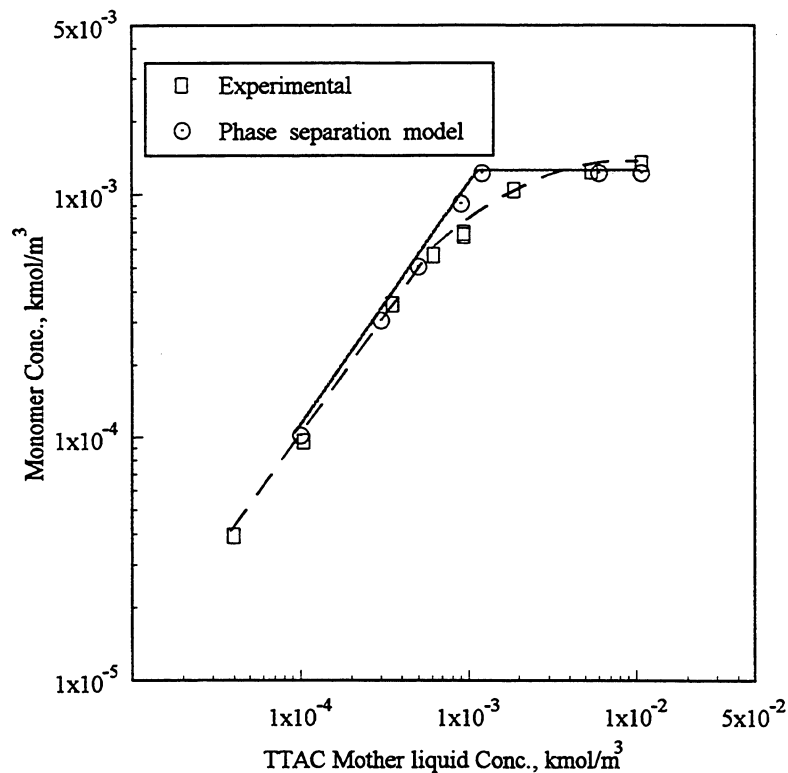


Figure 54 **Monomer concentration of Tetradecyltrimethylammonium chloride (TTAC) as the function of total concentration**

These results show that ultrafiltration method is suitable for separating monomers from micelles in this system. To compare the results from ultrafiltration tests with a prediction from the phase separation model, the monomer concentrations predicted by phase separation model are also plotted in figures 54 and 55. It can be found that experimental results and phase separation model are almost the same except around CMC. In this concentration range, the monomer concentrations obtained from ultrafiltration are lower than the concentrations predicted by phase separation model. This may indicate formation of some pre-micellar aggregates in solution, and this aspect merits further investigation.

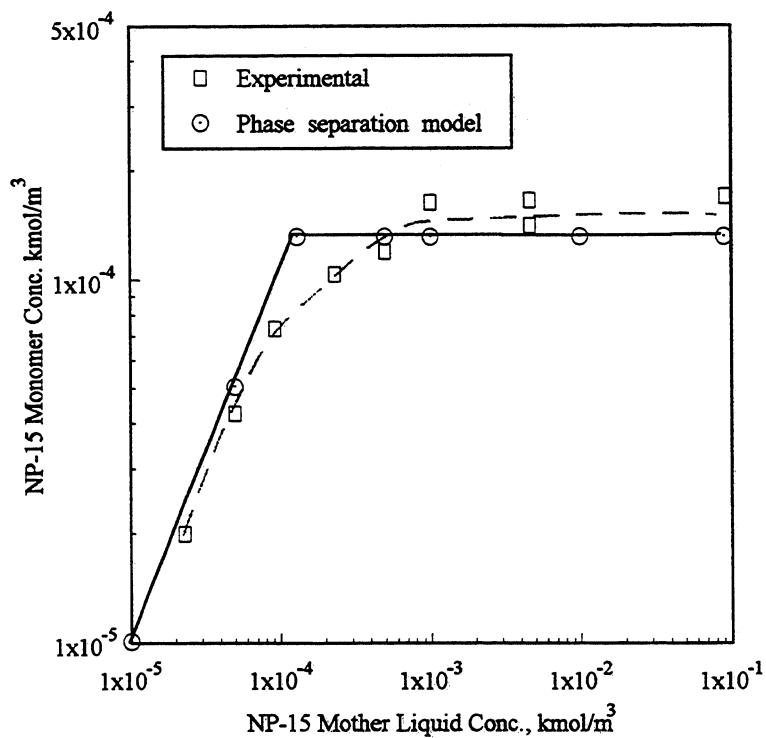


Figure 55 **Monomer concentration of pentadecylethoxylated nonylphenol (NP-15) as the function of total concentration**

Monomer concentrations of tetradecyl trimethyl ammonium chloride (TTAC) and Pentadecylethoxylated nonyl phenol (NP-15) in their mixed solutions

The monomer concentrations of both tetradecyl trimethyl ammonium chloride and pentadecylethoxylated nonyl phenol in their mixtures were measured using ultrafiltration. A YM-3 membrane from Amicon Company with a molecular weight cut-off of 3000 was used for ultrafiltration. All experiments were performed at an ionic strength of 0.2 M NaCl . The monomer concentrations of TTAC in its mixtures with NP-15 are shown in figure 56.

It is seen that the cationic TTAC monomer concentrations are lower in mixtures with the

nonionic NP-15 than for TTAC alone. With an increase of NP-15 content in the mixtures, the monomer concentrations of TTAC is further decreased. It is interesting to note that monomer concentrations of TTAC in the mixtures keep increasing even above the critical micelle concentration (CMC) of the mixtures. This is in contrast to the single surfactant system where the monomer concentration is relatively constant above the CMC. The TTAC monomer concentrations were also calculated using the regular solution theory¹⁴. Comparing the two it is seen that the TTAC monomer concentrations in this mixed surfactant system measured by ultrafiltration and calculated using regular solution theory are similar. This is not the case for NP-15 since the monomer concentrations measured by ultrafiltration are different from those calculated using regular solution theory (see figure 56). The ultrafiltration results show the monomer concentrations to be constant over the concentrations immediately above the mixed CMC (depending on mixed ratio), and then to increase at higher concentrations. Regular solution theory, however, predicts a decrease in monomer concentration above the mixed CMC. The above results clearly suggest that regular solution theory is not suitable for the TTAC and NP-15 mixture system.

Ionic strength can be expected to have a significant effect on the aggregation of the cationic surfactant which in turn will affect co-aggregation with the nonionic surfactant. To determine such effects, monomer concentrations of TTAC and NP-15 were measured at an ionic strength of 0.03 M NaCl. Two kinds of membranes, (YM-1 and YM-3) from Amicon Company with the molecular weight cut-off of 1000 and 3000 were used to separate TTAC and NP-15 monomers from the same sample: the YM-1 membrane was used to separate TTAC monomers from the mixed micelles and the YM-3 membrane was used to separate NP-15 monomer from the mixed micelles. The purpose of this experimental design was to ensure complete separation of all monomers from the mixed

micelles. The monomer concentrations of TTAC and NP-15 thus determined are shown in figures 58 and 59 for different mixing ratios. The monomer concentrations for both TTAC and NP-15 at the lower ionic strength (0.03 M NaCl) are higher than those at higher ionic strength (0.2 M NaCl) (see figure 56 and 57).

This is anticipated for TTAC since the critical micelle concentration (CMC) of ionic surfactants and correspondingly the monomer concentration do decrease upon the addition of salt. For NP-15, however, the monomer concentrations are identical at both the ionic strengths.

Although the CMC of NP-15 is not very sensitive to the addition of salt, particularly in this concentration range, in the case of its mixtures with TTAC, mixed micelles will be formed and any change in the activity of the ionic surfactant will alter aggregation between NP-15 and TTAC.

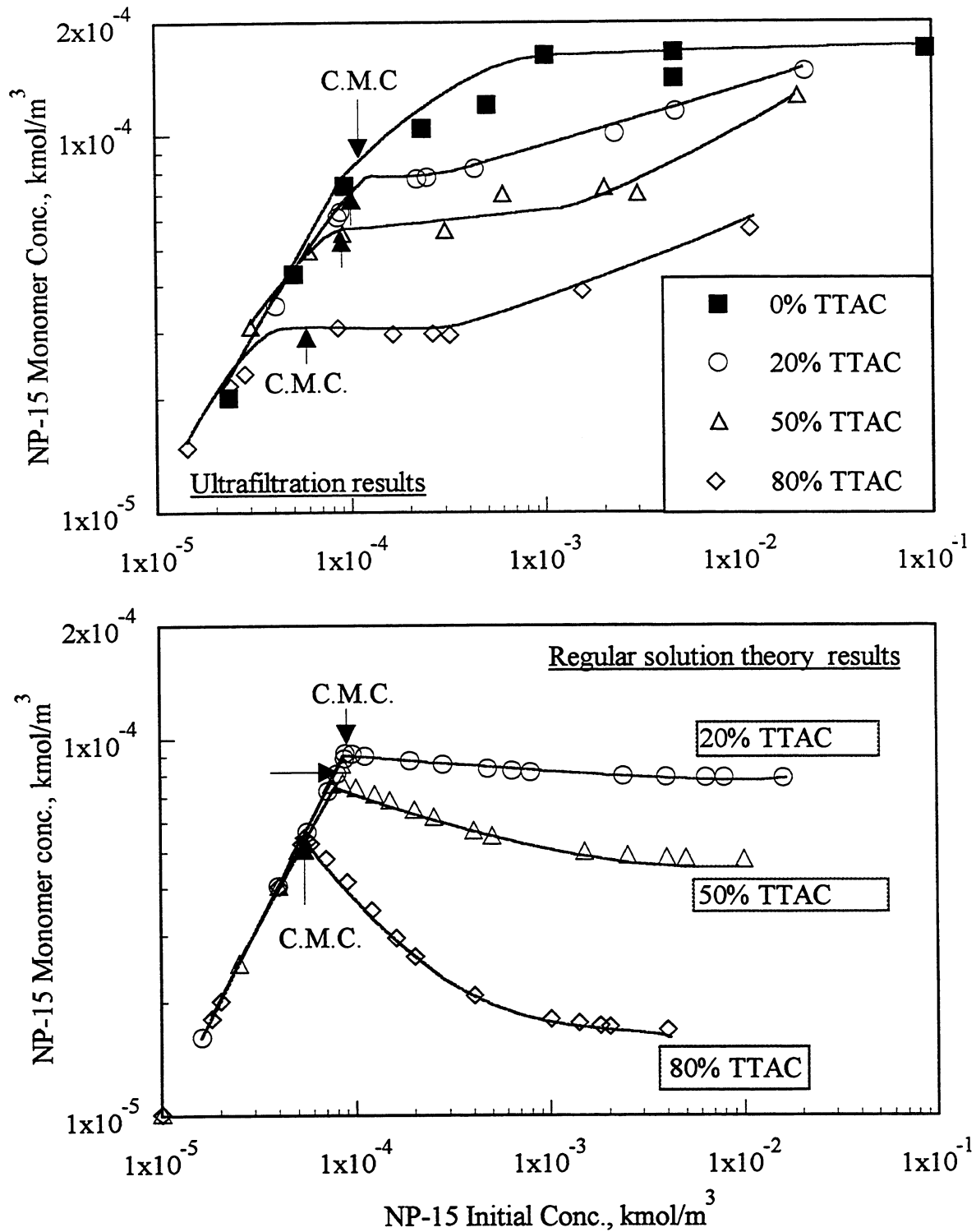


Figure 56 Monomer concentrations of NP-15 as measured by ultrafiltration compared with those calculated using regular solution theory.

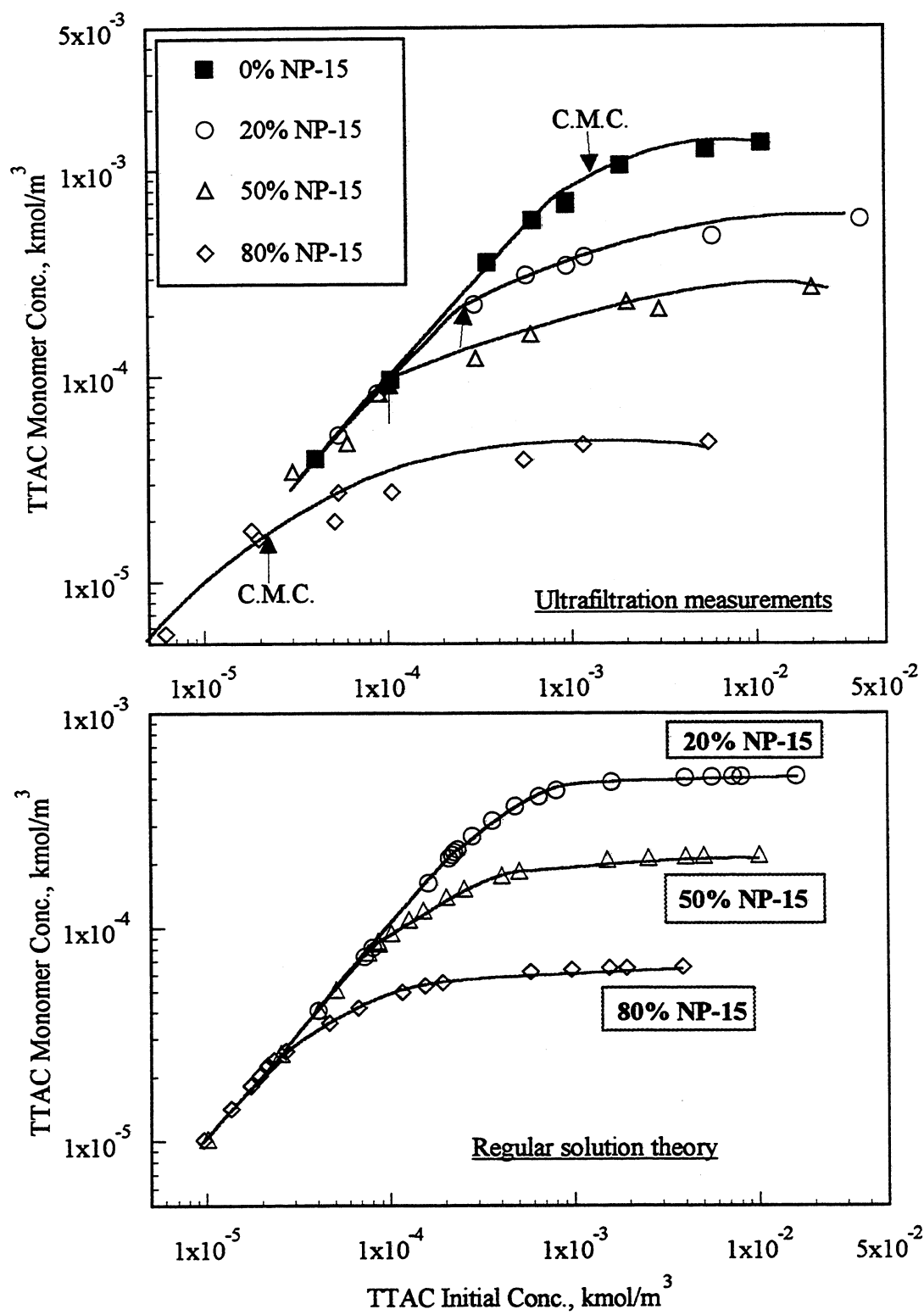


Figure 57 Monomer concentrations of TTAC in mixtures with NP-15 as measured by ultrafiltration and also calculated using regular solution theory.

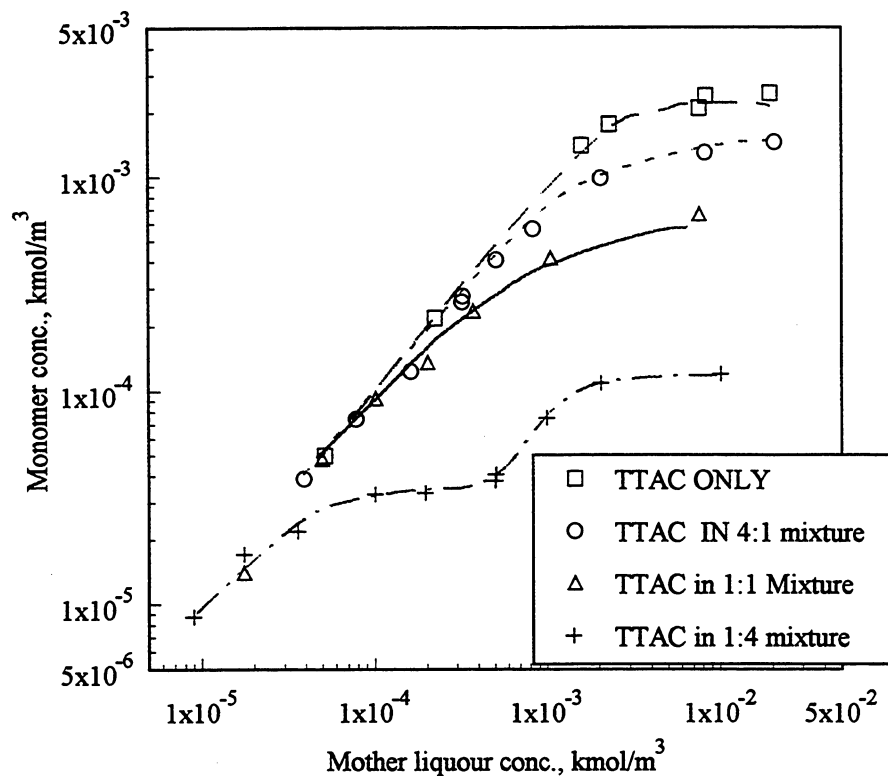


Figure 58 TTAC monomer concentrations in TTAC:NP-15 mixtures of different compositions. I.S. 0.03 M NaCl

It is interesting to note that monomer concentrations of both TTAC and NP-15 do not remain constant above the mixed CMC of the system. Considering that the mixed micelles are in equilibrium with these monomers, it can be expected that the composition of the mixed micelles will vary as the total concentration is increased above the CMC of the mixtures. The results obtained for monomer concentrations of pentadecylethoxylated nonyl phenol (NP-15) show that the monomer concentrations are constant over a short concentration range above the mixed CMC (depending on the ratio of mixing) and then increases at higher concentrations. The NP-15 concentrations at the mixed CMC are 8.8×10^{-5} mol/l, 8.5×10^{-5} mol/l and 5.4×10^{-5} mol/l for the 1:4, 1:1 and 4:1 TTAC:NP-15 mixing ratios respectively. The NP-15 concentration at the mixed CMC decreased with increase

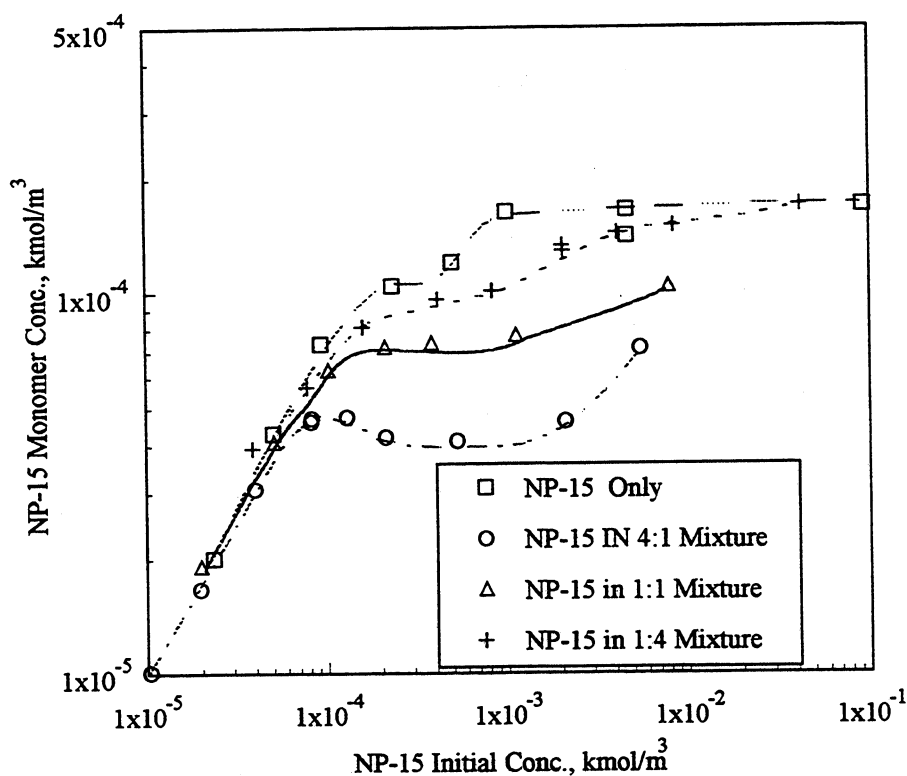


Figure 59 NP-15 monomer concentrations in TTAC:NP-15 mixtures of different composition. I.S. = 0.03 M NaCl

in TTAC content of the mixture suggesting enhanced synergism with increasing TTAC. Since NP-15 is more surface active than TTAC, it is reasonable to believe that only NP-15 can form micelles immediately above the mixed CMC, and TTAC molecules are then "dissolved" in the micelles of NP-15, similar to solubilization of organic compounds in micelles. At a fixed ionic strength, the TTAC that can be dissolved in NP-15 micelles will depend upon packing constraints of the two surfactants. With an increase in total surfactant concentration to the point at which TTAC itself can form aggregates, a new kind of TTAC-rich micelle may be formed. This may cause some of the TTAC molecules dissolved in the NP-15 rich micelles to rearrange into TTAC rich micelles. This is proposed

to be a reason for the increase in NP-15 monomer concentrations at high concentrations. For example, in the 1:4 TTAC:NP-15 mixture system, NP-15 rich micelles will form at an NP-15 concentration of 8.8×10^{-5} mol/l, into which some TTAC molecules can dissolve. This is indicated by a constant monomer concentration of TTAC over a certain concentration range. Above a TTAC concentration of 6×10^{-4} mol/l, TTAC rich micelles may form. The monomer concentrations of both TTAC and NP-15 are seen to increase and reach new plateau values, especially the NP-15 monomer concentration which is similar to that in the pure NP-15 system. In the 4:1 TTAC: NP-15 mixture system NP-15 rich micelles will be formed at an NP-15 concentration of 5.4×10^{-5} mol/l . Due to the strong synergism between NP-15 and TTAC in NP-15 rich micelles, the monomer concentration of NP-15 decreases slightly above the mixed CMC. On the other hand, the monomer concentration for TTAC did not change very much from that in the pure TTAC system. This could be due to the limit on the amount of TTAC that can dissolve in the NP-15 rich micelles. With an increase in total concentration, TTAC itself can form micelles and two kinds of mixed micelles (NP-15 rich and TTAC rich micelle) can co-exist. As a result, NP-15 monomer concentration increases and TTAC monomer concentration approaches a plateau.

Relationship between adsorption at the alumina-water interface and monomer concentration in a 4:1 tetradecyl trimethyl ammonium chloride (TTAC) to pentadecyl ethoxylated nonyl phenol (NP-15) mixture system

Surfactant adsorption at the solid-liquid is related to the chemical potential of the surfactant molecules (monomers) in the solution as well as to the nature of the solid. To better elucidate the mechanisms of adsorption of TTAC :NP-15 mixtures, their monomer concentrations of were

measured before and after adsorption and the results obtained are plotted in figures 60 and 61 as a function of equilibrium concentration. The monomer concentrations of both TTAC and NP-15 are similar before and after the adsorption. For tetradecyl trimethyl ammonium chloride (TTAC), the slope of monomer concentration curve after the adsorption is higher than that before the adsorption in the concentration range of 2×10^{-4} to 8×10^{-4} mol/l. This corresponds to the concentration range where TTAC solloids* are formed at the interface. For pentadecyl ethoxylated nonyl phenol (NP-15), the monomer concentration curve was shifted to lower concentrations due to the significant adsorption of NP-15 at the alumina interface. Clearly, the adsorption mechanisms for cationic TTAC are different from those for the non-ionic NP-15.

*Solloid, short form for *Surface colloid*, is a generic term for all types of adsorbed aggregates such as hemimicelles, admicelles, surface micelles , bilayer etc.

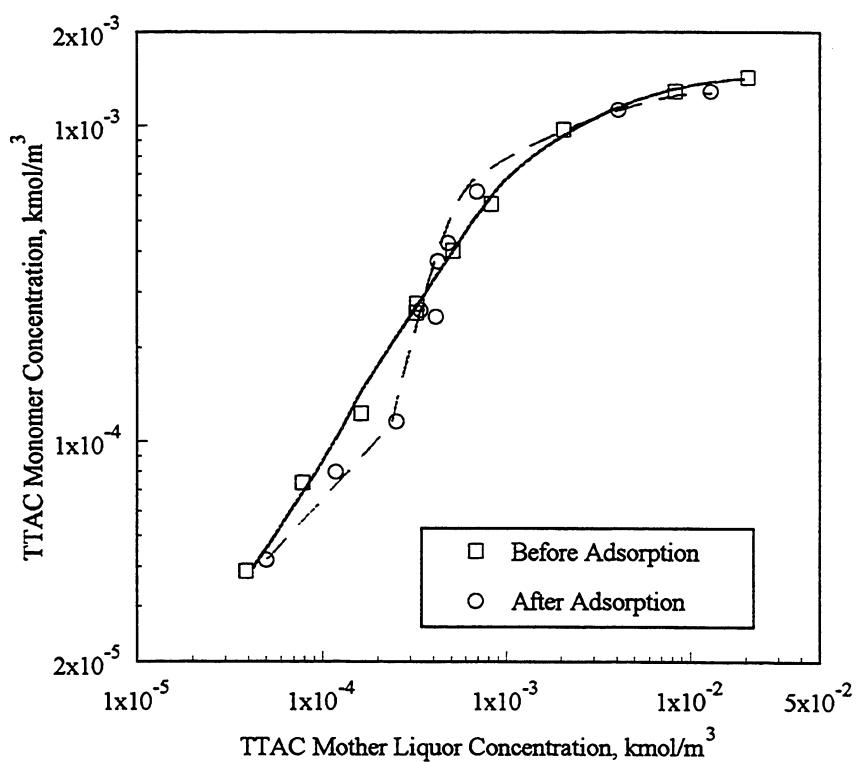


Figure 60 Change in TTAC monomer concentrations before and after adsorption on alumina from a 4:1 TTAC:NP-15 mixture.

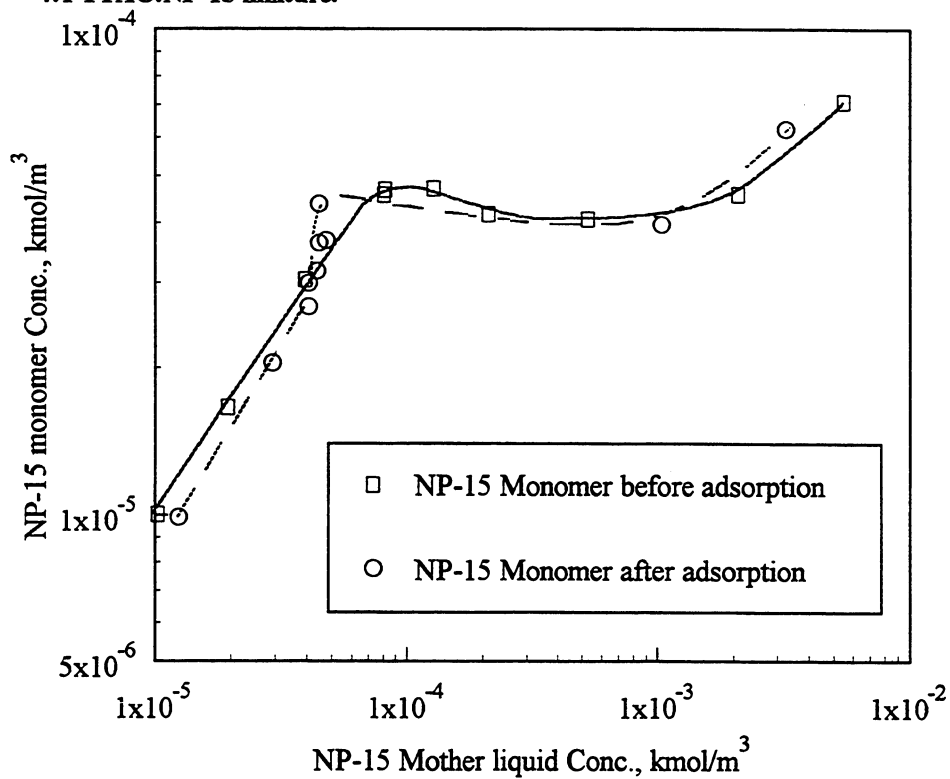


Figure 61 Change in NP-15 monomer concentrations before and adsorption on alumina from a 4:1 TTAC:NP-15 mixture.

The adsorption density is compared with the monomer concentrations for both TTAC and NP-15 in figures 62 and 63. The relationship between TTAC adsorption density and its monomer concentrations can be described by two straight lines with different slopes. The point of intersection of these two lines is around the TTAC monomer concentration of $3.5 - 4.0 \times 10^{-4}$ mol/l and the adsorption density corresponds to the surface coverage at which the alumina surface charge is neutralized. This indicates that there are two kinds of mechanisms involved in the adsorption of TTAC at this mixture ratio.

At low concentrations, the monomer concentration is equal to the total bulk concentration of the surfactant. The adsorption mechanism in this region is clearly electrostatic and can be described by the Stern-Graham equation¹⁵. At high concentrations, mixed micelles are formed and the monomer concentration is different from the total bulk concentration. The adsorption mechanism in this region is rather complex and merits further investigation. The adsorption mechanism for NP-15 is different from that of TTAC (see figure 63). There is a steady increase in adsorption density with increase in monomer concentration upto $\sim 3 \times 10^{-5}$ mol/l. Above this concentration, an increase in adsorption is accompanied by a decrease in monomer concentration. This is due to the more efficient solubilization of NP-15 into TTAC aggregates which are formed on the alumina surface at this stage. Strong synergy between adsorbed TTAC and NP-15 is indicated by this behavior. Subsequent to the initial extraction of residual NP-15 into the adsorbed aggregates, further increase in monomer

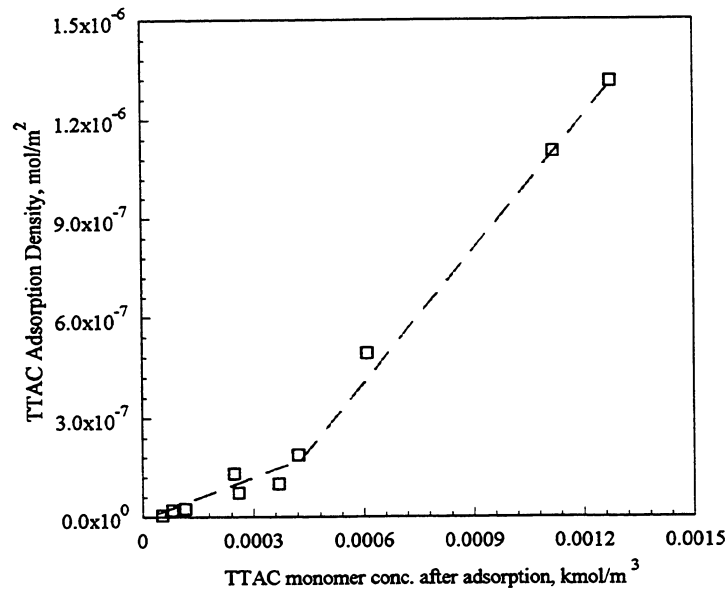


Figure 62 Relationship between TTAC monomer concentration and adsorption density for a 4:1 TTAC:NP-15 mixture system.

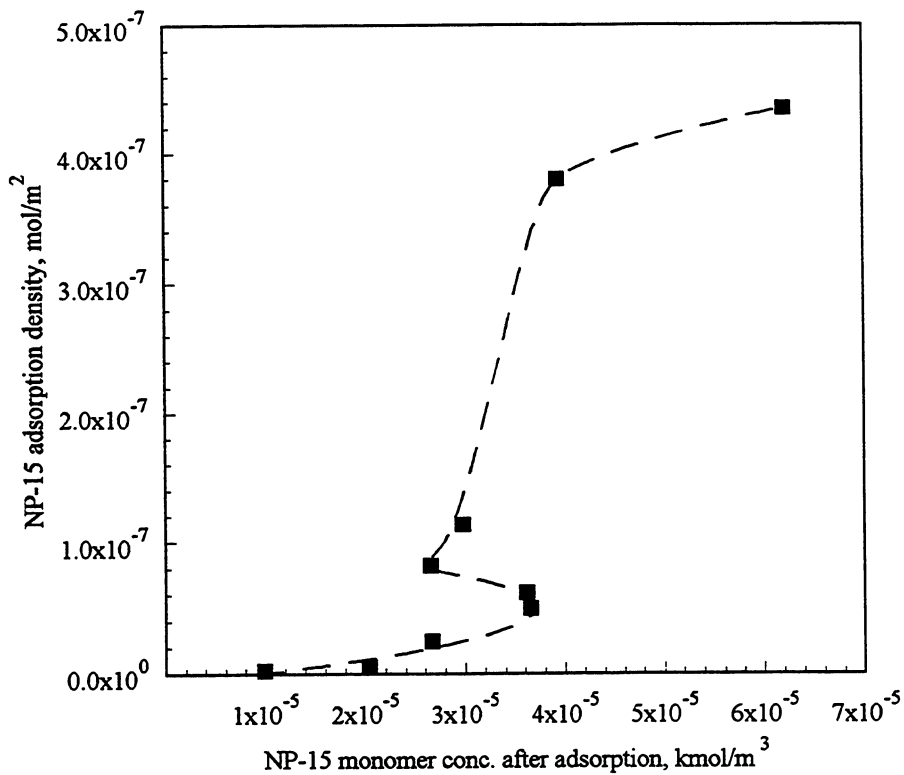


Figure 63 Relationship between NP-15 monomer concentration and adsorption density on alumina from a 4:1 TTAC:NP-15 mixture.

concentration leads to increased adsorption followed by surface saturation at high NP-15 concentrations.

It is interesting to examine the monomer ratio in the supernatant from the adsorption behavior point of view in the system (Figures 64 and 65). The ratio of surfactant mother liquor concentration to the monomer concentration can be used as an indication of mixed micelle formation. If no mixed micelles are formed, this ratio will be equal to 1 and ratios higher than 1 indicate the formation of micelles.

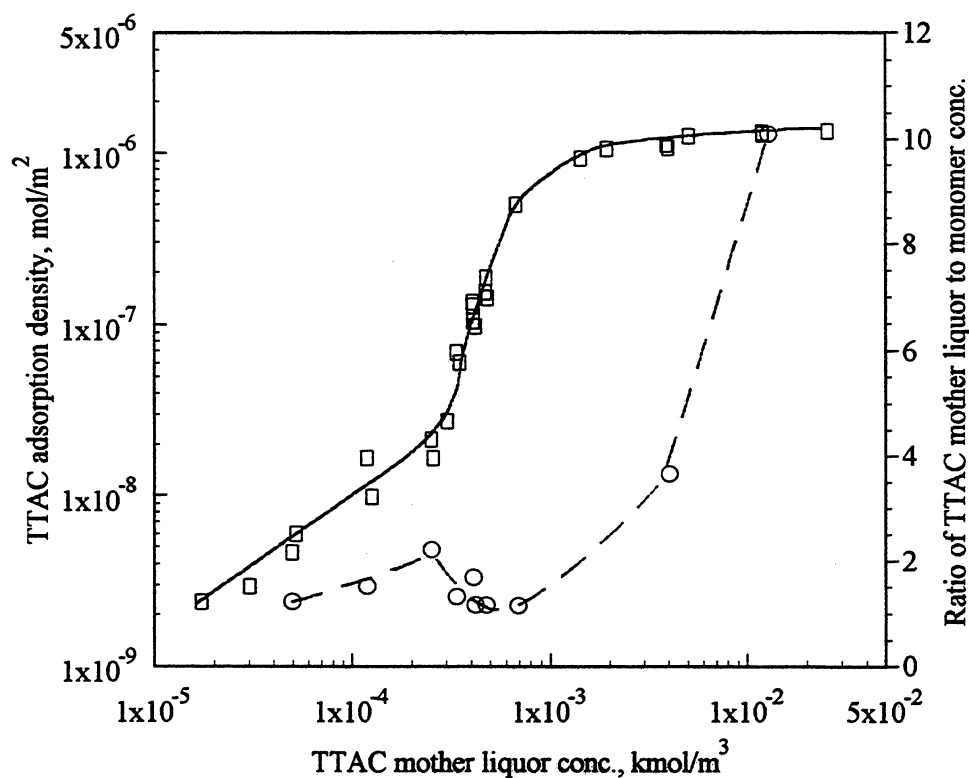


Figure 64 Correlation between adsorption density and monomer ratio after adsorption for TTAC from a 4:1 TTAC:NP-15 mixture.

The CMC for the 4:1 TTAC:NP-15 mixture is $\sim 2.7 \times 10^{-4}$ mol/l (total concentration). This corresponds to 5.4×10^{-5} mol/l NP-15 and 2.16×10^{-4} mol/l TTAC. From figures 35 and 36 it is seen that the adsorption densities for both TTAC and NP-15 continue to increase beyond these

concentrations. In single surfactant systems, formation of micelles in bulk solution is accompanied

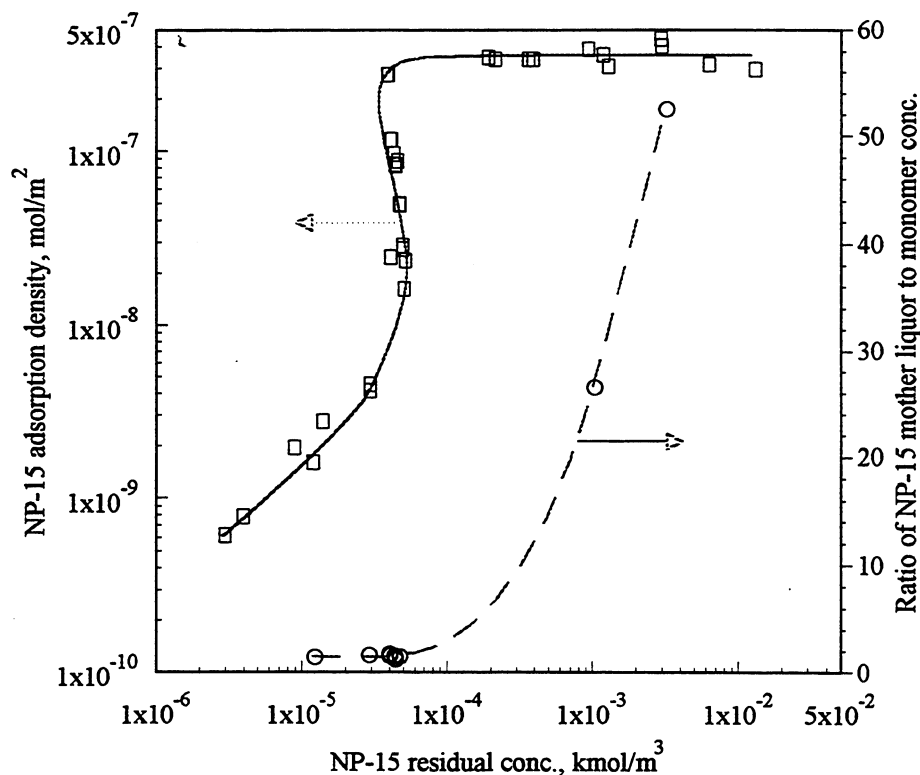


Figure 65 Correlation between NP-15 adsorption density and monomer ratio after adsorption from a 4:1 TTAC:NP-15 mixture.

by a plateau in adsorption. Adsorption of both TTAC and NP-15 from the 4:1 thus involve complex equilibria between micelles of different compositions and monomers. Clearly a full understanding of the change in micellization behavior of mixed surfactant systems should help in analyzing the adsorption processes. Since the regular solution theory is not suitable for the mixed surfactant systems, a new model to describe micellization of mixed surfactant systems is required.

SUMMARY

Adsorption/desorption of single surfactants and surfactant mixtures was studied on solids relevant to reservoir minerals. A marked effect of the structure of surfactant on determining its adsorption as well as the microstructure of the adsorbed layer has been demonstrated. Adsorption of surfactants from mixtures is invariably higher than when the surfactant was used alone in low concentration region. In the high concentration region, the relative adsorption density of surfactant from mixtures can be higher or lower depending on the structures of the surfactant components. In other words, steric hinderance between surfactants will play an important role in this high concentration region. This finding has important bearing especially because commercially used surfactants are always mixtures. The role of pH on the adsorption of surfactants was dependent upon the system studied. In ionic surfactant systems, increase in pH reduced the adsorption but in nonionic surfactants the effect was much less or insignificant. Adsorption/desorption of tetradecyltrimethylammonium chloride (TTAC) was studied at the alumina-water interface and significant hysteresis was observed at low surfactant concentrations. Also upon dilution the nature of the adsorbed layer was altered, and during desorption aggregates were present even at residual concentrations where no such aggregates had formed at those concentrations during initial adsorption. It is proposed that the initial aggregates undergo rearrange and do not desorb. This led to the observed hysteresis at lower concentrations.

Interactions between dissimilar surfactants (cationic and nonionic) modified the adsorption behavior of both the cationic (tetradecyl trimethyl ammonium chloride - TTAC) and the nonionic (pentadecylethoxylated nonyl phenol NP-15) surfactants. In the presence of TTAC, adsorption of NP-15 was induced on the substrate (alumina) where it normally does not adsorb. The presence of NP-15

lowered the adsorption of TTAC due to the shielding of the electrostatic interactions between the cationic surfactant and anionic substrate (pH 10). Desorption of TTAC from mixtures with low amounts of NP-15 was similar to that of TTAC alone. Since the nonionic NP-15 adsorption required the anchoring presence of the cationic TTAC, the desorption was also dependent upon TTAC desorption. In NP-15 rich mixtures, the desorption behavior is more complex and mechanisms are yet to be elucidated.

Regular solution theory was used to model the interactions between NP-15 and TTAC in solution. From the value of the interaction parameter it was evident that the interactions were not strong. Monomer concentration of mixtures were calculated and attempts made to correlate them with their adsorption behavior. Adsorption of TTAC was found to be dependent upon monomer concentrations but there was no such relation for NP-15 since its adsorption was dependent upon preadsorbed TTAC.

In addition to the cationic-nonionic system, interactions between an anionic surfactant (sodium dodecyl sulfate - SDS) and a nonionic surfactant (octaethylene glycol mono-n-dodecyl ether - $C_{12}EO_8$) with varying hydrocarbon chain length were also studied. Hydrophobic chain-chain interactions led to enhanced adsorption of both surfactants at solid-liquid interfaces. Interestingly, once the hydrocarbon chain length of the nonionic surfactant exceeded that of the anionic surfactant there was no further enhancement of SDS adsorption. This result can be used to guide the selection of mixed surfactants.

Size of aggregates of 1:1 mixtures of SDS/ $C_{12}EO_8$ adsorbed at the alumina-water interface was measured using dynamic pyrene fluorescence spectroscopy. Presence of the nonionic surfactant in the mixed aggregate with the anionic SDS reduced the electrostatic repulsion and increased the

total aggregate size. The SDS aggregate at the interface was smaller than that of the $C_{12}EO_8$ aggregate at similar adsorption densities. Also the number of SDS molecules in the mixed aggregate was smaller than that of the single component aggregate. Differences in the aggregate structure during adsorption and desorption can also be expected to cause differences in interfacial properties such as wettability and dispersion of the solid particles with significant effects on efficiency of micellar flooding.

To develop a model that can predict adsorption of surfactant mixtures as a function of their activity in the mixed surfactant system, the monomer concentrations of TTAC and NP-15 in mixtures at different ratios and different ionic strengths were measured using ultrafiltration technique. It was found the monomer concentrations measured by ultrafiltration method were different from the predictions of the regular solution theory. This result exposes the limitations of the regular solution theory for the mixed surfactant systems, and a more suitable model needs to be developed.

In conclusion, interactions between ionic and nonionic surfactants have been exploited to modify the solution and interfacial properties of the individual surfactants. Aggregate size, reduction of interfacial tension and adsorption/desorption characteristics were all modified markedly by a judicious selection of surfactant combinations. These findings have important bearings to enhance oil recovery using micellar flooding because commercial surfactants used invariably are mixtures.

REFERENCES

1. Z. Li and M.J. Rosen, *Analytical Chemistry*, **53**, 1981, 1516.
2. A. Sivakumar and P. Somasundaran, *Langmuir*, **10**, 1994, pp 131-134.
3. P. Somasundaran, E.D. Snell, E. Fu and Q. Xu, *Colloids Surfaces*, **63**, 1992, 49.
4. Erkan Koksal, R. Ramachandran, P. Somasundaran and C. Maltesh, *Powder Technology*, **62**, 1990, 251.
5. K. Kalyansundaram and J.K. Thomas, *J. Am. Chem. Soc.*, **99**, 1977, 2038.
6. D.N. Rubingh, "Mixed Micelle Solutions", in Solution Chemistry of Surfactants, K.L. Mittal (ed), Vol. 1, Plenum Press, 1978, pp 337-354.
7. R. Zana, in Surfactant Solutions: New Methods of Investigation, Surfactant Science Series, R. Zana (ed), Vol. 22, Marcel Dekker, New York, 1987.
8. J.H. Harwell, J.C. Hoskins, R.S. Schechter and W.H. Wade, *Langmuir*, **1**, 1985, 251.
9. R.L. Venabl and R.V. Naumann, *J. Phys. Chem.*, **68**, 1964, 3498.
10. P. Somasundaran, T.W. Healy and D. W. Fuerstenau, *J. Coll. Interf. Sci.*, **70**, 1966, 90
11. P.Chandar, P. Somasundaran and N.J. Turro, *J.Coll. Interf. Sci.*, **117**, 1987, 31.
12. S. Fukushima and S. Kumagai, *J. Coll. Interf. Sci.*, **42**, 1973, 539.
13. P. Somasundaran, E. Fu and Q. Xu, *Langmuir*, **8**, 1992, 1065.
14. L. Huang, C. Maltesh and P. Somasundaran, *J. Coll. & Interf. Sci.*, **177**, 1996, 222
15. P. Somasundaran, T. W. Healy, and D. W. Fuerstenau, *J. Phys. Chem.* **68**, 1964, 3562

Publications and Presentations

1. A. Sivakumar and P. Somasundaran, " Adsorption of Alkylxylene Sulfonates on Alumina: a Fluorescence Probe Study", *Langmuir*, **10**, 1994, p131.
2. Lei Huang, C. Maltesh and P. Somasundaran, " Adsorption Behavior of Cationic and Nonionic Surfactant Mixtures at the Alumina-water interface", *J. of Colloid & Inter. Sci.*, **177**, 1996, p222
3. Lei Huang, C. Maltesh and P. Somasundaran, in "Surfactant Adsorption and Surface Solubilization" (R. Sharma, ed) ACS Symposium series 615, Chapter 14.(1995)
4. Lei Huang, C. Maltesh and P. Somasundaran, " Spectroscopic Investigation of Adsorption and Desorption of Mixed Surfactant Layers." Presented at the 208th ACS National Meeting, Washington, DC August 21-25, 1994
5. Lei Huang and P. Somasundaran, "Changes in Micelle Composition and Monomer Concentrations in Mixed Surfactant Solution" Presented in 211th ACS National Meeting, New Orlean March 24-28, 1996